Diplomarbeit

Application and Improvement of Quasi-Dimensional Combustion Models for Turbocharged SI Engines

Alois Steiner

zur Erlangung des akademischen Grades eines Diplom-Ingenieurs
eingereicht am Institut für Verbrennungskraftmaschinen und
Thermodynamik an der Technischen Universität Graz

Institutsvorstand:
Univ.-Prof. Dipl.-Ing. Dr.techn. Helmut Eichlseder

Betreuender Professor:
Ao.Univ.-Prof. Dipl.-Ing. Dr.techn. Andreas Wimmer

Externer Betreuer:
Dr.-Ing. Jens Neumann

Februar 2010

STATUTORY DECLARATION

I declare that I have authored this thesis independently, that I have not used other than the declared sources / resources, and that I have explicitly marked all material which has been quoted either literally or by content from the used sources.

Ich erkläre an Eides statt, dass ich die vorliegende Arbeit selbstständig verfasst, andere als die angegebenen Quellen/Hilfsmittel nicht benutzt, und die den benutzten Quellen wörtlich und inhaltlich entnommenen Stellen als solche kenntlich gemacht habe.

Graz, 01.02.2010

(Alois Steiner)

ABSTRACT

In times of increasing requirements on CO_2-emissions and therefore the need to improve fuel efficiency, downsizing of combustion engines is an effective approach for future concepts.

In order to predict and optimize the expected combustion behavior concerning fuel consumption, performance, emissions etc., the simulation plays a key role nowadays. Due to the fact that the number of engine parameters is steadily rising, simulation methods which need less computational time like zero-dimensional models are required, especially in the early stages of the development process.

The objective of this thesis is to analyze, calibrate and develop quasi-dimensional combustion models for SI engines within the 1D-simulation-tool GT-Power. In the present work, a comparison was made between the commercial tool from Gamma Technologies Inc. “SI Turbulent Flame Combustion Model” and a combustion model created at BMW which was subject of the dissertation of Nefischer (TU Graz, 2009). This model has been enhanced and refined during this thesis.

The investigations on two turbocharged SI engine concepts (one highly turbocharged and one with variable valve timing) demonstrate different aspects of both models and their ability to meet requirements like accuracy, robustness, simulation time etc. The calculations are based on measurements at engine test benches.

ACKNOWLEDGEMENTS

This document is the last step in my course of studies at Graz University of Technology. I can look back to wonderful experiences, meeting exciting people, seeing different countries and cultures.

First of all, I want to thank my family and friends for their care and support throughout my whole life, always giving me a feeling of home, even when I was far away.

Second, I would like to thank Dr. Jens Neumann for his support and assistance during the creation of this thesis and the whole team of EA-301 which is responsible for the predevelopment of SI engines at BMW.

Finally, I want to thank my supervisor Prof. Dr. Andreas Wimmer from the Institute of Internal Combustion Engines and Thermodynamics at Graz University of Technology for his assistance and for giving me the possibility do write this thesis at BMW in Munich.

TABLE OF CONTENTS

1 Introduction

In the last century, the importance of combustion engines increased enormously and nowadays a life without them seems almost impossible. Despite a lot of upcoming new technologies, like hydrogen fuel cells and electric concepts, the traditional combustion engines and their development are still crucial for every car manufacturer. During the last decades, the greenhouse effect has become a major topic and the requirements for emissions rose steadily. In order to meet these requirements, car manufacturers are forced to reduce the fuel consumption and emissions of their cars. For this purpose, downsizing is an effective approach to improve the fuel efficiency of engines and to lower emissions.

Since 1876, when Nikolaus August Otto has patented his engine on the basis of the much weaker performing two-cycle gaseous-fuel engine of Lenoir developed in 1860, the SI engine has experienced about 130 years of development.

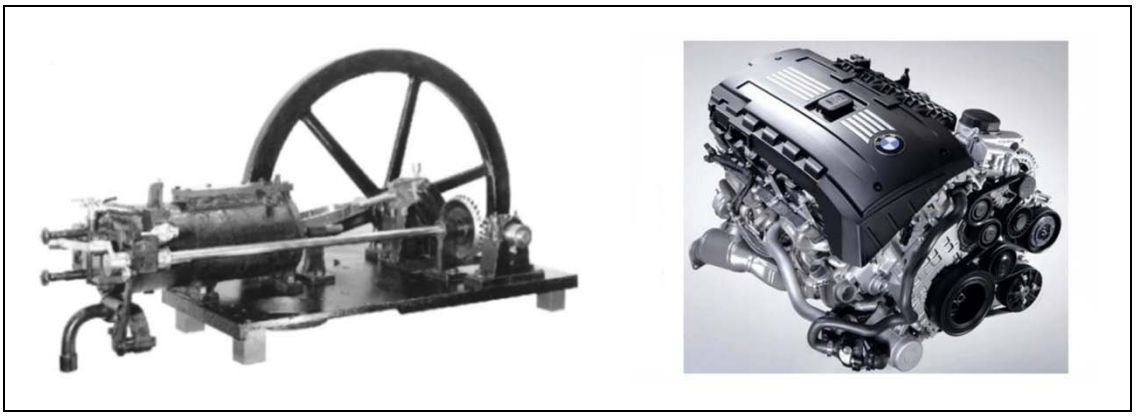

Figure 1-1: Comparison of the first engine from Nikolaus Otto with a modern TGDI engine from BMW

In order to predict and optimize the expected combustion behavior concerning emissions, performance, fuel consumption etc., the simulation nowadays plays a key role. Due to the fact that the number of engine parameters is steadily rising, simulation methods which need less computational time like zero-dimensional models are required, especially in the early stages of the development process. The simulation-tool GT-Power

from Gamma Technologies provides combustion models and sub-models, which can achieve quite good results but are not explained thoroughly in the documentation and therefore give the model a black-box-character. In order to understand the physical processes and to make a better usage of the software possible, a combustion model for GT-Power was created at BMW (Nefischer, 2009). It is based on the "Entrainment model", which was developed by Blizard and Keck (1976).

One of these combustion models is supposed to be used not only to predict the burn rates (rates of heat release) but also to simulate values like maximum pressures (which are important for the design engineers), mean effective pressures, torques and so on. It is also planned to integrate the model into power train and driving simulations.

The objective of this diploma thesis is to analyze, calibrate and compare combustion models for SI Engines within GT-Power: The SI Turbulent Flame Combustion Model "EngCylCombSITurb", which is integrated in GT-Power, and a User Model, created at BMW. These 2 models are applied to 2 different engine concepts: a Highly Turbocharged TGDI and a TGDI with Variable Valve Timing (TVDI). Incoming measurements from the engine test bench give the possibility to perform a "Three Pressure Analysis" (TPA) in GT-Power, which uses these measurements to calculate the burn rate. These results are taken as reference values and can be compared with the two competing models.

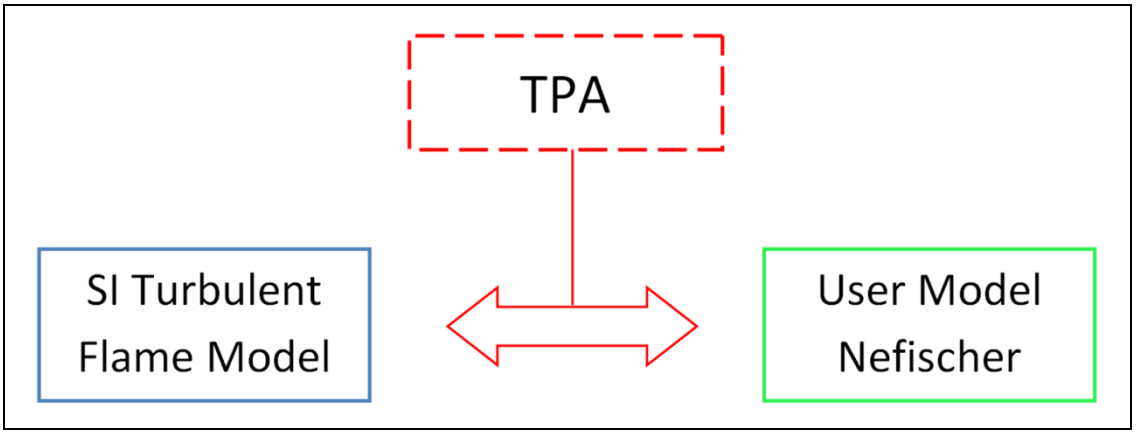

Figure 1-2: Competing models

2 Basics

This chapter is based on up-to-date literature regarding the main topics and technologies of the two investigated SI engines in this thesis.

2.1 Combustion Process of an SI Engine

In conventional SI engines, the homogeneous fuel-air mixture is ignited through a spark timing close to the top dead center. In the following premixed combustion process, a flame front is expanding from the position of the spark plug until it reaches the walls of the combustion chamber where extinction occurs. The high turbulence in SI engines is important for the high velocities of flames, which make high engine speeds possible.

So, the combustion process of an SI engine is strongly determined by the expansion of turbulent flames which depends on the one hand on the laminar flame speed and on the other hand on parameters of turbulence (e.g. turbulent length scale etc). As Figure 2-1 shows, increasing turbulence causes the warping of the laminar flame front which increases the reaction zone and causes faster flame propagation.

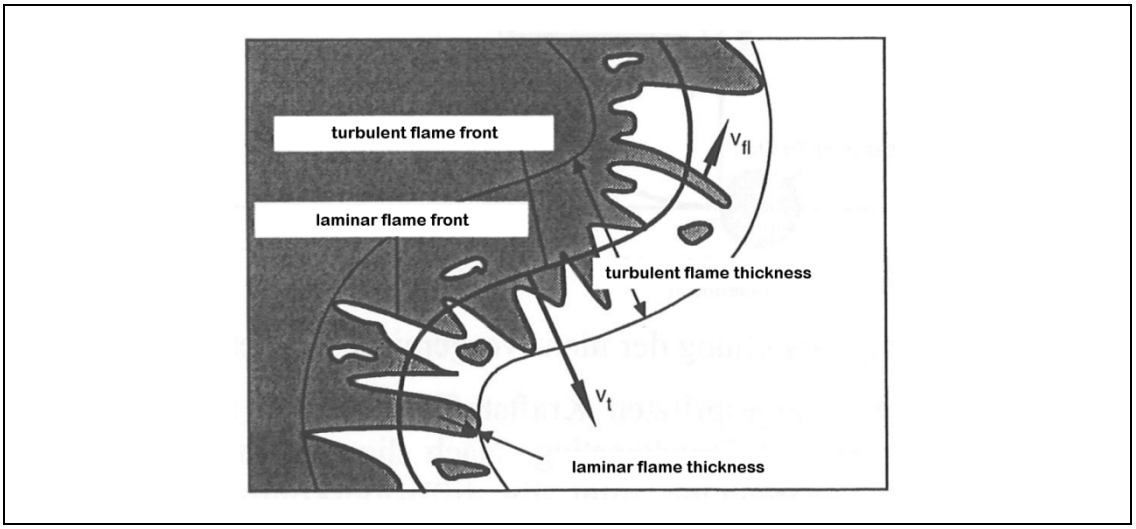

Figure 2-1: Laminar and turbulent flame propagation (Wimmer, 2004)

Whereas the ordinary combustion process is initiated through a spark from the spark plug, engine knocking is caused by compressed ignition of fuel-air

mixtures the flames front has not reached yet (tail gas). The sudden release of high rates of chemical energy leads to a high increase of pressure and temperature and to an expansion of high-frequency shock waves from 5-7 kHz with high amplitudes (Eichlseder, 2005).

The velocity of flame propagation determines not only the burnout, but has also direct impact on knock occurrences in SI engines. If the burnout of the tail gas is fast enough, engine knocking can be avoided (RWTH Aachen, 2000).

2.2 Downsizing

Downsizing is a procedure where engines with smaller displacements can achieve the same results concerning driving performance as engines with large displacements. The main goal is the increase of fuel efficiency and a decrease of CO_2-emissions. Due to the reduction of displacement, the used engines can be operated in areas with higher specific loads to reach the same performance, which leads to lower throttle losses. Thus, a higher degree of efficiency and a lower specific fuel consumption can be achieved (Van Basshuysen & Schäfer, Motorlexikon.de - Downsizing, 2009).

Hence, the goals for downsizing-concepts are:

- Decrease of fuel consumption and CO_2-emissions
- Reduction of weight compared to an engine with the same power but larger displacement
- Same power due to higher indicated mean effective pressures (IMEP)
- Compensation of the low torque (compared to engines with larger displacement) due to turbocharging

In order to achieve these goals, key technologies are:

- Gasoline Direct Injection (GDI)
- Supercharching (especially with the exhaust-driven turbocharger)
- Variable Valve Timing

Concepts for a variable compression ratio, which could bring further improvements to these engines, are also possible, but are not ready for serial production yet.

2.3 Technologies Used in the Investigated Engine Concepts

In order to further increase the performance and fuel efficiency, the 2 investigated engine concepts use technologies which will be described in this chapter.

2.3.1 Gasoline Direct Injection

The original purpose of gasoline direct injection was an increase in performance because of the cooling effect through evaporation in the combustion chamber. This leads to a higher volumetric efficiency, reduces the tendency of engine knocking at full load and permits a slightly higher compression ratio (Eichlseder, 2005).

Basically, there are 2 concepts to perform gasoline direct injection:

- **Homogeneous operation:** At high loads, gasoline is injected early during the intake stroke, the fuel-air mixture homogenizes and burns premixed with a stoichiometric air-fuel-ratio.
- **Stratified-charge operation:** Due to a late injection in the compression stroke at partial load, a stratification of the fuel-air-mixture can be achieved. This leads in average to a lean fuel-air mixture in the combustion chamber, but in the area of the spark plug there is an ignitable mixture.

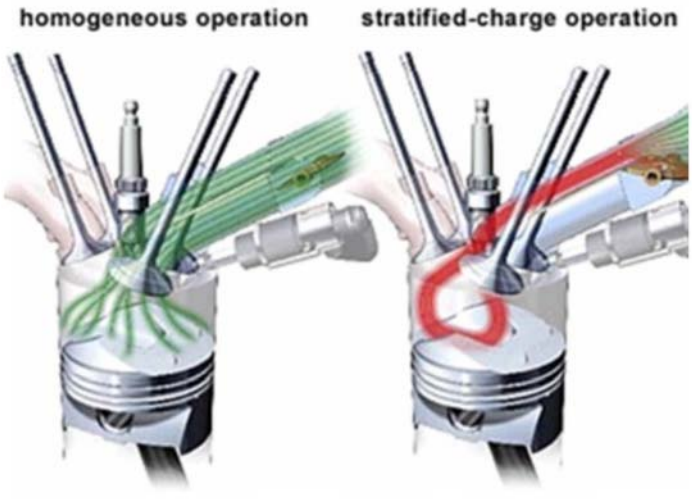

Figure 2-2: Basic concepts of Gasoline Direct Injection

At engines which are only operated homogeneously, like the two investigated engines in this thesis, the advantages because of the cooling effect, the shift of the knocking limit and advantages regarding the filling of the cylinder can be exploited totally. That way, the fuel efficiency increases in wide areas of the engine performance map up to 10%. In stratified-charge operation with variable high fuel-air mixtures, the engine can be run without a throttle which reduces the high losses of gas exchange of homogeneously operated SI engines. Because of higher air-fuel-ratios, the efficiency of the whole process increases and leads to improvements of efficiency at partial load of 10-30%.

Therefore, the decisive strengths of the SI engine with direct injection are the high potentials operating with fuel stratified injection. Additionally, this system has a good transient- and full load behavior. Nowadays, the whole exploitation of these potentials is limited by exhaust gas emissions. Due to the fact that with fuel stratified injection the cylinder is filled mostly with lean fuel-air mixture, there is a surplus of oxygen. This inhibits the possibilities of reduction and thus the conventional exhaust gas treatment with the three-way catalytic converter. In addition, the shorter time for fuel-mixture generation and the accumulation of fuel at the cylinder walls with the wall-guided method lead to much higher HC-emissions. According to the state in the engine performance map, SI engines with gasoline direct injection are

operated with different methods. Figure 2-3 gives an example for possible strategies (Eichlseder, 2005).

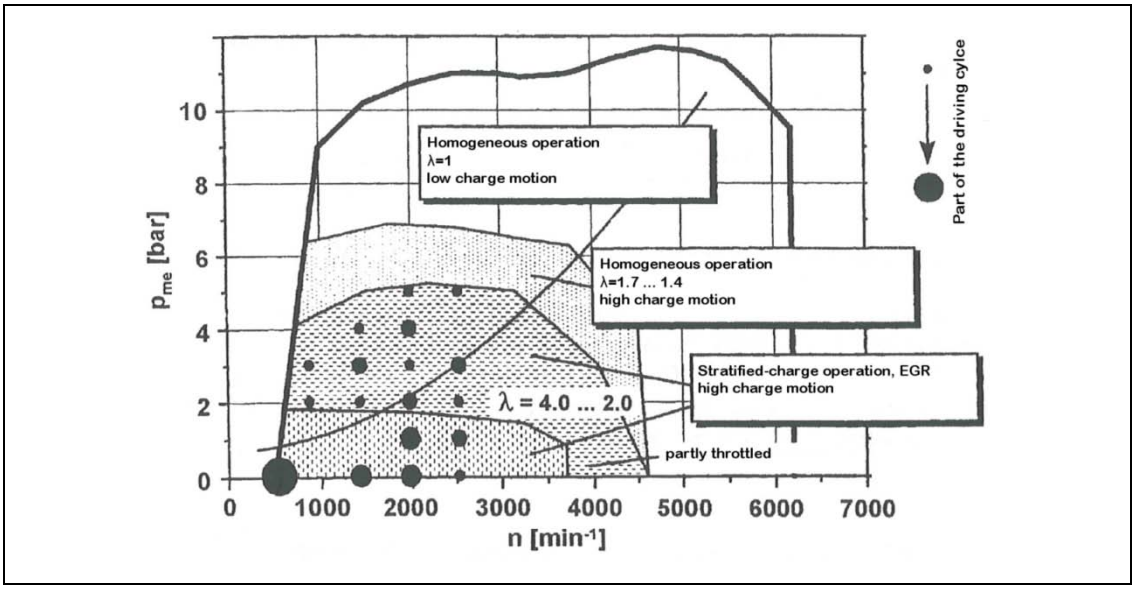

Figure 2-3: Operating strategies in the engine performance map (Eichlseder, 2005)

2.3.2 Variable Valve Timing

Variable Valve Timing (VVT) is usually realized by the use of a Variable Valve Train, called Valvetronic at BMW, which controls the valve lift and a variable camshaft setting system, called VANOS (short form for “Variable Nockenwellensteuerung”) at BMW, which controls the phase setting. There are upcoming electro mechanic concepts which are not fully developed yet.

The in- and outflow of gases changes depending on the engine speed and the throttle position. Variable Valve Timing permits the adjustment to different engine speeds and cylinder charges. With the variable camshaft setting system, the valve timing can be changed. At low engine speeds, the cylinder is already filled with the fuel-air mixture at BDC and an earlier IVC (ideally where the mass flow gets zero) avoids the backflow of gases in the intake part, which increases the volumetric efficiency. At higher engine speeds, there is less time to fill the cylinder and a later IVC permits the fuel-air mixture to flow in even after BDC leading to higher engine power (Eichlseder, 2005). Due to optimized valve overlap at partial loads, the internal exhaust gas recirculation (EGR) can be increased. High EGR-rates lead to a thermal

de-throttling which increases fuel efficiency and reduces NO_x-emissions (Backhaus, 2009).

Another goal is to reduce throttle losses which increases the fuel efficiency at partial load. This can be realized with partial de-throttling over even full de-throttling which supersedes the throttle. As Figure 2-4 shows, the TVDI (with VVT) has lower gas-exchange losses (orange area) than the homogeneously operated TGDI (blue area).

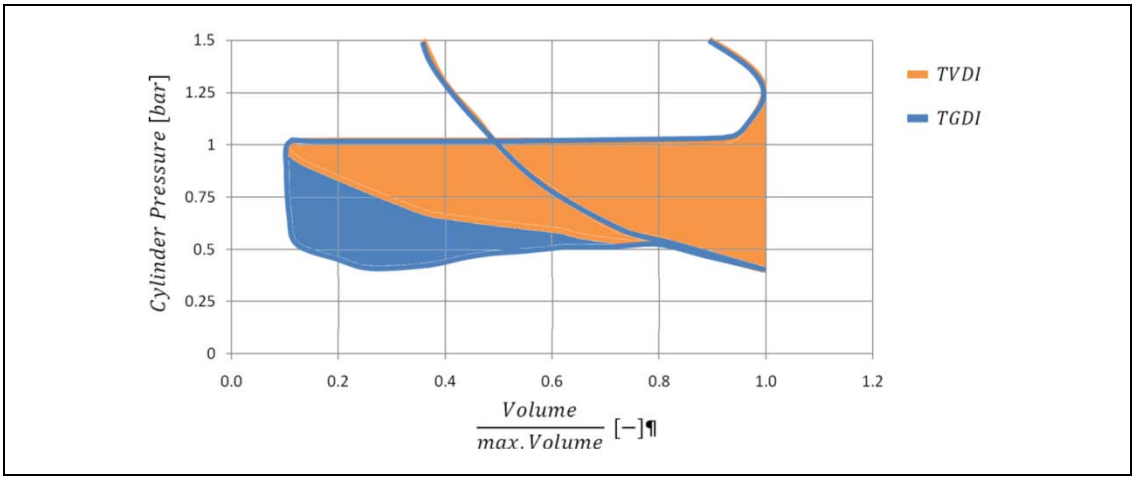

Figure 2-4: Reduced gas-exchange work with Variable Valve Timing (according to Kiefer et al., 2004)

Partial de-throttling can be realized by:

- Variable phase setting
- Exhaust gas recirculation
- Stratification operation at direct injection
- Supercharged engines with small displacements
- Variable compression ratio
- Cylinder cutoff

Full de-throttling can be realized by:

- Variable Valve Train
- Electro-mechanic valve train

2.3.2.1 Scavenging

If the time slots for intake and exhaust valves can be adjusted independently, due to variable valve timing, the intake valves at full load can be opened when the exhaust valves are still open. With this overlap of valve opening-periods and a positive pressure gradient between intake and exhaust manifold (which is the case for turbocharged engines), fresh air flows into the exhaust manifold and scavenges residual gases out of the cylinder. This cools the combustion chamber and additionally drags hydrocarbons and carbon monoxide out of the cylinders which react with this air and burn. Thus, the exhaust gas temperature and volume increase, leading to a higher exhaust gas flow and causing a higher pressure of the exhaust-driven turbocharger. Scavenging leads to higher torques at low engine speeds.

2.3.2.2 Phasing

Phasing describes the different intake valve lifts of a cylinder. If one of the intake valve lifts remains small, the biggest part of the fresh mixture flows through the other valve and causes swirl. So, it can increase the turbulent kinetic energy and make higher burn rates possible. This reduces the burn duration and, if the crank angle of 50% burn point stays the same, the ignition point can be set at higher crank angles. The higher turbulence increases combustion stability, which helps to apply higher fractions of residual gases. This increases the fuel efficiency because of partial de-throttling and makes procedures like the warm-up of the catalyst easier (Klaus et al., 2005).

The problem when trying to model phasing is that a higher degree of phasing causes of course a higher swirl, but measurements showed that it can also reduce tumble. So, this process is nonlinear and needs a sophisticated approach in order to model the real effects.

Figure 2-5 shows 3 different settings: the one in the middle with no phasing, where both intake valves have the same lift, one with mild phasing and the maximum phasing settings with the highest possible difference in valve lifts.

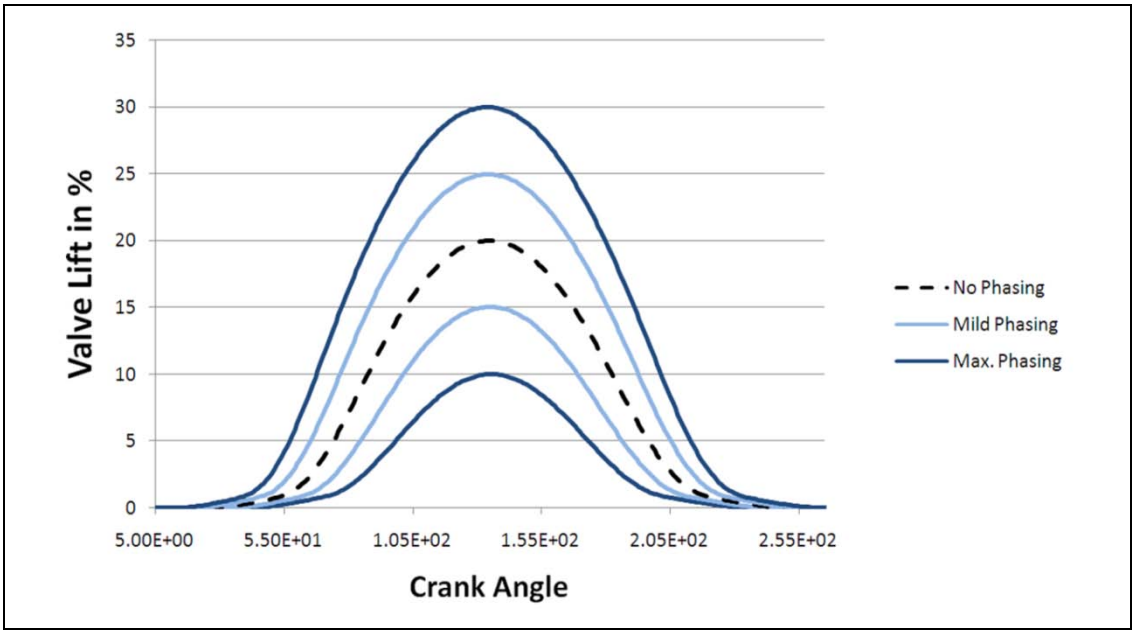

Figure 2-5: Different degrees of phasing

Phasing is used in areas with low engine loads, where throttling is applied in conventional SI engines. At full load, other parameters like the flow rate become more important and so the same valve lifts are applied. Figure 2-6 shows a characteristic diagram how phasing is used.

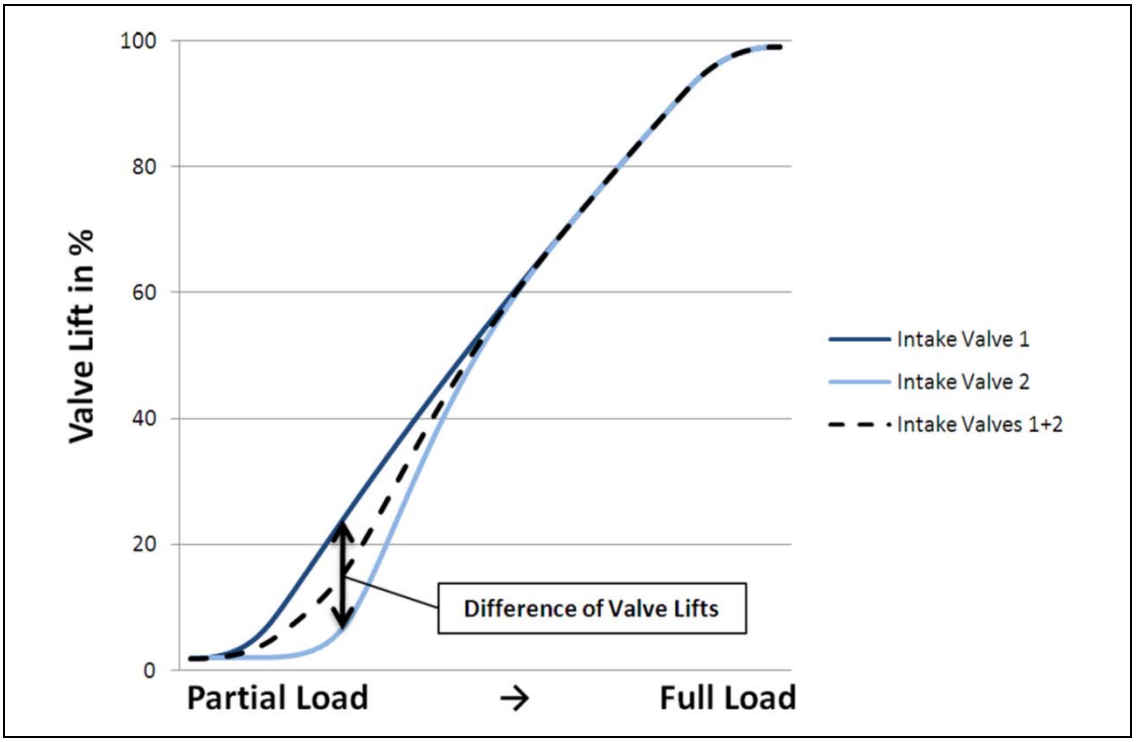

Figure 2-6: Phasing depending on load

2.3.3 Highly Turbocharged Engines

Highly turbocharged is not a well-defined term. For passenger car engines, the term highly turbocharged is used approximately above 18 bar indicated mean effective pressure. Modern Diesel engines reach 25 bar (Van Basshuysen & Schäfer, Motorlexikon.de - Hochaufladung, 2009). Highly turbocharged engines are usually used in downsizing concepts to achieve higher performance, higher torque already at low engine speeds and to reduce fuel consumption and emissions.

For higher degrees of turbocharging, larger turbocharger(s)/turbocharger concepts are necessary. Because of the increasing volumes and increasing inertias, the response behavior gets worse (turbo lag) and so a compromise between the advantages of turbocharging (e.g. higher torques), response behavior and costs (overall more advanced and more expensive concepts, e.g. additional variabilities) has to be made.

According to Backhaus (2009), double-stage turbocharging systems are the best solution for engines with higher specific engine power. Based on cost-benefit calculations, they see advantages compared to single-stage turbochargers with the expensive variable turbine geometry.

2.3.4 Twin Scroll Turbocharger

Exhaust driven turbochargers with variable turbine geometry are standard in modern diesel engines. With the higher exhaust gas temperatures of SI engines, more expensive material choices or thermodynamically less efficient solutions have to be pursued. So, other methods to improve the response behavior of the turbine were investigated. The Twin Scroll turbocharger has a double-flow construction of the turbine housing and exhaust manifold.

As Figure 2-7 shows, the pipes of cylinder 1 and 4 are separated from cylinder 2 and 3 in two scrolls, until the entrance into the turbine. This prevents disturbances of the impact energy of the adjoining flow in the exhaust manifold and avoids the weakening of turbine propulsion (Haider, 2008). Thus, the advantages of the Twin Scroll turbocharger are a better response behavior and a faster build-up of turbocharging pressure. Tests

have shown that the build-up of turbocharging pressure can already start slightly above idle speed which leads to a maximum torque at around 1500 rpm.

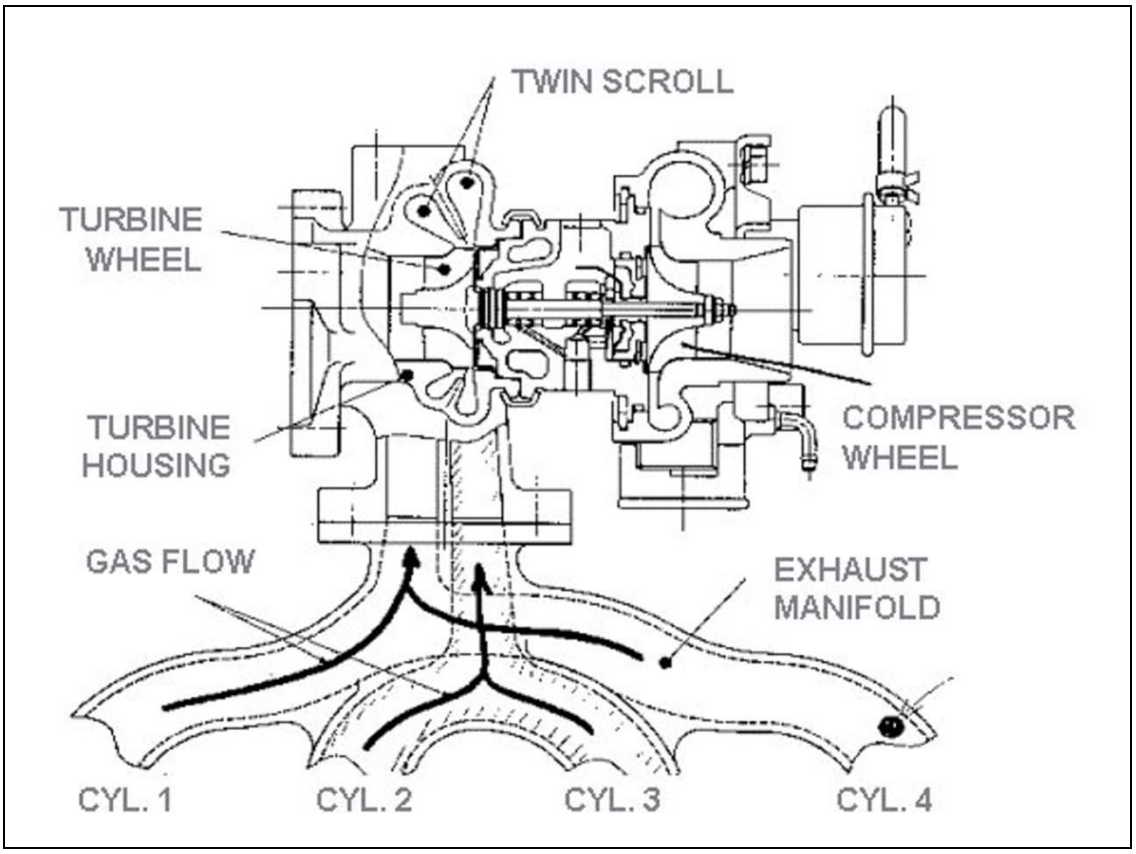

Figure 2-7: Construction of a Twin Scroll turbocharger (www.skyroadster.com)

2.4 Pressure Trace Analysis

The pressure trace analysis in a cylinder is a very important tool in the development of combustion engines. It is the most effective way to identify the knocking limit. By a thermodynamic analysis other values like the burn rate can be calculated.

Cylinder pressure is measured with piezo-sensors, which indicate a force proportional to the pressure in the combustion chamber. The conditions of the gases (pressure, temperature and internal energy) can be specified by the thermal equation of state, the mass balance and the energy balance. Due to the fact that the combustion process happens during the high-pressure-phase, the combustion chamber for this phase can be seen as a closed

system. This means that the flows of enthalpy across the system borders are zero. The blowby losses and the change of enthalpy through evaporation with gasoline direct injection are zero as well.

The internal energy depends on pressure, temperature and the composition of gases (Formula 2-1). The term dQ_w is subtracted because of the chosen orientation into the cylinder (Figure 4-1). The temperature of gases can be determined through the actual volume of the combustion chamber, the total gas quantity and the pressure measured in the cylinder (Merker, Schwarz, Stiesch, & Otto, 2004).

$$\frac{dQ_B}{dt} = \frac{dU}{dt} - \frac{dQ_W}{dt} + p\frac{dV}{dt}\left[-\frac{dm_{BB}}{dt}h_{BB}\left(-\frac{dm_{Br.,verd.}}{dt}\Delta h_{verd.}\right)\right]$$

Formula 2-1: Equation for the burn rate

Figure 2-8 shows the burn rate (blue) and some characteristic values which have been used in the simulation analysis (5.4.2.1).

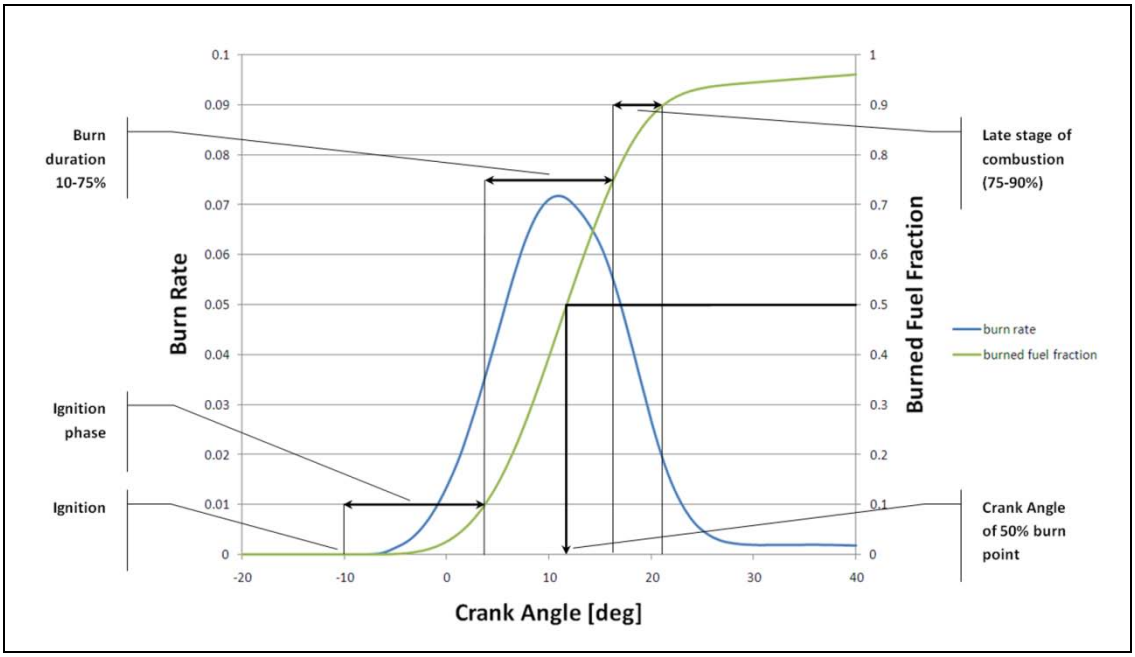

Figure 2-8: Characteristic values of the combustion process

3 Investigated Engine Concepts

In order to evaluate the simulations models, data from real engines is necessary. The engines described in chapter 3.2 and 3.3 have been modeled in GT-Power and are evaluated at the engine test bench, equipped with an indication system to track the required data. The cylinder pressures, which are necessary for a Pressure Trace Analysis (2.4), are measured with high-pressure piezo-sensors. Low-pressure piezo-sensors and thermocouples measure pressures and temperatures just before intake valves and after the exhaust valves, which helps to reduce the simulation model significantly to the region between these measurements. Additionally, the engines are equipped with many other measuring points for torque, power, exhaust gas analysis, fuel consumption etc. A conditioning system guarantees a constant environment (intake air, cooling water, fuel conditions etc.), which is necessary for a comparability of measurements. Both engines are turbocharged concept engines and use Gasoline Direct Injection with homogenous operation throughout the entire engine performance map.

3.1 Base TGDI

In the first development steps, the Nefischer User Model has been evaluated on the TGDI. In this thesis the transfer of the model to the engines described in chapter 3.2 and 3.3 has been evaluated. Both engines are based on the TGDI, one is highly turbocharged, the other one has been enhanced with Variable Valve Timing (VVT).

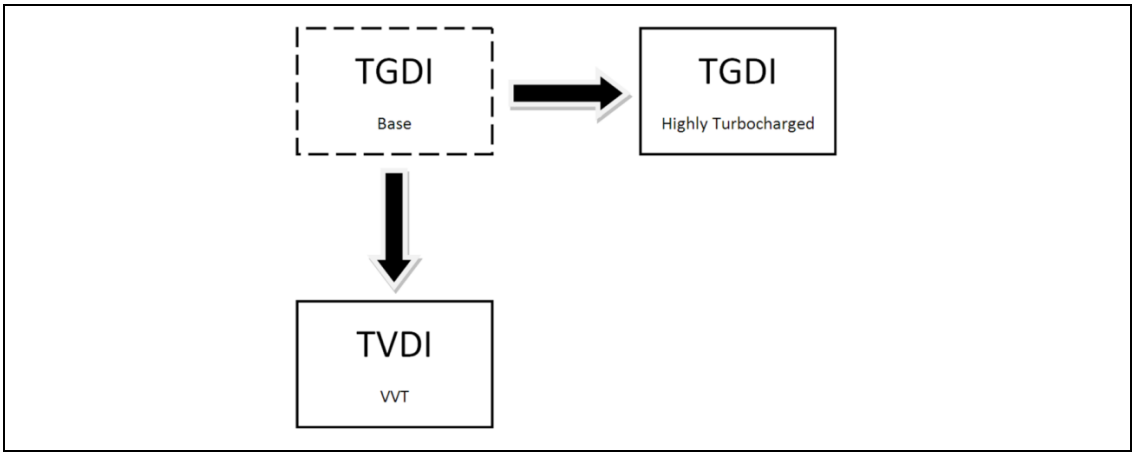

Figure 3-1: Engine concepts

3.2 Highly Turbocharged TGDI

The Highly Turbocharged TGDI is equipped with a double-stage exhaust driven turbocharger and VANOS for the intake and exhaust camshafts (Bi-VANOS). It is highly turbocharged (2.3.3) in order to realize a very high specific engine performance. Table 3-1 gives an overview of engine specifications.

Specifications Engine 1	
Operating process	Gasoline 4-stroke
Cylinders	4
Valves	4
Displacement	1600 cm^3
Bore	77 mm
Stroke	85.8 mm
Compression ratio	9.2

Table 3-1: Engine specifications (Highly Turbocharged TGDI)

3.3 TVDI

The second engine is a so called TVDI (Turbocharged Valvetronic Direct Injection) with a Twin-Scroll turbocharger (2.3.4) and Variable Valve Timing (2.3.2). Table 3-2 gives an overview of engine specifications.

Specifications Engine 2	
Operating process	Gasoline 4-stroke
Cylinders	6
Valves	4
Displacement	2979 cm^3
Bore	84 mm
Stroke	89.6 mm
Compression ratio	10.2

Table 3-2: Engine specifications (TVDI)

4 Simulation of Combustion Processes

This chapter shows a general classification of working process models and gives an overview of established combustion models which are nowadays used in simulation programs. It also describes how simulations are done with the software GT-Power.

4.1 Classification of Models for the Working Process

In order to classify models to analyze and simulate the working process, Wimmer (2004) has proposed the following classification:

- Zero-dimensional models
- Quasi-dimensional models
- One- and multidimensional models

4.1.1 Zero-Dimensional Models

Zero-dimensional models describe the time-dependence of variables but do not consider spatial phenomena. They are often used to develop empirically based models when fast and simple approaches are required.

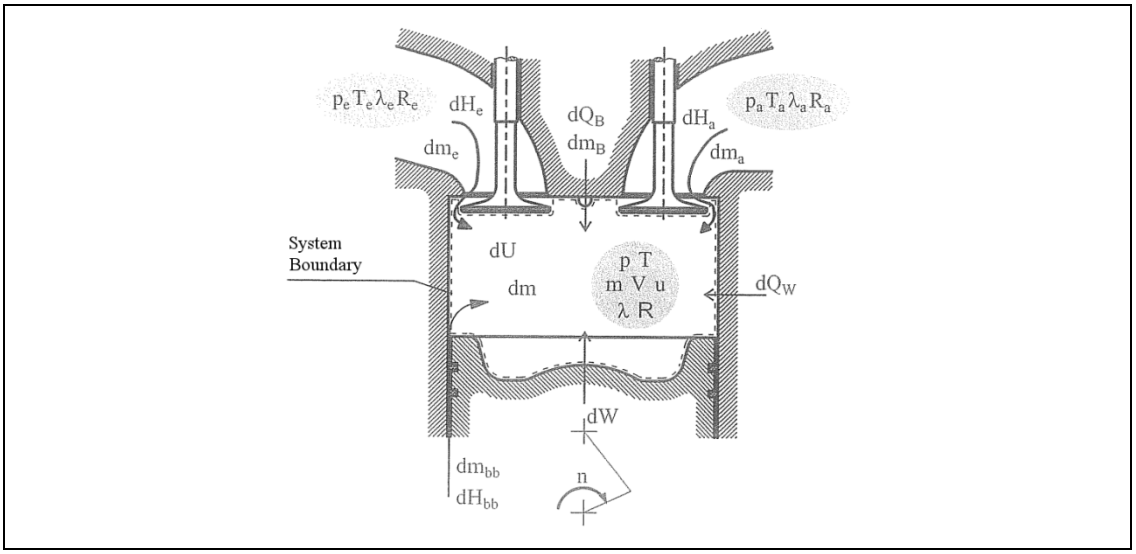

Figure 4-1: Cylinder model with 1 zone

The combustion chamber can be considered as 1 homogeneous zone (Figure 4-1) or can be divided into 2 or more zones. As Figure 4-2 illustrates, models with 2 zones divide the combustion chamber mostly into burned and unburned gases.

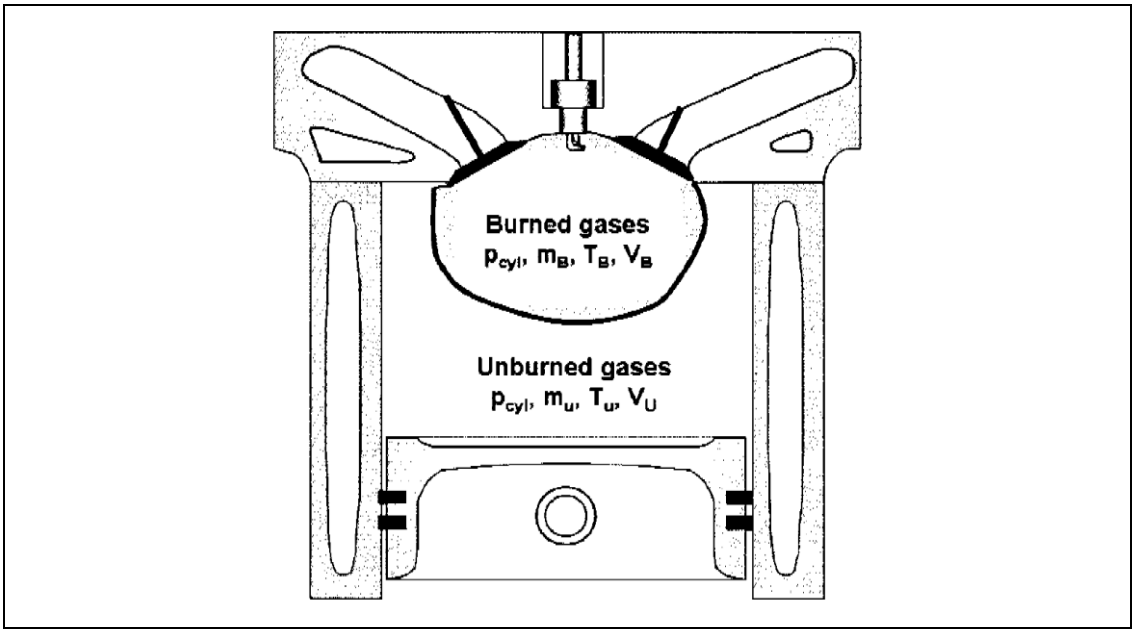

Figure 4-2: Cylinder model with 2 zones (Lämmle, 2006)

4.1.2 Quasi-Dimensional Models

Quasi-dimensional models are zero-dimensional calculations which consider spatial phenomena and geometric data. Therefore, spatial variables are implemented as a function of time.

4.1.3 One- and Multidimensional Models

One- and multidimensional models describe the dependence of variables from one or more spatial coordinates respectively. Due to the increasing computational power, 3 dimensional models become more and more important. CFD (Computational Fluid Dynamics) use numerical methods based on the Navier-Stokes equations to solve problems with fluids involved. In the area of combustion engines, so called 3D-CRFD (Computational Reactive Fluid Dynamics) are used.

Compared to zero-dimensional and quasi-dimensional approaches these models are much more sophisticated and can simulate flows of gases and

liquids, heat and mass transfer, moving bodies, multiphase physics, chemical reactions, fluid-structure interaction and acoustics through computer modeling (fluent.com, 2009). Hence, the disadvantages of this method are the higher effort which is needed to design the models and the much higher computational time compared to zero- or quasi-dimensional models.

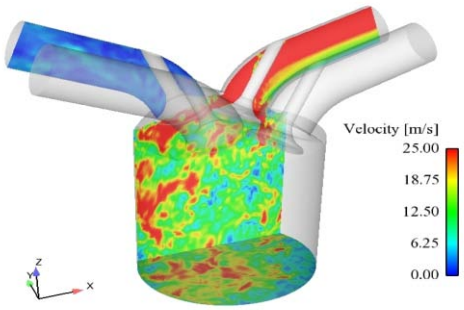

Figure 4-3: Example for a 3D-CFD model

4.2 Models for the Combustion Process

The combustion process describes the time dependent heat release in the combustion chamber. In order to model this process, substitution combustion processes like Vibe or phenomenological models (which precalculate the combustion process based e.g. on the injection rates) are used. Since the complexity of combustion procedures has increased (fuel stratified injection, multiple injections), numerical methods to describe the heat release have gained importance. The so called neural networks have to be trained with measurement results and are then able to find an adequate function for describing the heat release.

4.2.1 Vibe

Based on triangular burn rate functions Vibe (1970) has stated Formula 4-1 to describe the burned fuel fraction of the combustion process.

$$\frac{Q_B(\varphi)}{Q_{B,ges}} = 1 - e^{-a\left(\frac{\varphi-\varphi_{BB}}{\Delta\varphi_{BD}}\right)^{m+1}} \quad with \;\; \varphi_{BB} \leq \varphi \leq \varphi_{BB} + \varphi_{BD}$$

Formula 4-1: Burned fuel fraction according to Vibe

The heat release due to the combustion of the fuel in the combustion chamber can be calculated with the product of the fuel mass fraction in the combustion chamber and the lower heating value as Formula 4-2 shows.

$$Q_{B,ges} = m_B * H_u$$

Formula 4-2: Heat release

At the end of the combustion process, a certain percentage $\eta_{u,ges}$ of the energy provided from the fuel is meant to be realized. So $\eta_{u,ges}$ is called the degree of realization and can be calculated with Formula 4-3 (Merker, Schwarz, Stiesch, & Otto, 2004).

$$\eta_{u,ges} = \frac{Q_B(\varphi)}{Q_{B,ges}} \Big|_{\varphi=\varphi_{BB}} = 1 - e^{-a}$$

Formula 4-3: Degree of realization

In order to adjust the real burn rate graph to the Vibe-model, the 3 parameters *start of combustion*, *end of combustion* and the form factor *m* have to be determined. This can be done manually with help of mathematical procedures like the least square fit method. It is important that vital values like the maximum pressure, the indicated mean effective pressure and the temperature of exhaust gases of the Vibe-model have to correspond with the real data. Figure 4-4 shows the Vibe functions with different values for the form factors *m*.

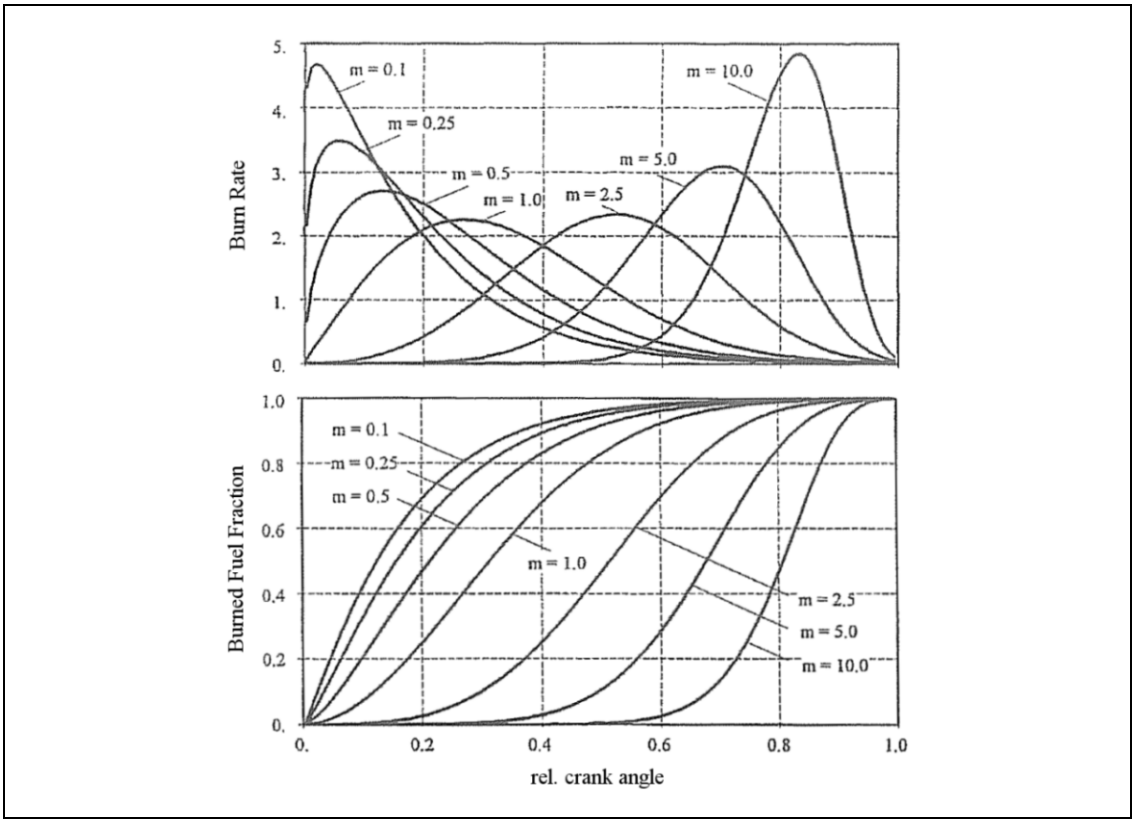

Figure 4-4: Vibe functions according to different form factors *m*
(Merker, Schwarz, Stiesch, & Otto, 2004)

4.2.2 Neural Networks

Because of the rising complexity of combustion processes (gasoline direct injection, pre- and post injections, fuel stratified injection etc.), simple substitution combustion processes like Vibe are not accurate enough anymore in order to describe all details.

Artificial Neural Networks (ANNs) are inspired by the way how biological nervous systems, such as the brain, process information. It is composed of a large number of highly interconnected processing elements (neurons). An ANN is configured for a specific application, such as pattern recognition through a learning process (Stergiou & Siganos).

Also, combustion processes can be calculated with neural networks. For instance, the Vibe-process can be combined with ANNs, which can be trained on finding the right Vibe-parameters based on experimentally determined combustion processes. One disadvantage of ANNs is that their

results are just valid in areas which have been in the training process. Extrapolation is not possible or will cause wrong results.

4.2.3 Entrainment Model

The Entrainment model was developed by Blizard and Keck (1976) and improved by Tabaczinsky (1980). This model is often used to compute heat release and flame propagation in SI engines. The model is based on physical dependencies and considers in-cylinder flows, the change of geometry, heat transfers and chemical reactions in order to calculate the combustion process. Figure 4-5 shows the basic principle of the entrainment model. The flame is propagating spherically from the spark plug until it interacts with the combustion chamber walls.

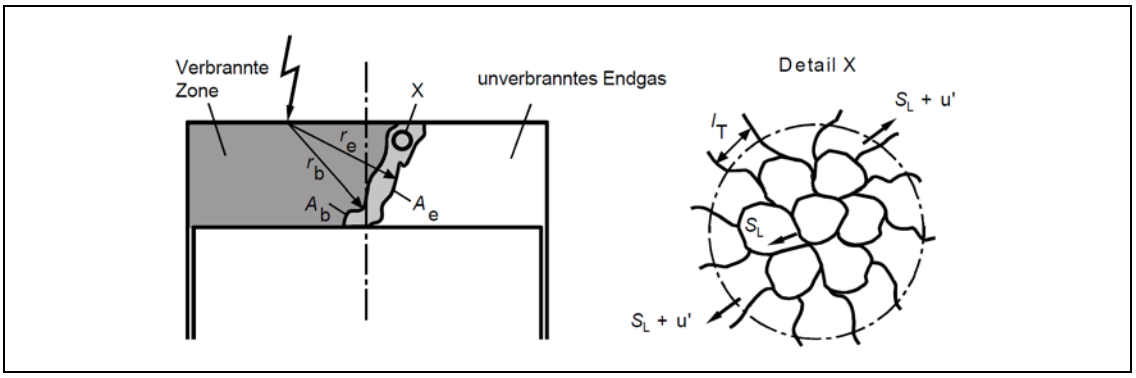

Figure 4-5: Basics of the entrainment model (Pischinger et al. 2002)

The entrainment model uses two separated processes to model the combustion. The first one describes the flame capturing (entraining) the unburned air-fuel mixture according to Formula 4-4 where ρ_u is the density of the unburned zone, A_T the turbulent flame surface and S_T the turbulent flame speed.

$$\frac{dM_e}{dt} = \rho_u * A_T * S_T$$

Formula 4-4: Entrained mass

Damköhler (1940) stated that the wrinkling of the flame front leads to an enlargement of the flame surface and thus calculates the turbulent flame

speed as sum of the laminar flame speed and the turbulent intensity u' according to Formula 4-5.

$$S_T = S_L + u'$$

Formula 4-5: Turbulent flame speed

The second process describes burn up process according to Formula 4-6. The entrained (M_e) but unburned ($M_e - M_b$) mass burns during the characteristic burn time τ, which is determined by the Taylor length scale λ, the laminar flame speed and a constant *C* (Nefischer, 2009).

$$\frac{dM_b}{dt} = \frac{(M_e - M_b)}{\tau} \; with \; \tau = C * \frac{\lambda}{S_L}$$

Formula 4-6: Burn up process

4.3 Turbulence Model

For the used entrainment models, the modeling of turbulence is very important, because it significantly affects the turbulent flame speed and thus the whole combustion process.

The k-ε turbulence model is frequently used in literature and was developed by Borgnakke et al. (1980). They observed that the flow field is inhomogeneous and anisotropic during the intake cycle but homogeneous and isotropic during the compression phase next to the top dead center.

Based on these observations, they proposed the following two equations to calculate the turbulent kinetic energy k and the turbulent rate of dissipation ε (Nefischer, 2009).

$$dk = \frac{2}{3}(1 + a)k\frac{d\rho}{\rho} - \varepsilon + F_k$$

Formula 4-7: Turbulent kinetic energy

$$d\varepsilon = \frac{4}{3}\varepsilon\frac{d\rho}{\rho} - C_2\frac{\varepsilon^2}{k} + F_\varepsilon$$

Formula 4-8: Turbulent rate of dissipation

The coefficient a considers anisotropy, the terms F_k and F_ε describe the transport of turbulent values between the zones at models with more than one zone.

For the use in Diesel engines with direct injection, Pivec (2001) used the basic approach of Borgnakke et al. (1980) and extended it by a term for the injected fuel mass m_k, which is brought in with the flow velocity u_k and leads to Formula 4-9 (Nefischer, 2009).

$$dk = \frac{2}{3}(1+a)k\frac{d\rho}{\rho} - \varepsilon + \frac{\dot{m}_k}{m}u_k$$

Formula 4-9: Turbulent kinetic energy according to Pivec (2001)

4.4 Investigated Entrainment Models

Both investigated models, the SI Turbulent Flame Combustion Model and the Nefischer User Model, use the entrainment concept and will be described in the following chapters. Due to the fact that the SI Turbulent Flame Combustion Model is a proprietary model of Gamma Technologies, a lot of information regarding the exact processes and formulas used are retained, thus giving the model a black-box-character. The following information was accessible in user manuals and the website (www.gtisoft.com).

4.4.1 SI Turbulent Flame Combustion Model (GT-Power)

The SI Turbulent Flame Combustion Model from GT-Power is an Entrainment model (4.2.3) and based on the propagation of flames due to turbulent cylinder flows. The template is called “EngCylCombSITurb”. It takes the cylinder geometry, air motion, spark timing and fuel properties into account. Via the submodel “EngCylFlame”, the location of the spark plug and geometry data of the combustion chamber can be defined. Additionally, STL-files (exported from CAD) can be included if the head and piston do not have

simple dome and cup geometries. The computational time for the SI Turbulent Flame Combustion Model is substantially higher than for non-predictive models like the Vibe combustion model, which is also integrated in GT-Power.

Based on predefined spark timing, spark size, spark position and parameters for the laminar and turbulent flame speed, the model is used to predict in-cylinder burn rates for spark-ignited engines. It is well suited for homogenous air-fuel mixtures but may be used to impose non-homogeneous air-fuel mixtures (with the attribute “Entraining Mixture Phi”) for direct injected engines as well. The following equations describe the mass entrainment rate into the flame front and the burn-up rate with the time constant τ (Gamma Technologies Inc., 2006).

$$\frac{dM_e}{dt} = \rho_u A_e (S_T + S_L)$$

Formula 4-10: Mass entrainment rate into the flame

Formula 4-10 states that the unburned fuel-air mixture is entrained into the flame front through the flame at a rate proportional to the sum of the laminar and turbulent flame speed. Formula 4-11 indicates that the burn-up rate is proportional to the amount of unburned mixture behind the flame front divided by the time constant τ.

$$\frac{dM_b}{dt} = \frac{(M_e - M_b)}{\tau} \; mit \; \tau = \frac{\lambda}{S_L}$$

Formula 4-11: Burn-up rate

4.4.1.1 Turbulence Model

The modeling of turbulence is done by the reference object “EngCylFlow”, which is used to calculate the in-cylinder flow velocity and turbulent intensity. As Figure 4-6 shows, it divides the cylinder into 4 regions.

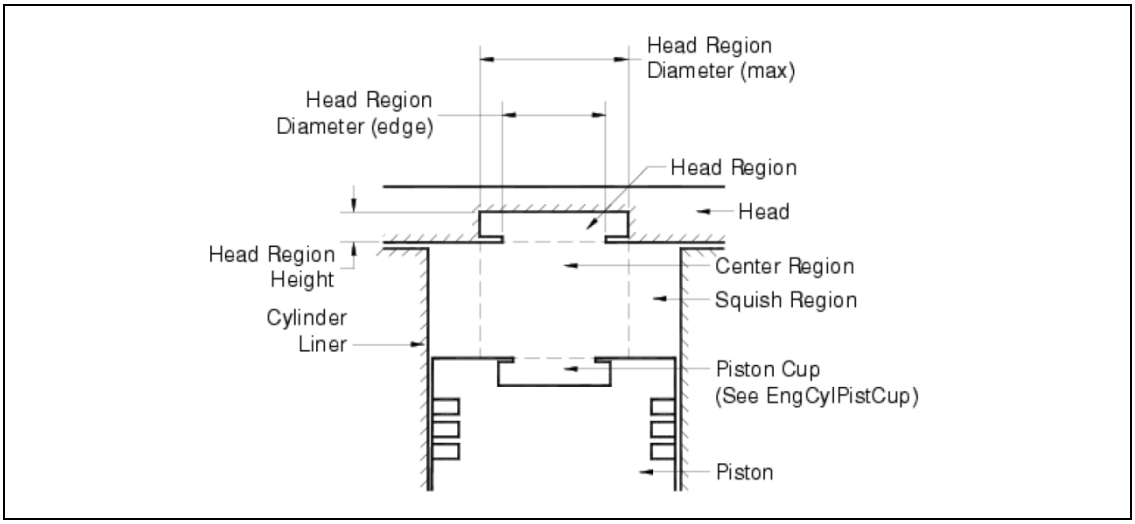

Figure 4-6: 4 regions of the cylinder

Taking into account the cylinder chamber geometry, the piston motion, flow rate, swirl and tumble of the incoming and exiting gases through the valves, the model calculates the mean radial velocity, axial velocity and swirl velocity for each time step in each region. Then it solves the equations for turbulence kinetic energy and turbulence dissipation rate and uses these results to calculate instantaneous mean turbulence intensity and turbulence length scale (Gamma Technologies Inc., 2006).

4.4.1.2 Flame Speed

The laminar flame speed is calculated as stated in the GT-Power User Manual according to Formula 4-12. It considers the maximum laminar flame speed for the used fuel, pressure, temperature and the influence of dilution.

$$S_L = \left(B_M + B_\phi(\phi - \phi_m)^2\right)\left(\frac{T_u}{T_{ref}}\right)^{\alpha}\left(\frac{p}{p_{ref}}\right)^{\beta}(1 - 2.06 * Dilution^{DEM*0.77})$$

Formula 4-12: Laminar flame speed

The turbulent flame speed was not stated explicitly by Gamma Technologies but they referred to the work of Morel et al. (1988) and Wahiduzzaman et al. (1993). Their assumption was that the unburned gas entrainment rate is limited by the laminar flame speed when the flame kernel is small. With growing size of the flame the turbulence induced component starts dominating the rate of the flame propagation. Thus, the turbulent flame speed

can be calculated according to Formula 4-13, considering the turbulence intensity u', which is calculated from the object "EngCylFlow", flame radius R_f, turbulent length scale L_t and 2 constants (C_s depending on the fuel type and C_k regarding the flame kernel growth).

$$S_T = C_s * u' * \left(1 - \frac{1}{1 + C_k * \frac{R_f^2}{L_t^2}}\right)$$

Formula 4-13: Turbulent flame speed

4.4.1.3 Settings

Additionally, the model offers five different data tabs, which allow the adjustment of several parameters as described in Table 4-1.

Data tab	Purpose, Parameters
Main	Defines the location, timing and size of the spark. Additionally, there is a parameter "Entraining Mixture Phi", which specifies the equivalence ratio at the flame front as a function of the mass fraction of burned fuel (only needed for stratified-charge operation).
LamSpeed	Defines the settings for the laminar flame speed considering different parameters like the fuel type, a maximum speed, dilution etc. Alternatively a user model can be implemented.
TrbSpeed	Defines the settings for the turbulent flame speed with factors for the flame speed, kernel growth rate and taylor length scale. Alternatively a user model can be implemented.
Advanced	The standard knock model from GT-Power can be used and calculations for NO_x, CO and HC can be added to the simulation.
Startup	In order to improve the computation time, a simple burn curve (Vibe), which can be defined with this tab, can be imposed for the initial cycles of the simulation.

Table 4-1: Parameters of the SI Turbulent Flame Combustion Model

4.4.2 Nefischer User Model

This chapter describes the basic structure and formulas of the User Model, which was developed by Nefischer (2009) and implemented as FORTRAN Code. Basically, it is based on the entrainment model (4.2.3) and uses approaches from Heywood (1988) for the laminar flame speed and Gülder (1990) for the turbulent flame speed.

4.4.2.1 Turbulence Model

The turbulence model is based on the k-ε turbulence model (chapter 4.3). Based on the work of Pivec (2001), Schubert et al. (2005) proposed to approximate the turbulent length scale by the cube root of the cylinder volume and to drop the differential equation for the turbulent rate of dissipation. According to this approach, the following formulas are used in the model.

$$dk = \frac{2}{3}(1+a)k\frac{d\rho}{\rho} - c_{diss}\frac{k^{\frac{3}{2}}}{l_T}$$

$$l_T = c_L\sqrt[3]{V_{zyl}}$$

Formula 4-14: Turbulent kinetic energy and turbulent length scale according to Schubert et al. (2005)

4.4.2.2 Flame Propagation

The spherical flame propagation is basically divided into 2 parts, one which calculates the flame surface from the flame center going towards the cylinder head and one towards the piston. The flame center position can be defined with the excentricity *exc* and the vertical position *vert* according to Figure 4-7.

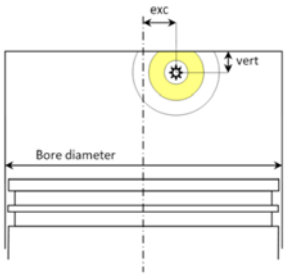

Figure 4-7: Excentricity *exc* and vertical position *vert* of the flame center

4.4.2.3 Flame Speed

The calculation of the laminar flame is done according to Heywood (1988), who stated the following Formula 4-15.

$$S_L = S_{L0}\left(\frac{T_{zyl}}{T_{ref}}\right)^{\alpha}\left(\frac{p_{zyl}}{p_{ref}}\right)^{\beta}(1-\gamma * f)$$

Formula 4-15: Laminar flame speed

S_{L0}, α, β and γ are constants considering different fuels, equivalence ratio and burned gas diluents fraction.

Taking a look at the burning velocity for different fuel types, they all show a peak slightly above the stoichiometric ratio. This fact is included in the calculation of S_{L0}, with a maximum value B_m and a negative value B_ϕ, which is multiplied with the square of the deviation from the equivalence ratio ϕ_m at B_m.

$$S_{L0} = B_m + B_\phi(\phi - \phi_m)^2$$

Formula 4-16: Laminar flame speed depending on equivalence ratio

The factor f in Formula 4-15 represents dilution and has been implemented according to Formula 4-17 (identical to the SI Turbulent Flame Combustion Model).

$$\mathrm{f} = \mathrm{Dilution}^{\mathbf{dilution_{exp}}*\mathbf{0.77}}$$

Formula 4-17: Dilution exponent in the User Model

Combining Formula 4-15 and Formula 4-16 leads to the same approach to calculate the laminar flame speed as used for the SI Turbulent Flame Combustion Model (Formula 4-12).

The turbulent flame speed is calculated according to Nefischer (2009), who modified an approach by Gülder (1990) and stated Formula 4-18.

$$S_T = a * S_L * Re^{\frac{1}{4}} + b * u' * Da^{\frac{1}{4}}$$

$$Re = \frac{l_T}{\delta_L} * \frac{u'}{S_L}$$

$$Da = \frac{l_T}{\delta_L} * \frac{S_L}{u'}$$

Formula 4-18: Turbulent flame speed according to Nefischer (2009)

It considers the Reynolds- and Damköhler-number (Re, Da) and the type of flames, which can be represented in the Peters/Borghi-Diagram.

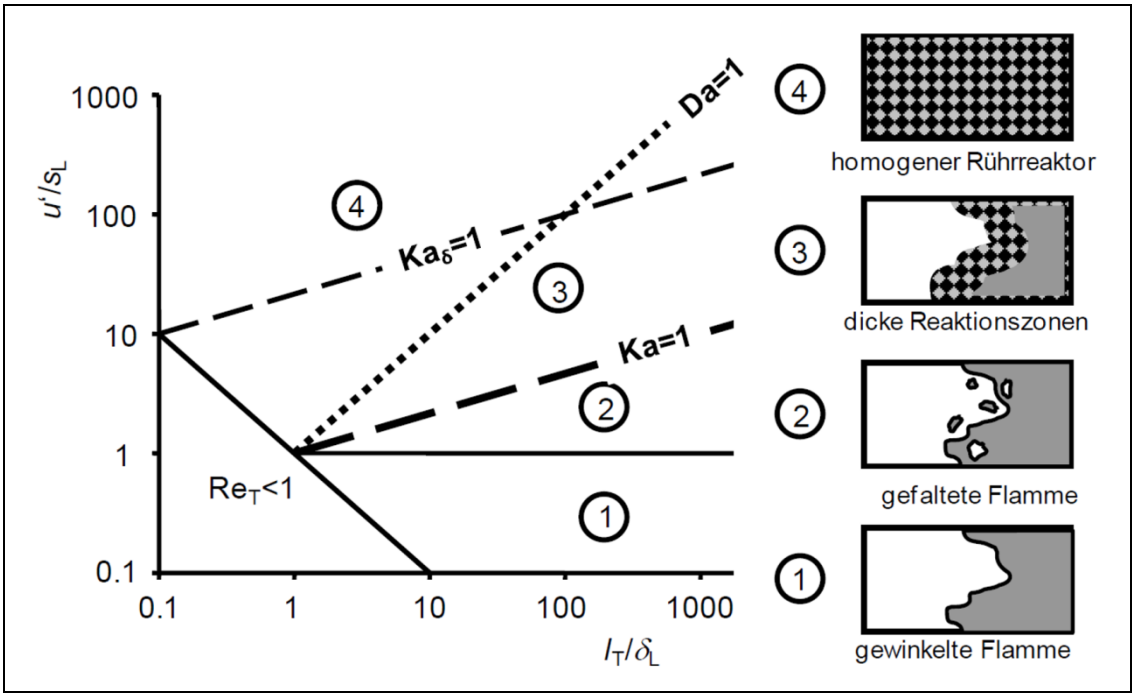

Figure 4-8: Peters/Borghi-Diagram according to Messner (2007)

Depending on the the type of flames, a and b have the following relation (Nefischer, 2009):

- Wrinkled flamelets (zone 1, e.g. H_2) a > b
- Corrugated flamelets (zone 2) a ~ b
- Thick reaction zone (zone 3) a < b

The flames of gasoline are between zone 2 and 3. Investigations of Nefischer (2009) showed that a relation of $a: b \approx 1:2$ can be seen as reasonable for gasoline and therefore can be used for the optimization process within this work.

4.4.2.4 Initial Kernel Growth – Ignition Delay

For modeling ignition delay, there are basically 2 concepts. The first one is to consider the initial kernel growth. It is assumed that the flame is propagating laminar at the beginning and that the turbulence plays a key role as soon as the flame exceeds a certain radius.

The following correlation stated by Lipatnikov and Chomiak (2002) defines the relation of the adjusted ($S_{T,k}$) to the original turbulent flame speed.

$$\frac{S_{T,k}}{S_T} = \sqrt{1 + \frac{\tau}{t} * \left(e^{-\frac{t}{\tau}} - 1\right)} \quad with \quad \tau = C * \frac{l_T}{u'}$$

Formula 4-19: Initial kernel growth

Figure 4-9 shows the development of the adjusted turbulent flame speed, which has a steep rise at the beginning and then slowly converges to 100% of turbulent flame speed.

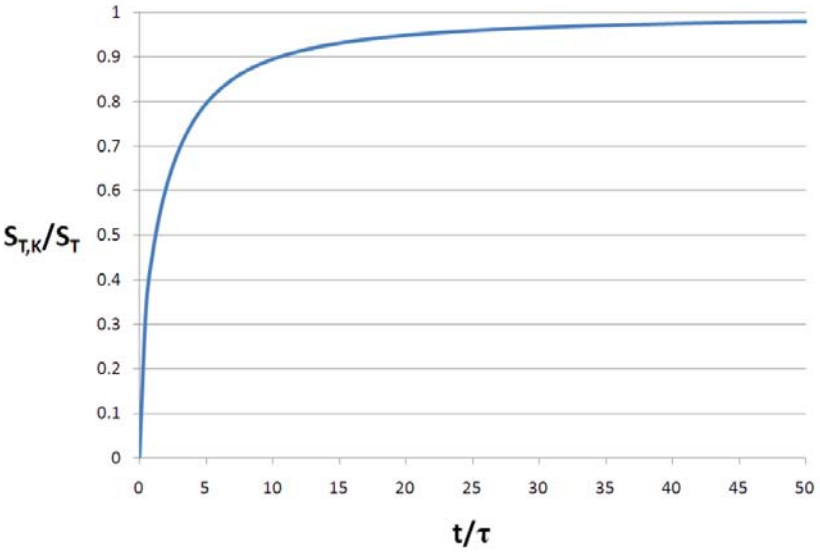

Figure 4-9: Relation of adjusted and original turbulent flame speed

Figure 4-10 illustrates that with an increase of parameter C and thus τ the combustion process starts at the same point, but the effects of turbulent flame speed are delayed.

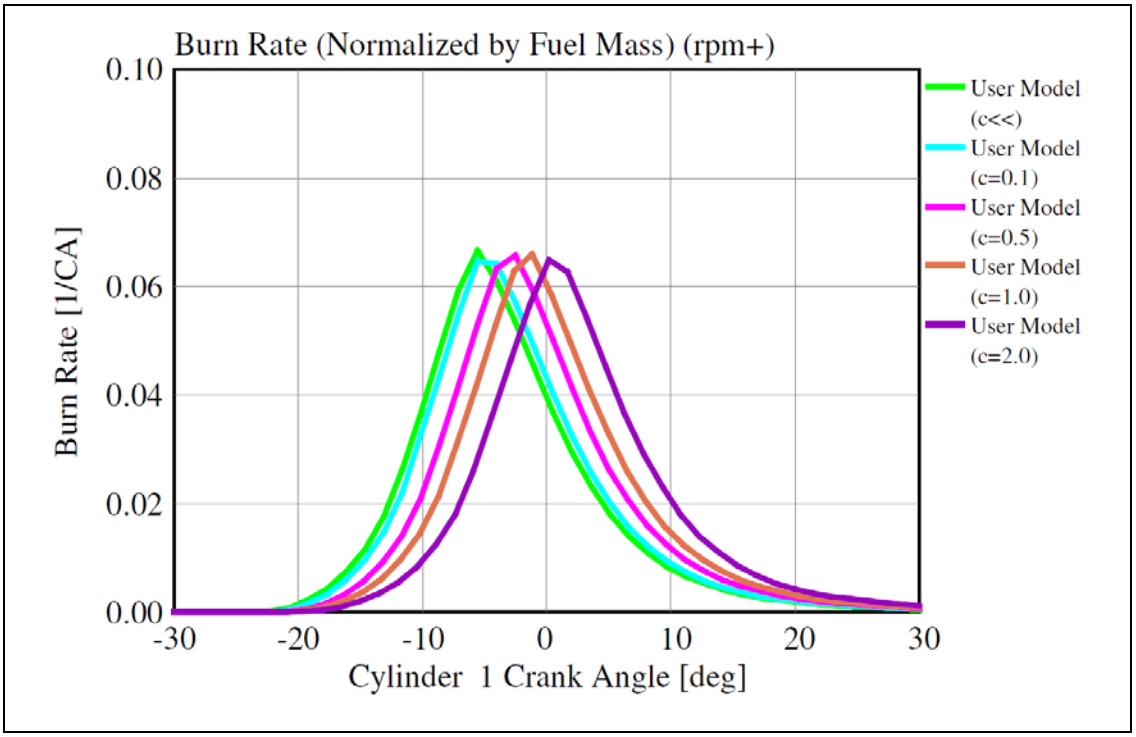

Figure 4-10: Comparison of burn rates with different values for *C*

The second concept is based on the integration of the term $1/\tau$ (where τ represents the ignition delay time), until it reaches a certain threshold value and arises from approaches to model knocking occurrences and auto-ignition (HCCI). Then, the combustion starts with full turbulent flame speed.

Livengood and Wu (1955) stated Formula 4-20, where knocking occurs if the integral reaches the threshold value 1.

$$\int \frac{1}{\tau} dt = 1$$

Formula 4-20: Integration of an ignition delay time

The ignition delay time τ is based on an approach according to Arrhenius depending on pressure, temperature and a constant A (Formula 4-21).

$$\tau = A * p^z * e^{\frac{T_a}{T}}$$

Formula 4-21: Arrhenius-approach for ignition delay time

This approach was extended by Jobst et al. (2005), as shown in Formula 4-22. c_{O_2} and c_K represent the concentration of oxygen and fuel in the cylinder.

$$\frac{1}{\tau} = r_A = A_{Arr} * {c_{O_2}}^x * {c_K}^y * p^a * e^{\frac{-T_a}{T}}$$

Formula 4-22: Extended approach for ignition delay time

Investigating the relation of ignition delay and total residuals at combustion start showed a clear correlation between them. Figure 4-11 and Figure 4-12 show the correlation of the ignition delay for both engines (from ignition point IP to 2% BFF and to 10% BFF) as a function of the total residuals.

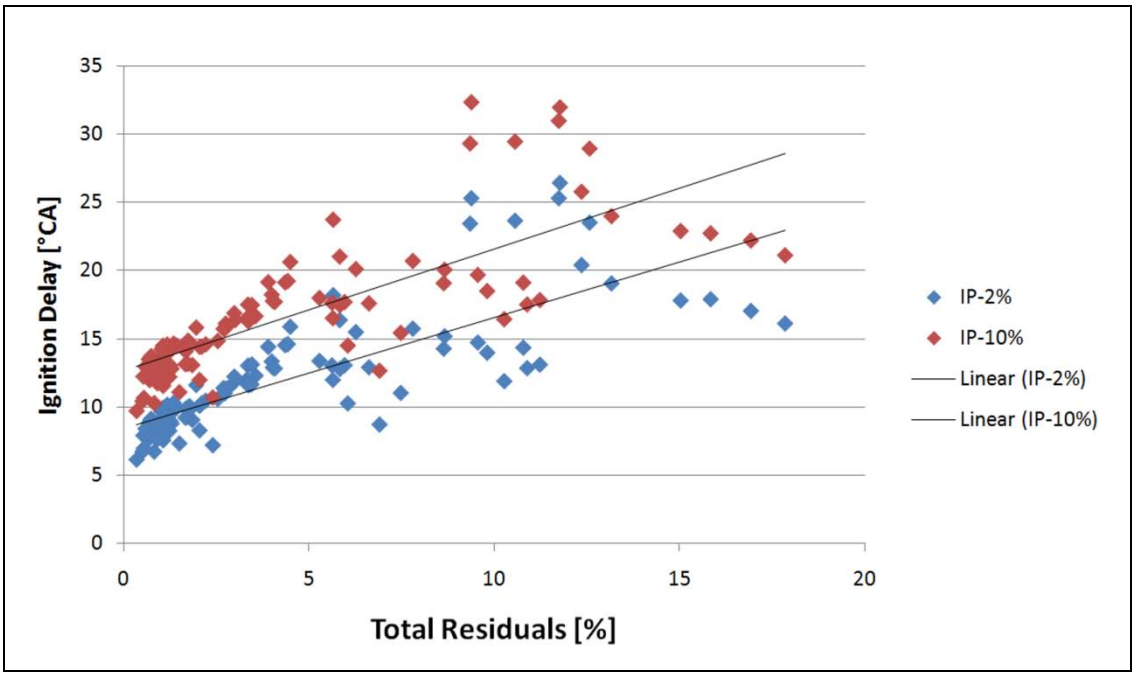

Figure 4-11: Correlation ignition delay and total residuals (Highly Turbocharged TGDI)

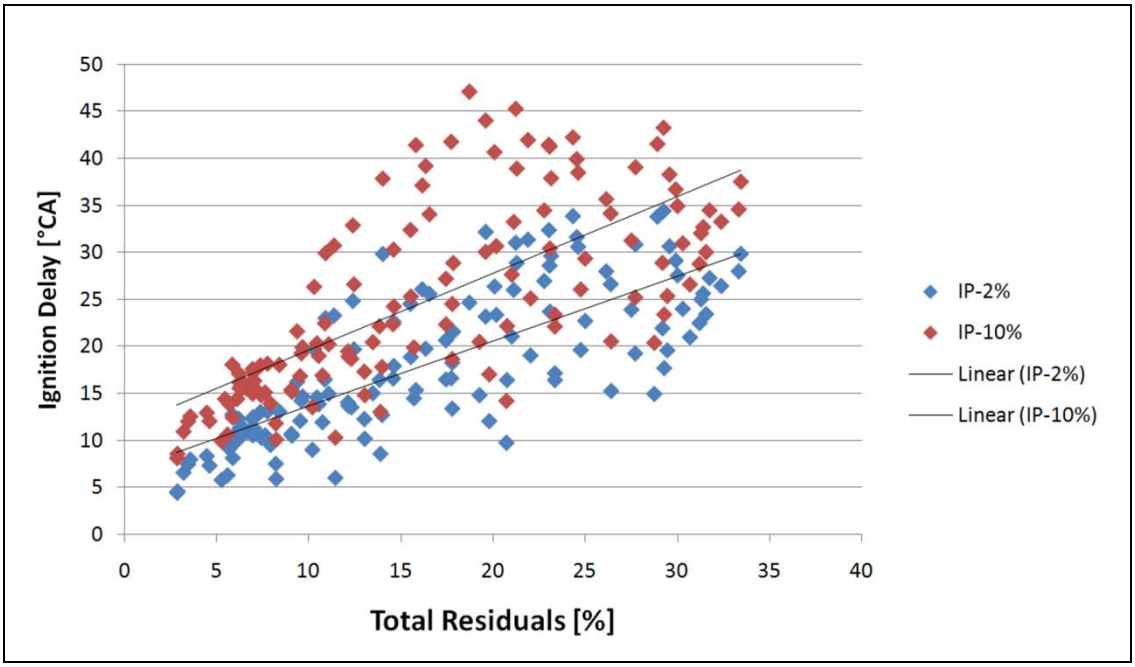

Figure 4-12: Correlation ignition delay and total residuals (TVDI)

Additionally, Chmela et al. (2006) proved that also the turbulence has an influence on the ignition delay

Considering these different aspects, the following ignition delay model has been implemented in the User Model:

$$\int \frac{1}{\tau} dt = 1$$

$$\tau = \frac{A * {c_{RG}}^{y} * p^{z} * e^{\frac{T_a}{T}}}{k^{x}}$$

Formula 4-23: Implemented ignition delay model

c_{RG} represents residual gases and k the turbulent kinetic energy in the combustion chamber. Figure 4-13 shows the impact of the implemented ignition delay model when the constant A increases. As soon as the threshold value is passed, the combustion process starts with full turbulent flame speed (i.e. without initial kernel growth).

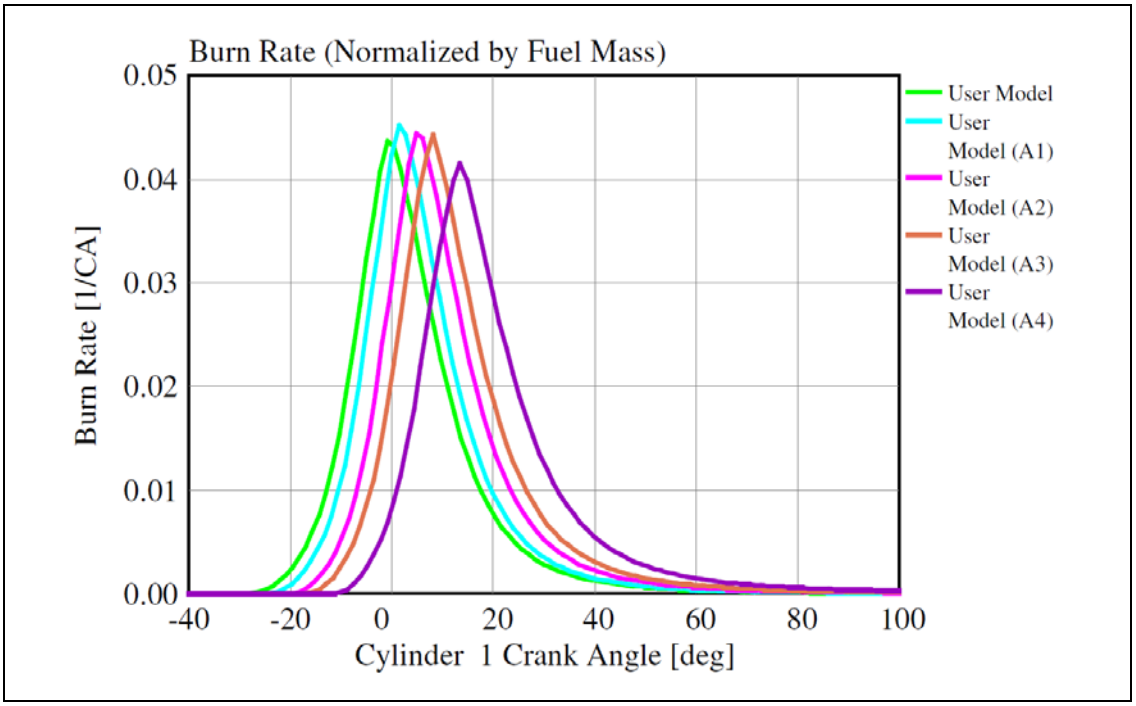

Figure 4-13: Comparison of burn rates with different values for *A*

4.4.2.5 Structure of the User Model in FORTRAN

The implementation of the User Model is basically done by the use of a dynamic linked library file (dll), which is created by the FORTRAN compiler. GT-Power calls the subroutine ENGCOMBUSER, if this option has been chosen in the settings. In this subroutine, where the basic code is available from Gamma Technologies and can be modified, a further call of the entrainment model is placed, which itself is structured and divided in different functions as Figure 4-14 shows.

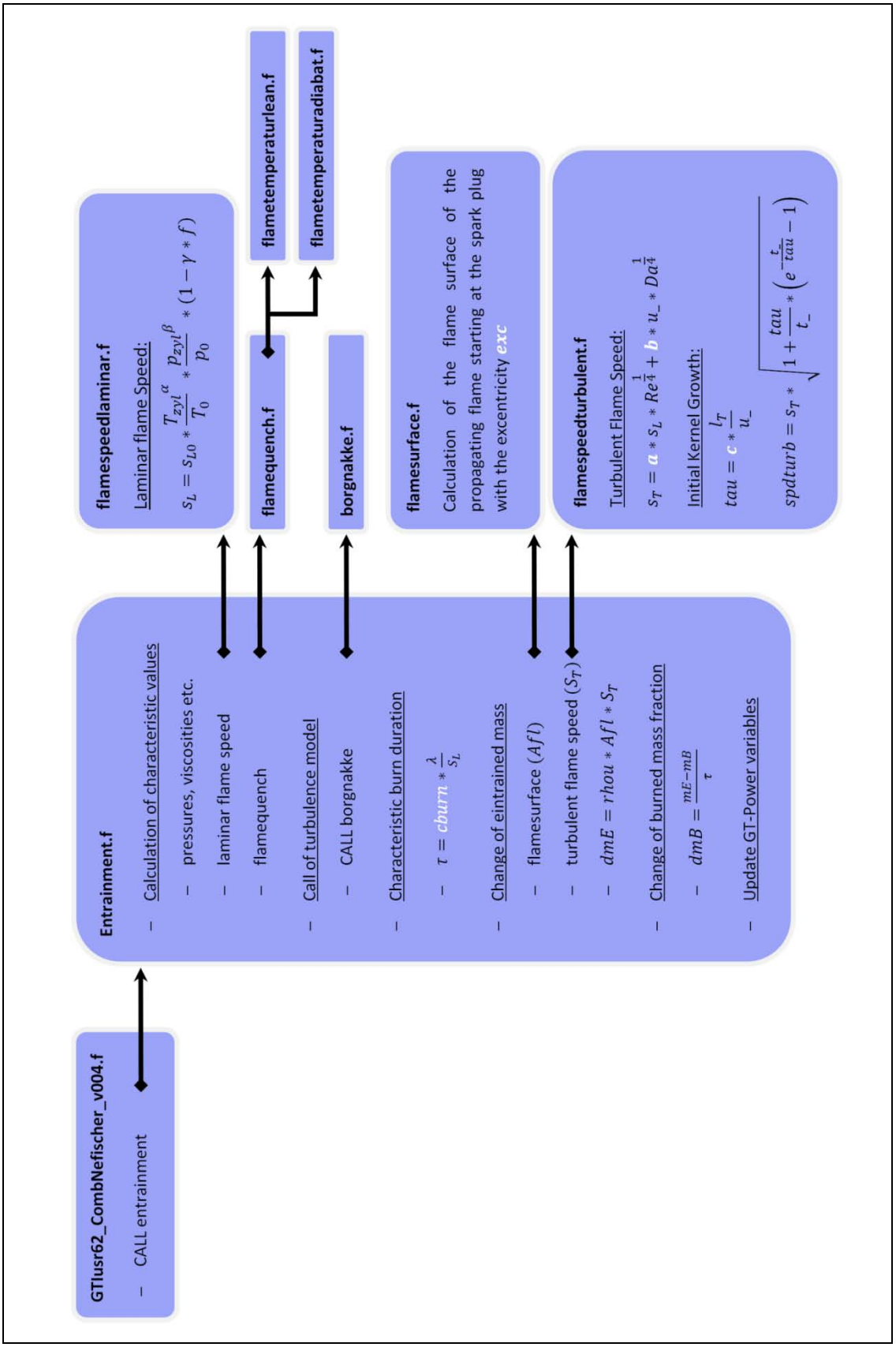

Figure 4-14: Basic structure of the User Model in FORTRAN

4.5 Model Generation and Simulation with the Software GT-Power

GT-POWER is the industry leading engine simulation (sometimes referred to as cycle simulation) tool used by many engine manufacturers worldwide. The software is used to perform a variety of both steady state and transient analyses. Table 4-2 gives examples for main functions of GT-Power (Gamma Technologies Inc., 2009).

Steady state studies	**Transient studies**
• Torque, power, and volumetric efficiency curves for SI and CI engines • Engine downsizing studies • Variable Valve Train simulations • Cylinder pressure analysis • Injection rate shaping for minimum NO_x • Intake and exhaust system acoustics	• Turbocharger response, turbo lag studies • Control system analysis • Air-fuel ratio response • Intake and exhaust system drive-by noise levels

Table 4-2: Examples for GT-Power main functions

If pressure and temperature measurements from an engine test bench are available, the models can be simplified significantly. The measuring points, which are located just before and after the cylinder, represent the boundaries of the simulation model and provide the possibility to perform a pressure trace analysis, the so called “Three Pressure Analysis” in GT-Power (4.5.1). It is not necessary to model the intake and exhaust system of an engine and the focus can be put on the combustion process, which reduces computing time. The second point, which also makes the simulation faster, is to reduce the number of cylinders from 4 or rather 6 to 1. If the response behavior of the turbocharger etc. is supposed to be modeled, these simplifications can not be made. Figure 4-15 shows an exemplary 4-cylinder model with EGR and a simulated muffler.

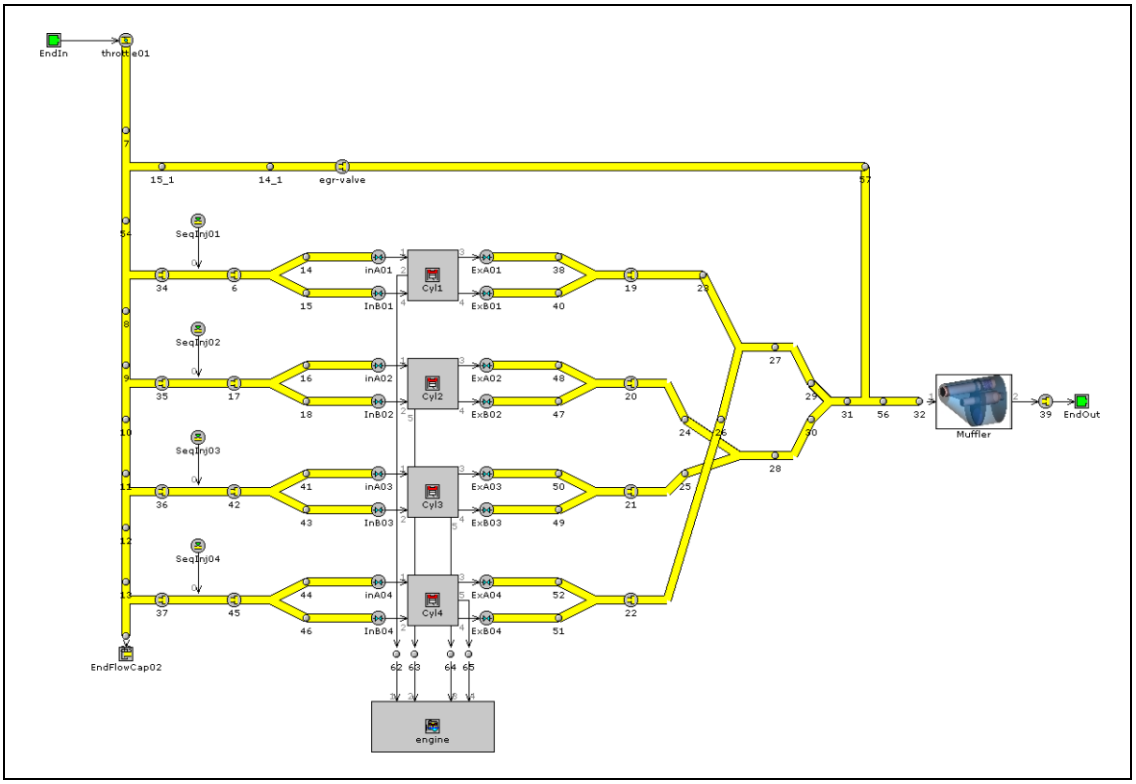

Figure 4-15: 4-cylinder model with EGR in GT-Power

4.5.1 Three Pressure Analysis

GT-Power has an integrated tool to perform a pressure trace analysis (2.4), which is called Three Pressure Analysis (TPA). In this technique, measured instantaneous intake and exhaust pressures (if available from the engine test bench) are used in conjunction with the measured cylinder pressure to determine not only burn rates, but also to compute the exact contents of the cylinder (air flow, residual content, fuel quantity) at the start of combustion (Gamma Technologies Inc., 2009). The TPA has been used to calculate the reference values for the comparison of the combustion models.

4.5.2 Wiring Harness

With the template “Wiring Harness”, GT-Suite can be coupled with the software MATLAB SIMULINK or a user-developed subroutine that is programmed using GT-SUITE’s user functions. It has been used to do parameter optimization processes with the help of MATLAB (5.4.2.1) and also to transfer data from GT-Power to the user model.

As Figure 4-16 shows, the Wiring Harness module in this case has one input, the least square error, which is sent to SIMULINK and three outputs, in this case the three optimization parameters for the SI Turbulent Flame Combustion model, sent from SIMULINK.

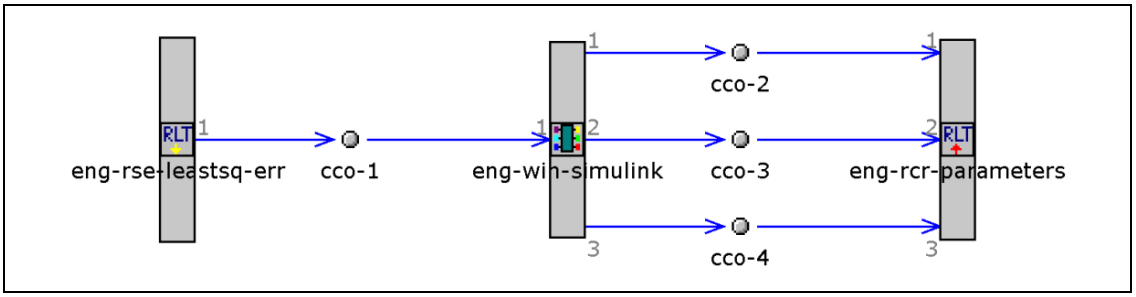

Figure 4-16: Wiring Harness module in GT-Power

4.5.3 Implementation of a User Model

In order to implement user models (e.g. the combustion user model from Nefischer), GT-Suite provides the template “UserModel”. It is used to pass data to a user subroutine, which is located in a dll-file in the corresponding folder where the gtm-file is located, in the case of this thesis created by the FORTRAN compiler. Figure 4-17 shows the combustion object “EngCombUser”, which used the template “UserModel”.

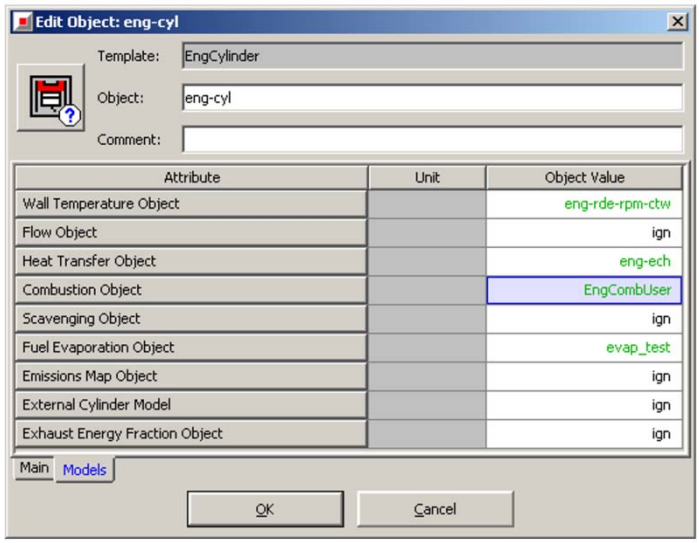

Figure 4-17: Implementation of a user model

4.5.4 Computing Specific Burnt Fuel Fraction Values

GT-Power provides standard values like the crank angle at 50% burned fuel fraction and the burn duration from 10-75%. In order to do more detailed investigations, for instance to analyze the ignition phase and the late stage of combustion, values for 5%, 10%, 75% and 90% burned fuel fraction have been calculated.

Due to the fact that the exact values are not available, but only values next to them, the interpolation block according to Figure 4-18 has been added.

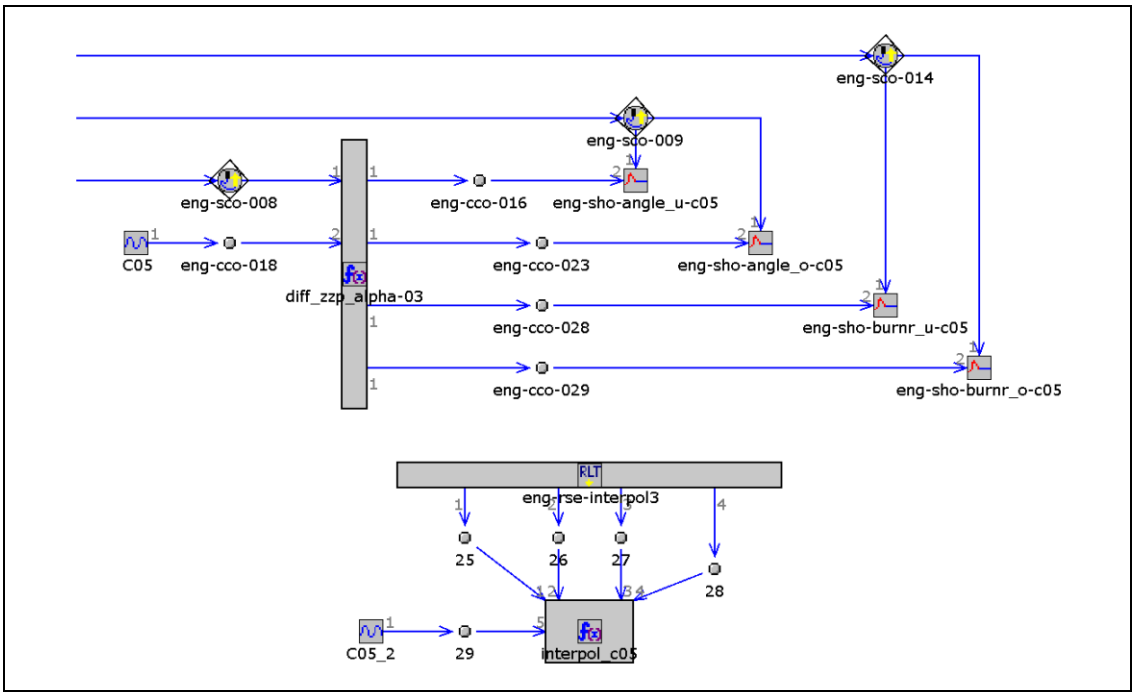

Figure 4-18: Interpolation with GT-Power

This block collects 4 values (2 for crank angle and 2 for burned fuel fraction) just next to the desired value and does an interpolation according to Formula 4-24 (in this case for the crank angle at 5% BFF φ_{05}).

$$\varphi_{05} = \varphi_{05_{low}} + \left(\varphi_{05_{high}} - \varphi_{05_{low}}\right) \times \frac{BFF_{05} - BFF_{low}}{BFF_{high} - BFF_{low}}$$

Formula 4-24: Interpolation for the calculation of the crank angle at 5% burned fuel fraction

5 Simulation Analysis

This chapter describes the procedure of comparing the different combustion models. The basic approach of the comparison was to take the results from the Three Pressure Analysis (4.5.1), which consider measurements from the engine test bench in their calculation, as a reference and to compare them with the SI Turbulent Flame Speed Model from GT-Power and the Nefischer User Model, which have been adjusted first.

5.1 Reference Model

Basically, the TPA has been used as reference model but some adjustments had to be done in order to receive decent results. First results showed a very good match of measured and calculated pressure for most points in the engine performance map (e.g. Figure 5-1).

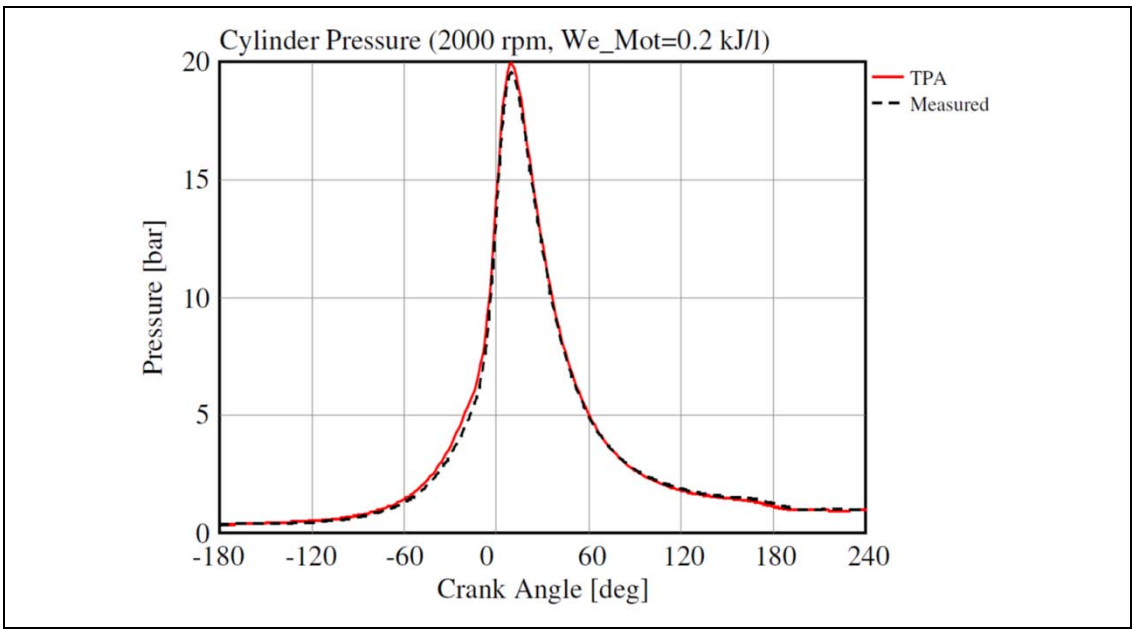

Figure 5-1: Comparison of measured pressure and calculated pressure (TPA)

5.1.1 End of Calculation Override

In order to help avoiding problems caused by noise in the pressure signal, the TPA provides an option called “End of Calculation Override”. It allows defining a certain Crank Angle, where the high-pressure part of the calculations automatically will stop.

After investigating the burn rate function for all points in the engine performance map for the 2 investigated engines, a value of 60°CA seemed to be reasonable and properly working.

5.1.2 Combustion Efficiency Control

As Figure 5-2 shows, jitters in the pressure signal and thus the calculated burn rate of the TPA result in lower combustion efficiencies of around 85-90% (blue curve). This distorts the further analysis and needs to be corrected in order to get a reasonable comparison with the other combustion models. Only with the End of Calculation Override option, this could not be totally corrected.

The settings of the TPA provide an option called “Apply fuel LHV (lower heating value) multiplier”. This option corrects the fuel energy in order to compensate for other inaccuracies in the process (measurement errors etc.). Thus, a good pressure match may be achieved even with major input errors in the calculation (Gamma Technologies Inc., 2009).

According to Formula 5-1, this option corrects H_U in order to realize a target burned fuel fraction of 100% unless other values have been defined (if measurements of unburned fuel in the exhaust gases are available).

$$\eta_u = \frac{\int Q_B(\varphi)}{m_B * H_U}$$

Formula 5-1: Degree of realization

Figure 5-2 shows how this option corrects the burn rate up to nearly 100%, which is vital for the further evaluation and the comparability with the 2 models.

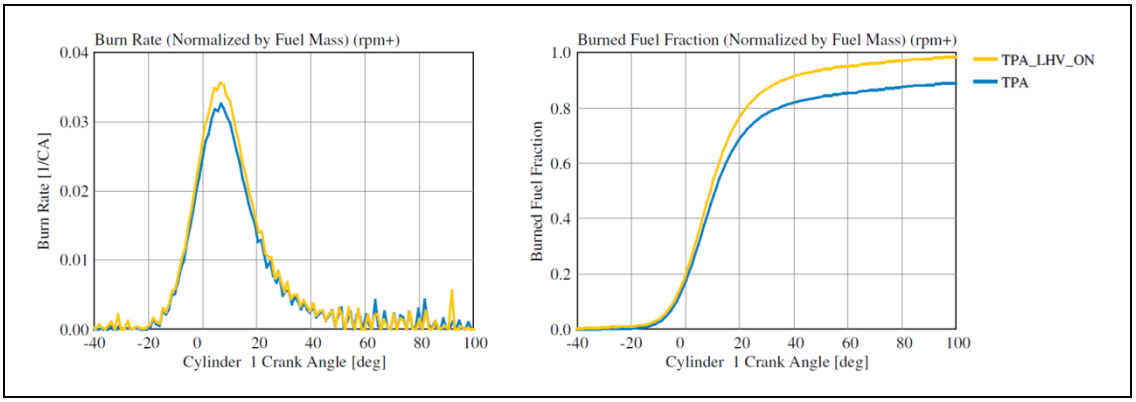

Figure 5-2: Application of the LHV multiplier

In order to consider these corrections in the fuel energy also for the 2 investigated combustion models, the lower heating values for the SI Turbulent Flame combustion model and the User Model have been adjusted according to Formula 5-2.

$$LHV_{new} = LHV_{original} * Fraction\ of\ Fuel\ burned * LHV\ Multiplier$$

Formula 5-2: Adjustment of LHV

By using the End of Calculation Override combined with this option, the TPA showed a proper behavior throughout the entire engine performance map and can be seen as a reliable reference. Figure 5-3 illustrates the behavior of burn rates and burned fuel fraction using once the LHV multiplier only (yellow) and combined with the End of Calculation Override at 60° CA (red).

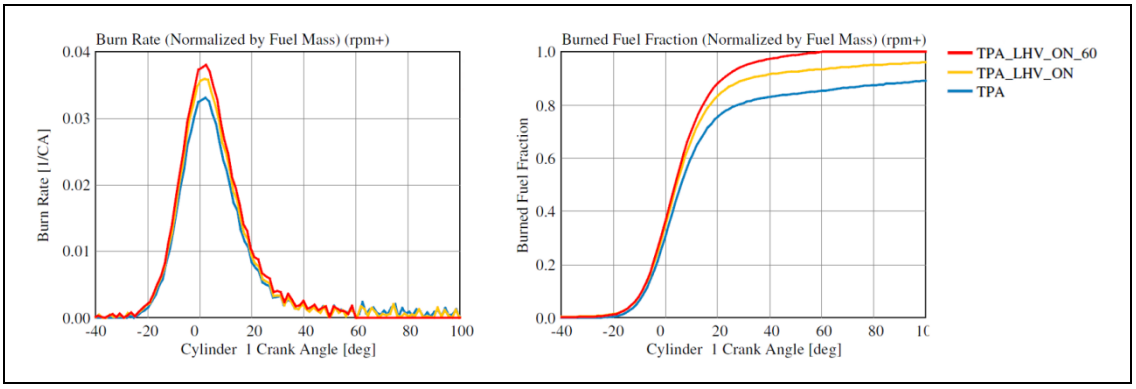

Figure 5-3: Application of the LHV multiplier combined with End of Calculation Override

5.2 Adjustment of the SI Turbulent Flame Combustion Model

The SI Turbulent Flame Combustion Model from GT-Power has several parameters, which need to be adjusted in order to get decent results. Three parameters have been selected (see 5.2.1) and after a manual pre-adjustment the further optimization has been done with the help of MATLAB (5.4.2.1).

5.2.1 Optimized Parameters

The SI Turbulent Flame Combustion Model from GT-Power has a lot of different parameters. Some of them are redundant and it would exceed the timeframe to adjust all of them. Former investigations from Busch (2007) and Madel (2008) brought up information about the importance of parameters and provided suggestions for starting values of the optimization process.

So, the focus has been on the following three parameters:

- **Turbulent Flame Speed Multiplier (TFM):** is used to scale the calculated turbulent flame speed or the name of a dependency reference object. It influences the overall duration of combustion. The larger the number, the higher the speed of combustion (default value = 1.0).
- **Dilution Exponent Multiplier (DEM):** is used to scale the effect of dilution (residuals and EGR) on the laminar flame speed or the name of a dependency reference object. Increasing this value will reduce the effect of dilution on the laminar flame speed and increase the burn rate (default value = 1.0).
- **Flame Kernel Growth Multiplier (CK):** is used to scale the calculated value of the growth rate of the flame kernel or the name of a dependency reference object. This variable influences the ignition delay. The larger the number, the shorter the delay, advancing the transition from laminar combustion to turbulent combustion (default value = 1.0) (Gamma Technologies Inc., 2006).

5.3 Adjustment of the Nefischer User Model

The Nefischer User Model also has a lot of parameters. The most important one, which has to be adjusted before a further optimization, is the turbulent kinetic energy (TKE). If TKE has been matched with CFD-data, an optimization process for the other parameters including the ignition delay can be started.

5.3.1 Turbulent Kinetic Energy

The turbulent kinetic energy is a very important parameter in the User Model and needs to be adjusted before further optimizations with MATLAB can be done. It is calculated within the turbulence sub-model (see 4.4.2.1). The change of turbulence can be described with Formula 5-3 (Nefischer, 2009).

$$Change\ of\ turbulence = Production + Diffusion - Dissipation$$

Formula 5-3: Change of turbulence

TKE values for several points in the engine performance map were available from CFD calculations (e.g. Figure 5-4 shows the TKE progress for 5500 rpm for the Highly Turbocharged TGDI).

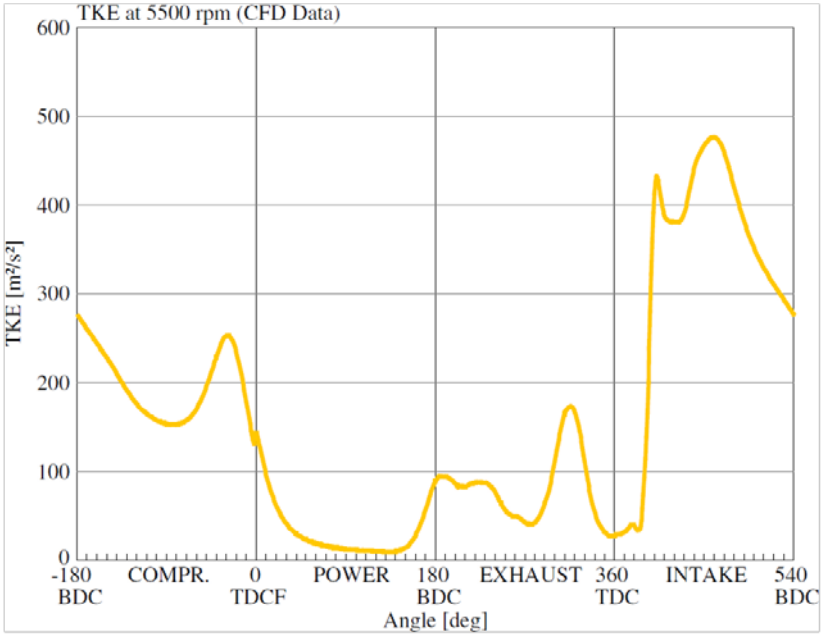

Figure 5-4: TKE progress at 5500rpm (CFD Data)

5.3.1.1 TKE at IVC

Nefischer (2009) proposed to define an initial value of TKE at IVC. According to Grill et al. (2006) and Nefischer (2009), this value only depends on the mean velocity of the piston, which can be calculated from the engine speed n. So, an extrapolation for all the other points can be done with Formula 5-4.

$$k_{IVC} = C * n^{x}$$

Formula 5-4: Turbulent kinetic energy at IVC

All geometrical dependencies are represented by the constant C. Empirical studies from Linse et al. (2009) showed that a good approximation can be done with x = 2.4, studies from Messner (2007) determined x = 3.4 as best value.

In order to get a good match for the progress of the TKE curve, the parameters in Table 5-1 need to be adjusted in the model.

Parameter	Purpose
c_diss	Dissipation
anisotropy_const	Anisotropy
TKE_AT_IVC	Turbulent Kinetic Energy at IVC

Table 5-1: Parameters for the TKE model

For both engines, the TKE parameters have been matched with the available CFD-data. Figure 5-5 shows that the beginning of the curve and peak values were matched quite well but the strong decline caused deviations after 0° CA.

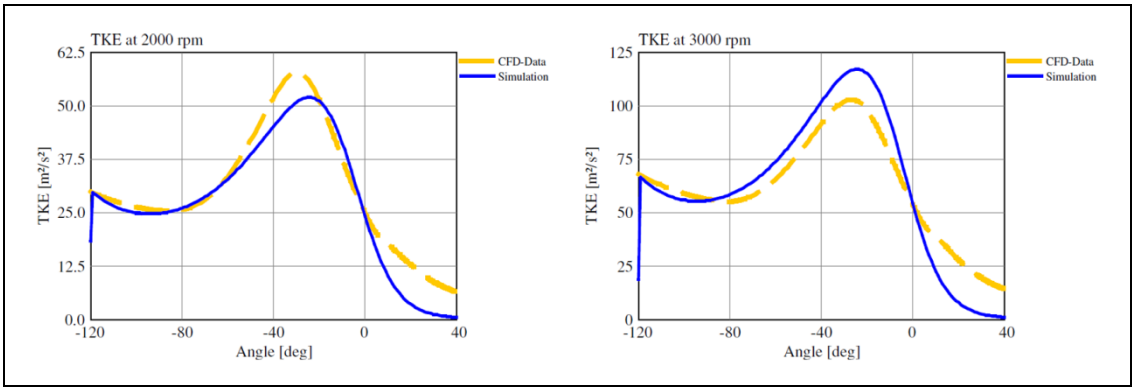

Figure 5-5: TKE at 2000 and 3000 rpm (TVDI)

An analysis of the entire engine performance map showed problems at points with very late ignition points (after approximately 5° CA). Figure 5-6 shows an example for high deviations of the User Model burn rate from the TPA.

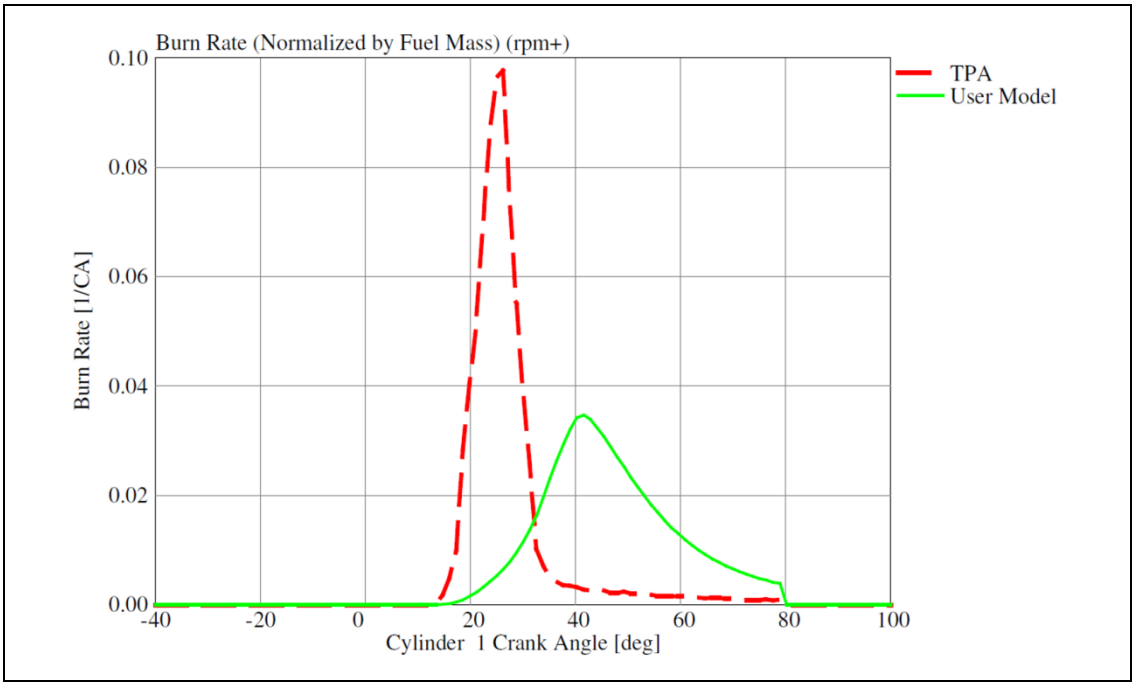

Figure 5-6: Problems at cases with late ignition point

This led to the consideration that there might be too little turbulent kinetic energy, which is caused by the already mentioned strong decline after 0°CA.

In order to increase TKE, the following three approaches have been considered:

- Increase of TKE at IVC
- Increase of Anisotropy
- Decrease of Dissipation

The first approach to vary TKE at IVC showed an interesting result (Figure 5-7). Even 4 times higher or lower values did not noticeably affect the progress of TKE after 0°CA.

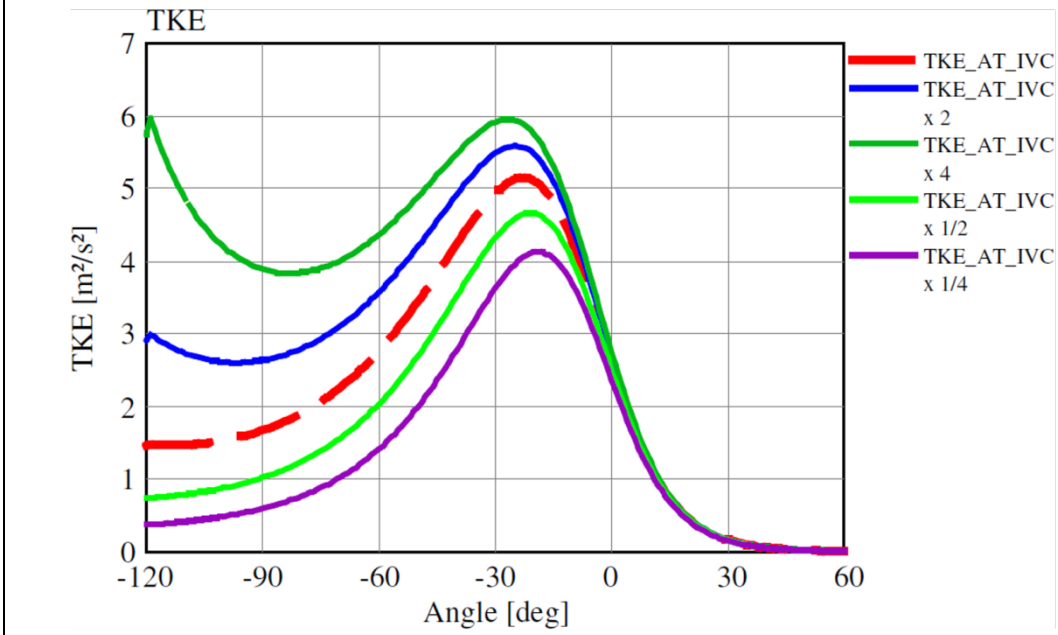

Figure 5-7: TKE progress for different TKE at IVC values

So, the next step was to change the parameters Anisotropy and Dissipation.

Figure 5-8 analyses the effects of these two parameters. The first row shows a much higher TKE peak with an Anisotropy value 3 times higher than before, which did not change the burn rate in this point at all (the green and blue dotted curve are overlapping, the red dotted curve shows the burn rate of the TPA, which is the target curve). At first glance, this was surprising but the zoom at the right side clearly shows that this high value for Anisotropy causes a higher peak but also an even stronger decline at the end. So, the

new TKE curve crossed the old one at about 10°CA and is higher before and lower after this point. This leads to the consideration that only the TKE values during the ignition phase are vital for the further progress of the combustion.

The second row shows the higher peak TKE value for a 50% lower Dissipation value and a quite good match of the burn rate with the modified TKE progress. The zoom makes clear that lower Dissipation leads to a flatter progress at the end of the curve. The TKE values with the new setup are higher than the old ones until 30°CA and are significantly higher during the ignition phase.

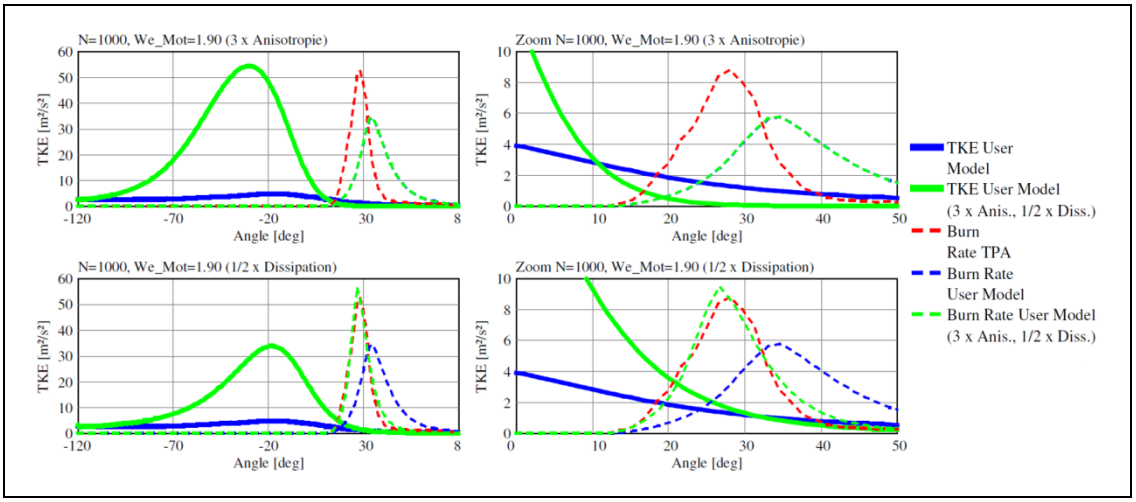

Figure 5-8: TKE and burn rates for different values of Anisotropy and Dissipation

These results led to the conclusion that TKE is very important for the further development of the combustion, especially during the ignition phase. According to these findings, a new approach for modeling TKE has been implemented (see chapter 5.3.1.3).

5.3.1.2 720° TKE approach

Theoretically, the most desirable approach would be to model TKE over the whole combustion cycle. Thus, the effects of e.g. the exhaust stroke (scavenging etc.) or the fuel injection could be modeled too.

Basically, the User Model has the following parameters in order to adjust the TKE progress to the CFD-data:

- Anisotropy constant
- Dissipation constant
- Intake constant
- Exhaust constant
- Squish constant
- Injection constant

Figure 5-9 shows the modeled TKE-progress (for 5000 and 6000 rpm) in comparison with the CFD data. After an optimization over the whole cycle, especially the TKE values in the area of the combustion process were not good. As already expected, because of the investigation shown in Figure 5-7, the TKE progress during the exhaust cycle or generally far before the combustion has almost no effect.

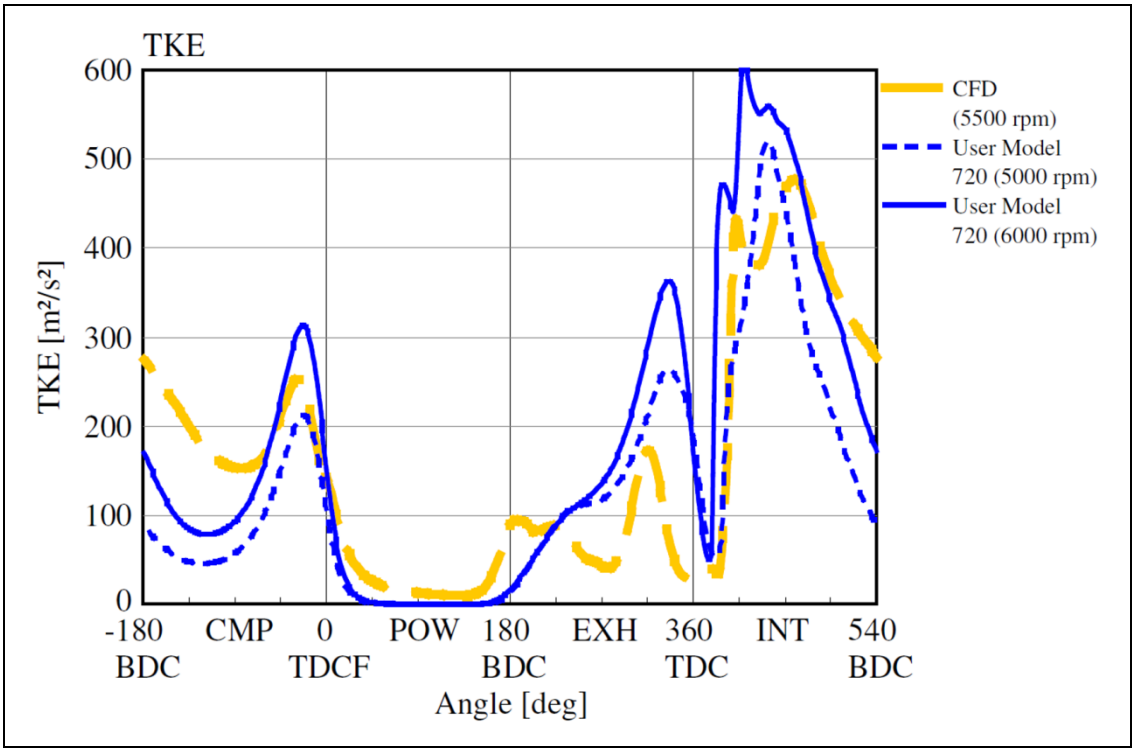

Figure 5-9: 720° TKE approach

These findings confirmed the idea to bring in a new, much more practicable TKE approach, which shifts the TKE start value closer to areas where ignition happens.

5.3.1.3 New TKE approach

The considerations in the previous chapters made clear that the progress of TKE before about -50°CA has no big effect on the combustion process and the approach to adjust TKE at IVC (at -120°CA) does not seem to be relevant.

So, the new procedure is based on the goal to get a good match of the TKE curve to the CFD data throughout the regions where ignition and combustion happens. Grill (2006) also proposed to solve the differential equation for turbulent energy starting approximately at the peak of the tumble decay and recommended values between -40 and -20° CA.

In order to ensure that the TKE progress is adjusted from the ignition point on, the new Crank Angle for the TKE start value was set before the earliest ignition point. The closer this ignition point to the peak of the TKE curve, the better the match of the TKE function to CFD data. If the start value is set earlier, the factor Anisotropy has to be increased in order to reach the appropriate peak values and this causes a strong decline at the end and thus much too low TKE-values at higher crank angles. The appropriate start values are calculated using a parabolic function fitted to CFD-data based on Formula 5-4.

Settings TVDI

In order to get a good match for the CFD data available for 2000, 3000 and 5800 rpm, Formula 5-4 has been extended with a constant C_3. As start value at -40°CA, the TKE Peak Values seemed to be reasonable and the parabolic function has been calculated according to Formula 5-5.

$$k_{-40°CA} = C_1 * n^{C_2} + C_3$$

Formula 5-5: TKE at -40°CA

Using the parameters C_1, C_2 and C_3 in Table 5-2 fitted the parabolic TKE-function to the CFD data shown in Figure 5-10.

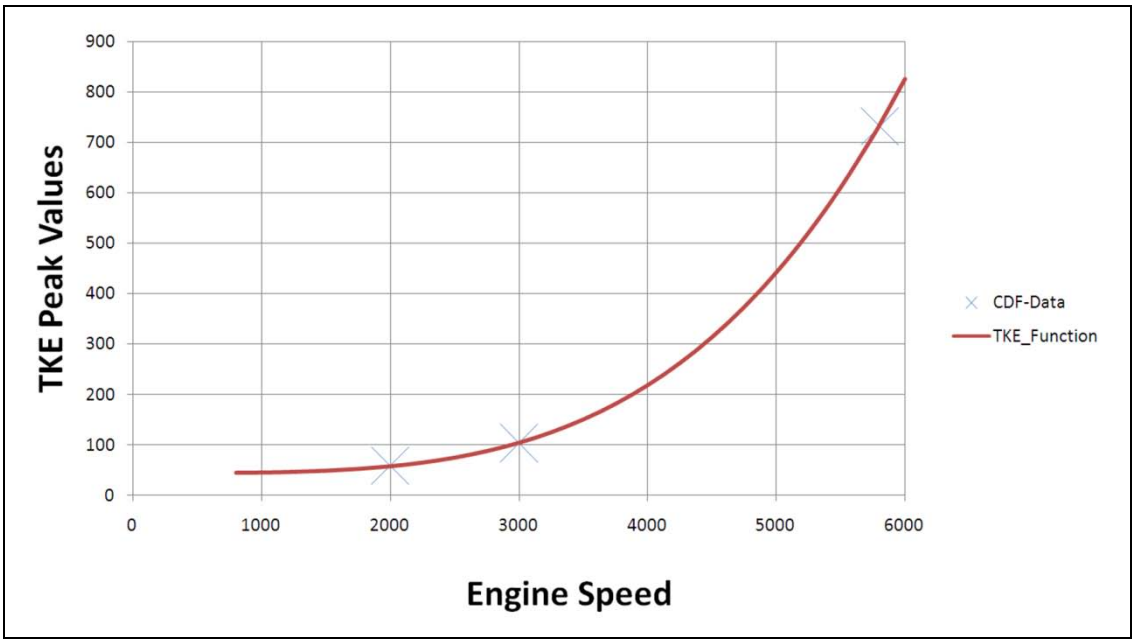

Figure 5-10: Parabolic function for TKE peak values (TVDI)

After defining the start value, the parameters Anisotropy and Dissipation were adjusted and showed the best behavior with the parameters in Table 5-2.

TKE Parameters	
C_1	8.2E-12
C_2	3.7
C_3	44
Anisotropy	1
Dissipation	0.8

Table 5-2: TKE parameters (TVDI)

This led to the new TKE settings which are shown in comparison to the old ones (Figure 5-11). Especially the Zoom on -40 to 20°CA (second row in Figure 5-11) shows the much better matching with the new configuration for 2000 and 3000rpm.

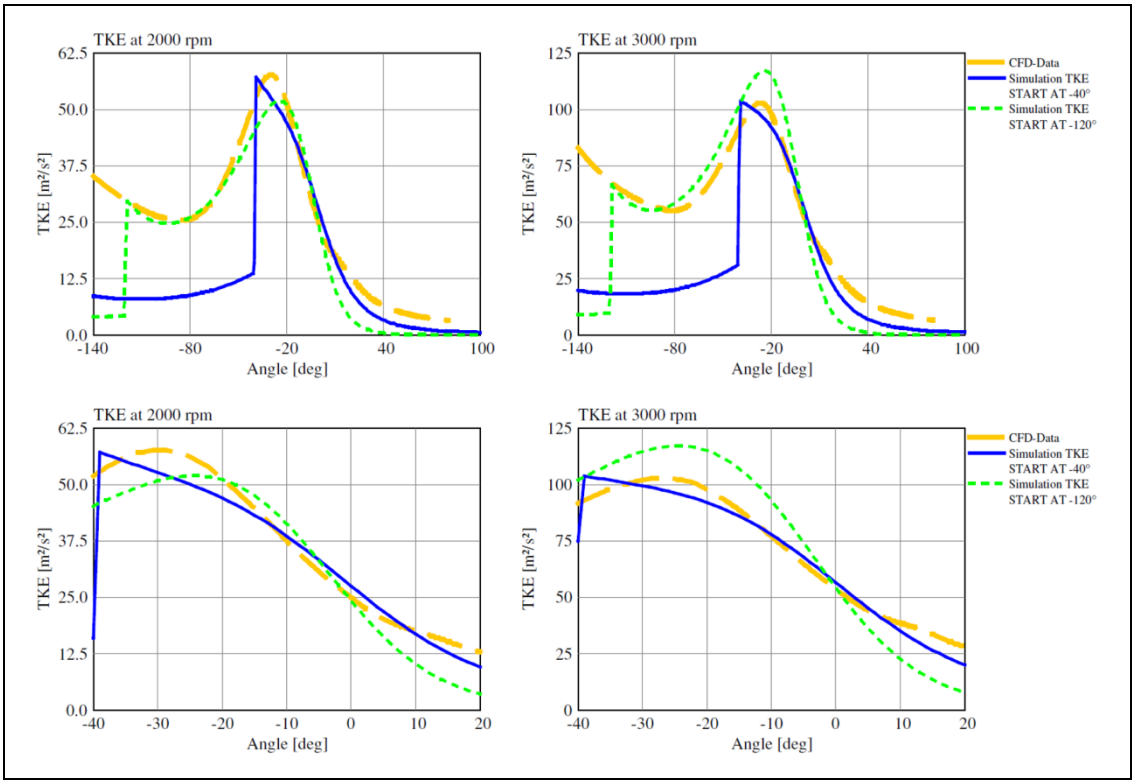

Figure 5-11: Comparison old and new TKE settings (TVDI)

Settings Highly Turbocharged TGDI

For the Highly Turbocharged TGDI, CFD data were only available for 5500 rpm. The parameter C_2 = 2.4 has been taken from the investigations of Linse et al. (2009) and parameter C_3 has been estimated using the same relation as the TKE peak values from the TVDI and the Highly Turbocharged TGDI.

Parameters	
C_1	2.51E-7
C_2	2.4
C_3	15
Anisotropy	1
Dissipation	0.8

Table 5-3: TKE parameters (Highly Turbocharged TGDI)

Applying the value from Table 5-3, the following parabolic function for the TKE peak values used for -40° CA can be found (Figure 5-12).

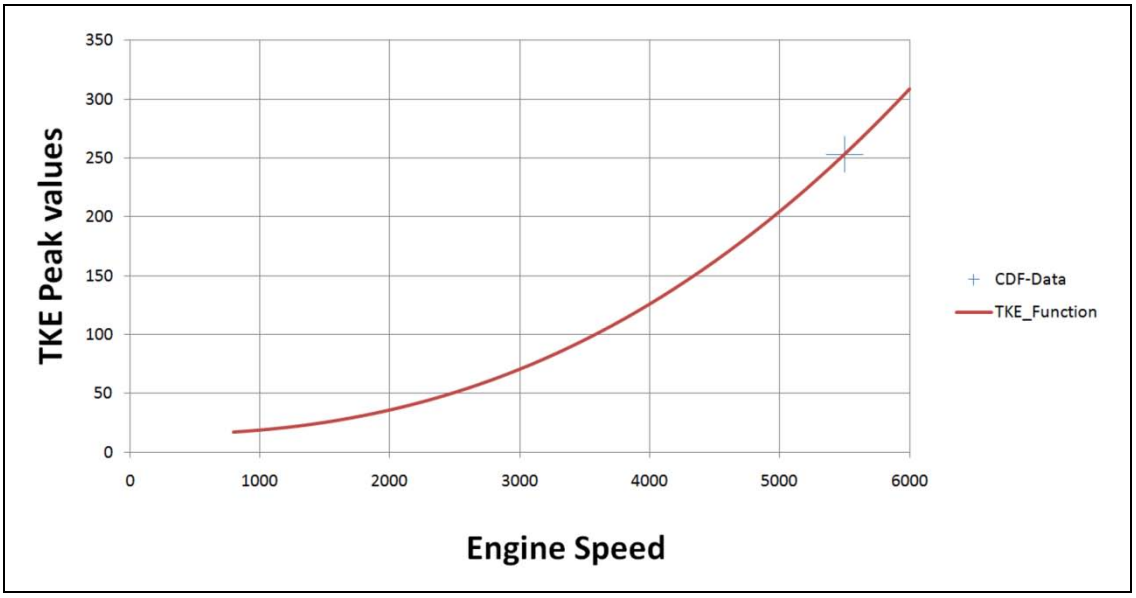

Figure 5-12: Parabolic function for TKE peak values (Highly Turbocharged TGDI)

With the values from Table 5-3, the TKE function from CFD-data for 5500 rpm is well located between the simulated TKE functions for 5000 and 6000 rpm, which seems to be the best possible solution. Again the comparison with the old settings shows the improvements especially after 0°CA (Figure 5-13).

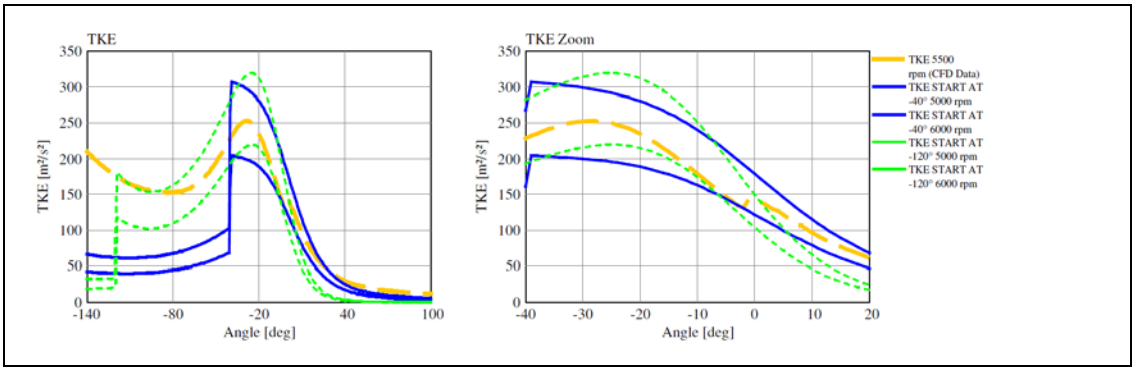

Figure 5-13: Comparison old and new TKE settings (Highly Turbocharged TGDI)

5.3.2 Ignition Delay

The adjustment of the ignition delay has been done with separate Excel sheets. A characteristic number of points have been chosen for each engine in order to match the ignition delay to the behavior of the TPA.

Figure 5-14 shows the burn rate of the TPA in blue and the ignition integral in pink (on the secondary axis), which is supposed to hit the threshold of 1 when the TPA starts to burn.

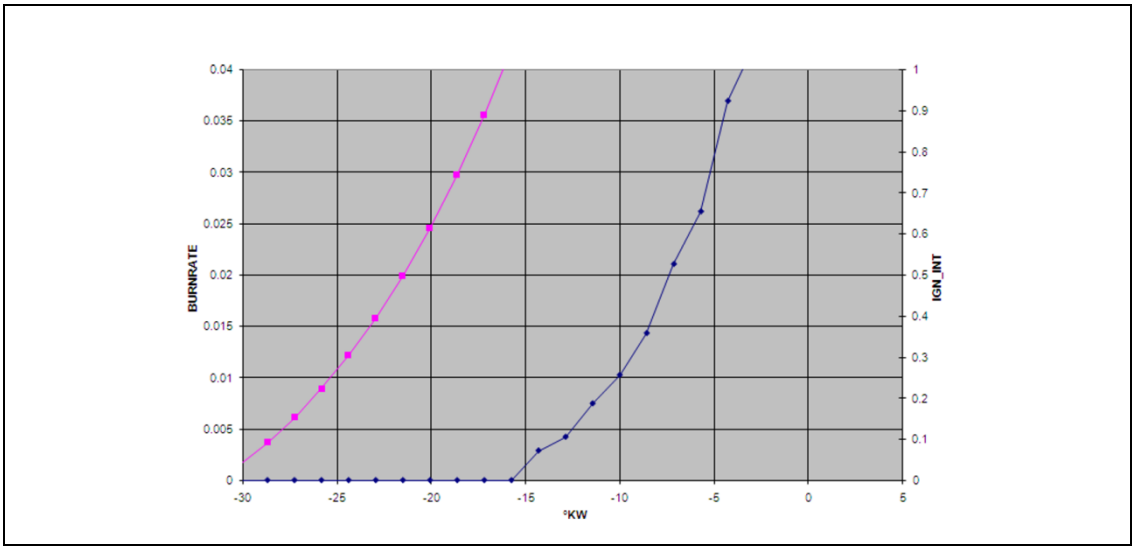

Figure 5-14: Adjustment of the ignition delay

The optimization process done with Excel, with the goal to get a match for all characteristic points, resulted in the following parameters according to Formula 4-23 shown in Table 5-4.

Parameter	Highly Turbocharged TGDI	TVDI
A	2*10^-6	2*10^-5
T_a	3800 K	3800 K
x	0.3	0.3
y	4	3
z	1.5	1.5

Table 5-4: Used parameters for ignition delay

Figure 5-15 shows the improvements by the implementation of the ignition delay model for the Highly Turbocharged TGDI.

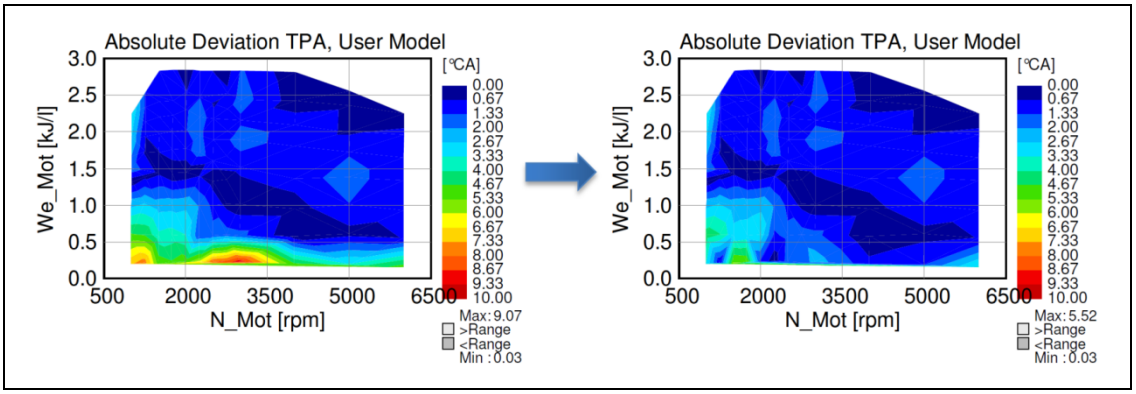

Figure 5-15: Improvements at 5% BFF because of the application of the ignition delay model (Highly Turbocharged TGDI)

5.3.3 Optimized Parameters

After the adjustment of TKE and ignition delay, the following 6 parameters shown and explained in Table 5-5 were optimized.

Parameter	Purpose
a, b	Have an impact on the turbulent flame speed (Formula 4-18) and can be compared to the TFM of the SI Turbulent Flame Combustion Model.
c	Has an impact on the initial kernel growth rate (Formula 4-19) and can be compared to the CK value of the SI Turbulent Flame Combustion Model.
cburn	Influences the characteristic burn duration and is realized as pre-factor for the time constant τ in Formula 4-11.
exc	Specifies the excentricity *exc* of the flame center according to Figure 4-7. It influences the wall interactions and therefore the maximum burn rate.
dilution_exp	Has the same function as the Dilution Exponent Multiplier of the SI Turbulent Flame Combustion Model and is used to scale the effect of dilution (residuals and EGR) on the laminar flame speed.

Table 5-5: Optimization parameters of the Nefischer User Model

5.4 Comparison of the Models

In order to perform a fair comparison of the two models, a structured procedure needs to be applied to optimize both of them. After this process, some characteristic values will be illustrated and compared.

5.4.1 Basic Approach

Generally, the goal was to match the burn rates of the 2 models to the burn rates of the TPA. Basically, the best procedure for an optimization process on the burn rates would be to minimize the total square error of all points in the engine performance map.

Due to the chosen MATLAB optimization (5.4.2.2), which accesses (full-cylce-) dat-files created by GT-Power, a separated optimization only for the high-pressure process could not be realized. So, the optimization process was very time consuming and a compromise had to be found. Thus, the final optimization has been done with MATLAB on 6 well-distributed points in the engine performance map. In case of a desired robust model, good results for these 6 points lead to good results throughout the engine performance map.

To find reasonable start values for the optimizer, a manual parameter pre-adjustment has been done first (details in 5.4.2). After the optimization process with MATLAB, all points in the engine performance map have been calculated with the discovered parameters.

5.4.2 Optimization Methods

The used optimization methods surely have an effect on the quality of the results. As already mentioned, a manual pre-adjustment based on preliminary simulations, which was necessary to get reasonable start values, has been done before the linear optimization with MATLAB. Chapter 5.4.2.3 shortly discusses other optimization possibilities which could bring further improvements.

5.4.2.1 Manual Parameter Pre-adjustment

The manual parameter pre-adjustment was based on simulation trials and the observation of their effects on the pre-calculated results. Because of available pre-studies for the SI Turbulent Flame Combustion Model, this method already achieved good results. In case of the Nefischer User Model, the parameters interacted much more with each other and so the manual adjustment was done more roughly just to get reasonable start values for the MATLAB optimization.

5.4.2.2 Linear Optimization with MATLAB

In order to find the best combination for the used parameters, a linear optimization with MATLAB has been integrated in the optimization process. The interconnection of MATLAB and GT-Power has been accomplished with MATLAB SIMULINK according to Figure 5-16.

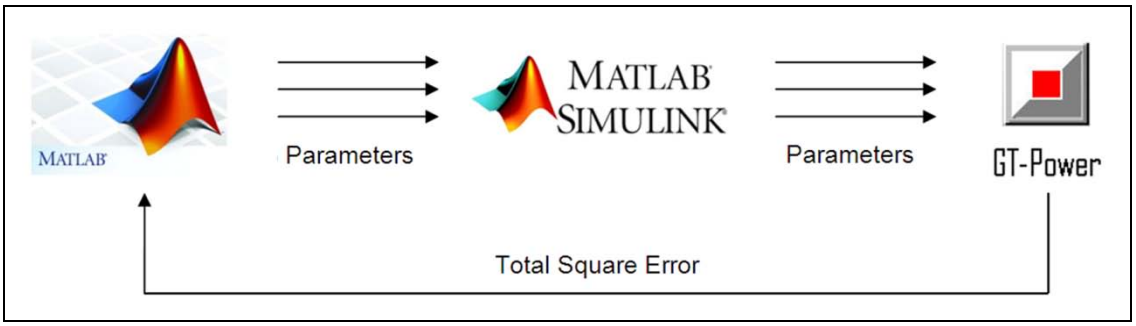

Figure 5-16: Interconnection of MATLAB and GT-Power

With help of the Wiring Harness template from GT-Power (4.5.2) and the SIMULINK block for GT-SUITE, the communication between MATLAB and GT-Power can be established. Thus, the MATLAB optimizer can set values for the parameters and retrieve the square errors calculated in GT-Power, which are supposed to be minimized.

As already mentioned, MATLAB can only access dat-files and not the Case Setup of GT-Power. Therefore, 6 single points (i.e. 6 single-case dat-files), which include an engine speed as well as a load spread, have been chosen in order to cover most regions of the engine performance map.

Figure 5-17 and Figure 5-18 show all the calculated cases in the engine performance maps, including the respective 6 points chosen for the MATLAB optimization process.

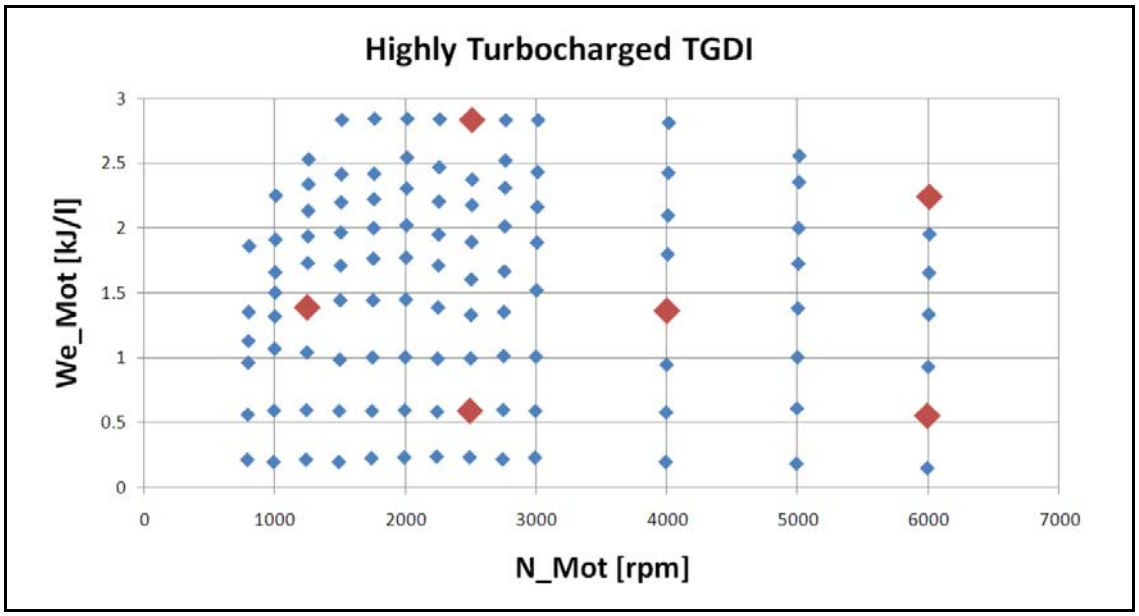

Figure 5-17: Points for MATLAB optimization (Highly Turbocharged TGDI)

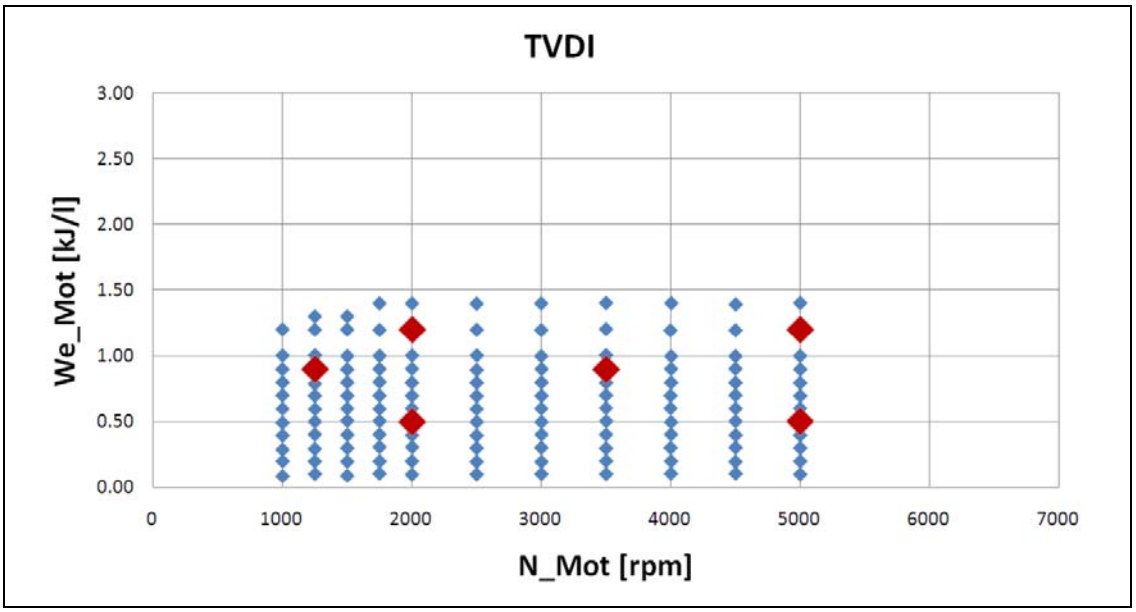

Figure 5-18: Points for MATLAB optimization (TVDI)

In order to show the lower level of mean effective pressures of the TVDI compared with the Highly Turbocharged TGDI, the same y-axis has been used for both figures.

For the optimization process, the linear MATLAB optimizer (fminsearch), which uses the Simplex-Method, has been used. The basic idea of this algorithm is to gradually find a solution with a higher objective function value. This is realized by “walking” along the edges of a polytope (whose dimension depends on the number of parameters), always taking the neighbor with the higher value (Figure 5-19). The algorithm terminates when a local maximum (or respectively minimum) is reached.

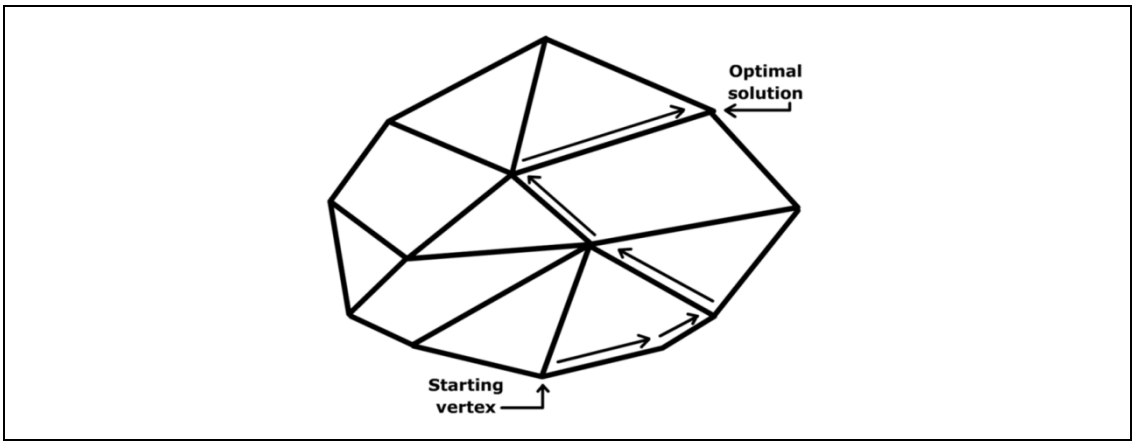

Figure 5-19: Principle of the Simplex-Algorithm (Wikipedia, 2010)

So, the optimizer improves the solution until the algorithm finds a minimum of total square errors of the 6 burn rates. It needs to be mentioned that this might be a local minimum and the global minimum can only be achieved with a different algorithm or different start values. The following chapter discusses methods to improve this situation.

5.4.2.3 Further Possibilities for the Optimization Process

For a further improvement of the optimization process, there are 2 possibilities to be mentioned. The first one, as already mentioned, is the separation of the engine process calculations and the high-pressure process calculations. If the gas-exchange processes are calculated once until IVC and the optimization later is done just for the high-pressure process until EVO, a lot of computational time can be saved. Thus, more points or even all points in the engine performance map can be taken for the optimization process, which would improve the overall results.

The second possibility is to improve the optimization method used for the 6 points. As a lot of different parameters are used for the optimization, which additionally interact with each other, a linear optimizer will find a local minimum but probably not the best possible solution.

Genetic algorithms, for instance, could bring further improvements. Inspired by evolutionary biology, they try to find the best possible solution using techniques like selection, crossover and mutation. Starting with randomly created conditions, the best results are combined and randomly mutated to the "next generation" similar to the principle "survival of the fittest".

Using genetic algorithms could avoid obtaining poor performing local minimums because of bad starting values for the optimization.

5.4.3 Result Plots

In order to present the results, 3 different plots have been used and are explained in the following chapters. The plots have been created with GT-Post, a postprocessor program for GT-Power, which provides a graphical view of data with additional functions to treat and compare the calculated results, and Microsoft Excel.

5.4.3.1 Variation of Engine Speed and Load

The combination of plots with varying engine speed (at constant load) and varying load (at constant engine speed) prove the ability of the models to adapt to an engine speed spread as well as a load spread. For the result plots, 4 points with constant engine speed and load have been chosen.

5.4.3.2 Map-Plots

Map plots are a very demonstrative way to show the analyzed values over the entire engine performance map (x = engine speed, y = load, z = analyzed value). In this thesis, deviation plots from the TPA measured in percent or in degree CA are used. Grey areas in this plot indicate deviations higher than 10°CA or 25% respectively.

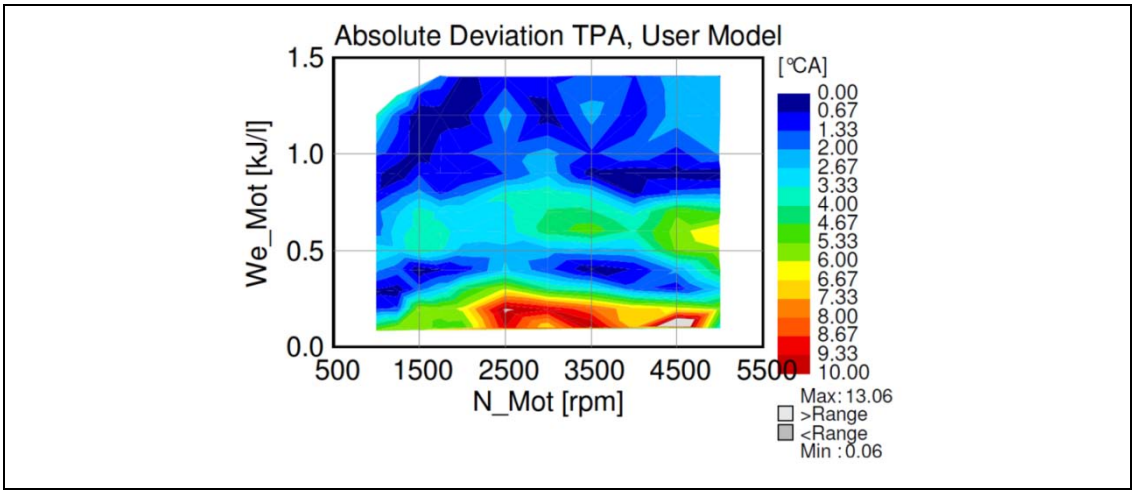

Figure 5-20: Map-Plot of 5% BFF (Deviations from TPA)

Generally, it is possible to get a good overview of the entire engine performance map, but only with a combined look at the burn rates it is possible to do a detailed evaluation.

It has to be mentioned that in some special cases the map plot can be misleading. As Figure 5-20 shows, there are very high deviations from the TPA at 4500 rpm and 0.1 kJ/l. A further look at the burn rate showed the following result (Figure 5-21). The burn rates of the simulation almost perfectly matches the burn rate of the TPA, but due to jitters in the TPA burn rate caused by jitters in the measured pressure signal, the reference 5% Burned Fuel Fraction was detected much too early.

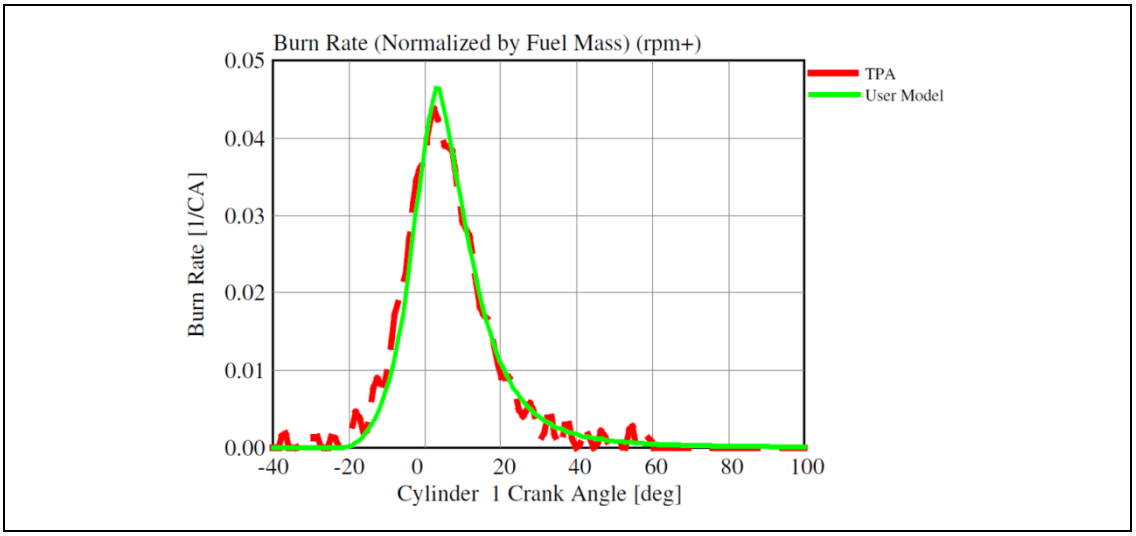

Figure 5-21: Example for a burn rate causing problems

Therefore, it is always important to take a further look at the burn rates in areas with high deviations.

5.4.3.3 Correlation of Measuring Points

Correlation or co-relation indicates the strength and direction of a linear relationship between 2 random variables and is often measured as a correlation coefficient ρ. In general statistical usage, several coefficients, adapted to the nature of data, are measuring the degree of departure of 2 random variables from independence (Wikipedia, the free encyclopedia, 2009).

The best known coefficient, which is also integrated in Microsoft Excel and has been used for the result plots, is the Pearson correlation coefficient. It is defined according to Formula 5-6.

$$\rho_{X,Y} = \frac{E((X - \mu_X) \times (Y - \mu_Y))}{\sigma_X \times \sigma_Y}$$

Formula 5-6: Pearson correlation coefficient

A correlation coefficient of +1 indicates an increasing linear relationship, -1 a decreasing linear relationship. A coefficient of 0 points out that the variables are independent and so the closer this number is to either -1 or 1, the closer is the correlation between these variables.

The correlation coefficients in the result plots are calculated considering all points in the engine performance map and compare the values from the TPA with the respective values from the 2 models. In case of the combustion models, a linear relationship and thus a value of +1 are desired.

6 Simulation Results

In chapter 6, the results of the preliminary survey, which has been done on the Base TGDI and the results of the Highly Turbocharged TGDI as well as the TVDI are presented. Additionally, they are compared to each other and discussed.

6.1 Preliminary Survey: Base TGDI

A preliminary survey done on the TGDI, following the same scheme for the simulation analysis (with an optimization on the burn rates of the 6 points shown in Figure 6-1), showed a 22% lower total least square error for the Nefischer User Model.

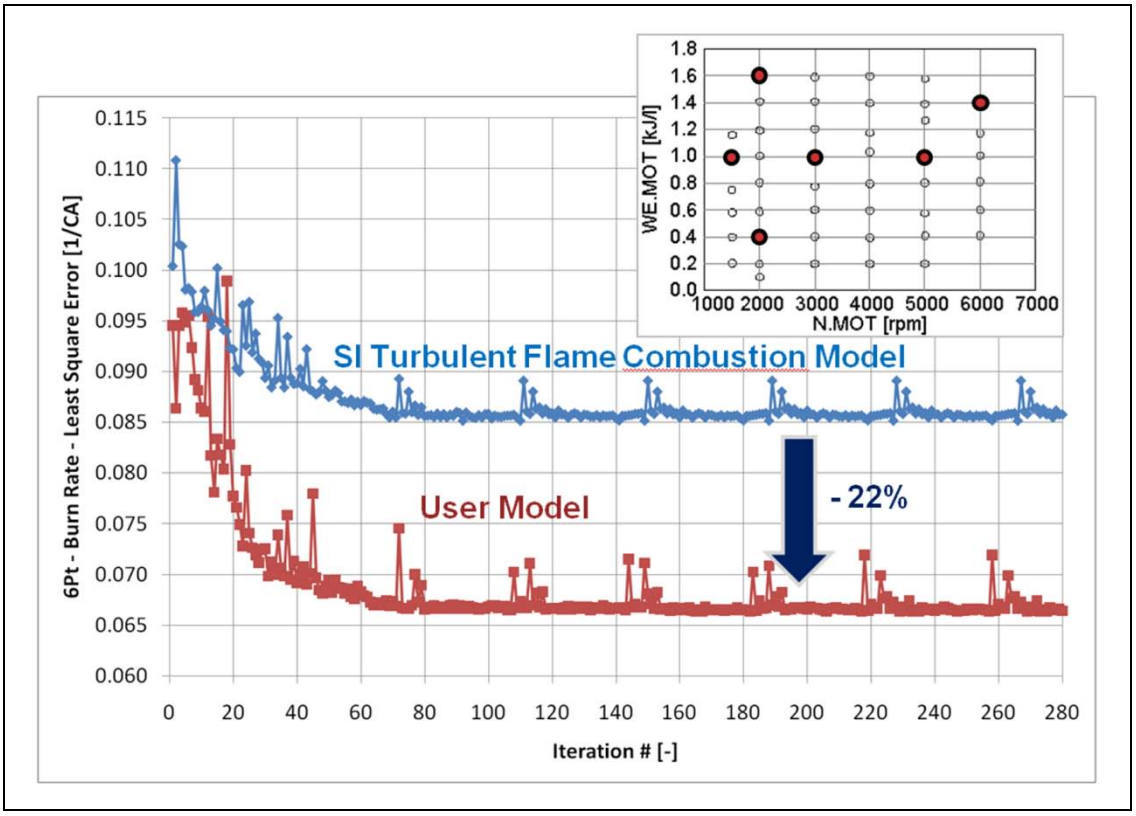

Figure 6-1: Comparison of Optimization Progresses (Base TGDI)

Also the variation of engine speed and load pointed out a slightly better behavior of the Nefischer User Model.

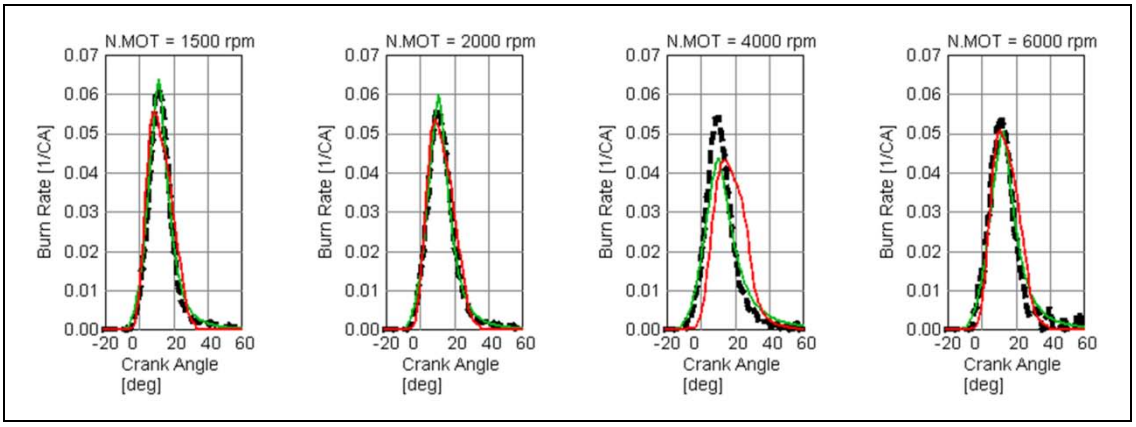

Figure 6-2: Variation of engine speed (TPA in black, Nefischer User Model in green and SI Turbulent Flame Combustion Model in red, Base TGDI)

The variation of engine speed (Figure 6-2) was done at We_Mot = 0.8 kJ/l and the variation of load (Figure 6-3) was taken at 4000 rpm.

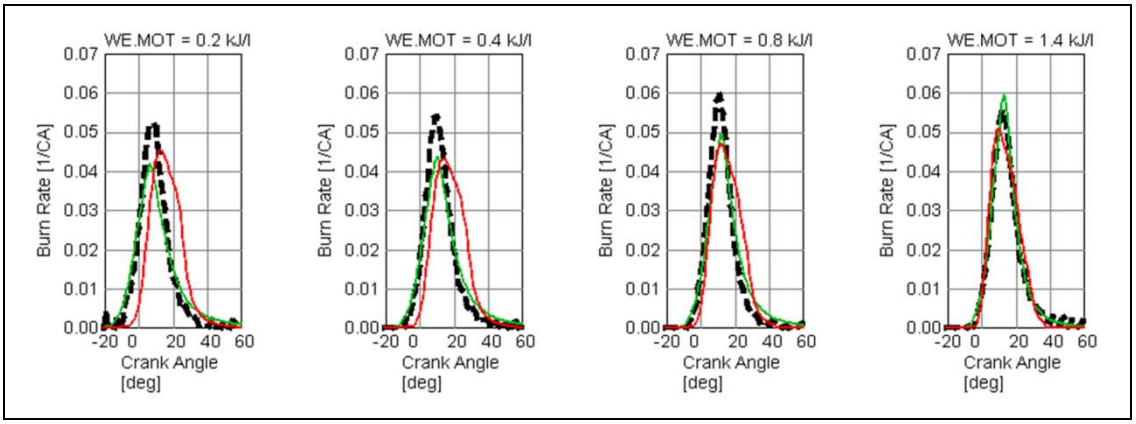

Figure 6-3: Variation of load (TPA in black, Nefischer User Model in green and SI Turbulent Flame Combustion Model in red, Base TGDI)

The 50% Burn Point results of the Nefischer User Model showed very little deviations, whereas the SI Turbulent Flame Combustion Model had serious problems at high engine speed and low load (Figure 6-4). For the maximum cylinder pressure, the Nefischer User Model showed deviations up to 10 % (area of green color), whereas the SI Turbulent Flame Combustion Model showed deviations of 20% at high engine speed and low load.

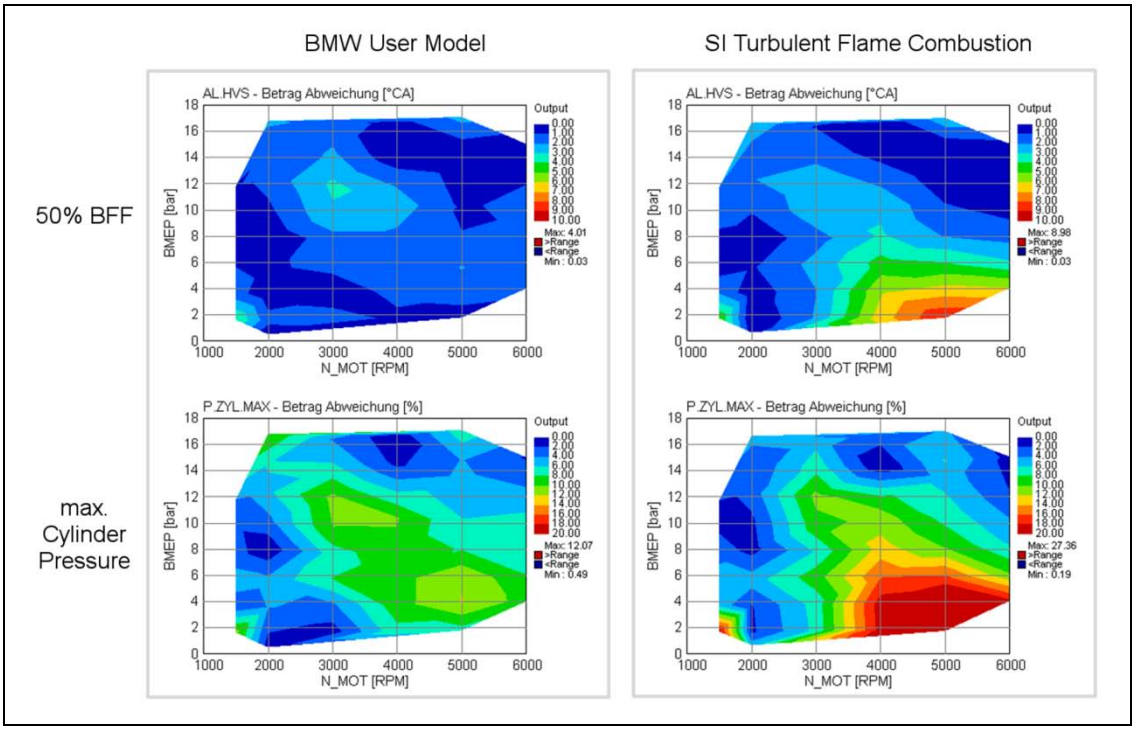

Figure 6-4: 50% BFF and maximum cylinder pressure, deviations from TPA (Base TGDI)

6.2 Highly Turbocharged TGDI

Both combustion models lead to acceptable results for the Highly Turbocharged TGDI. First, the progresses of the 2 optimizations are compared, and then burn rates, cylinder pressures and indicated mean effective pressures are evaluated.

6.2.1 Optimization Progress

Due to available pre-studies for the behavior of parameters for the SI Turbulent Flame Combustion Model, the pre-adjusted model already showed acceptable results and the further MATLAB optimization only brought improvements of 12% (Figure 6-5).

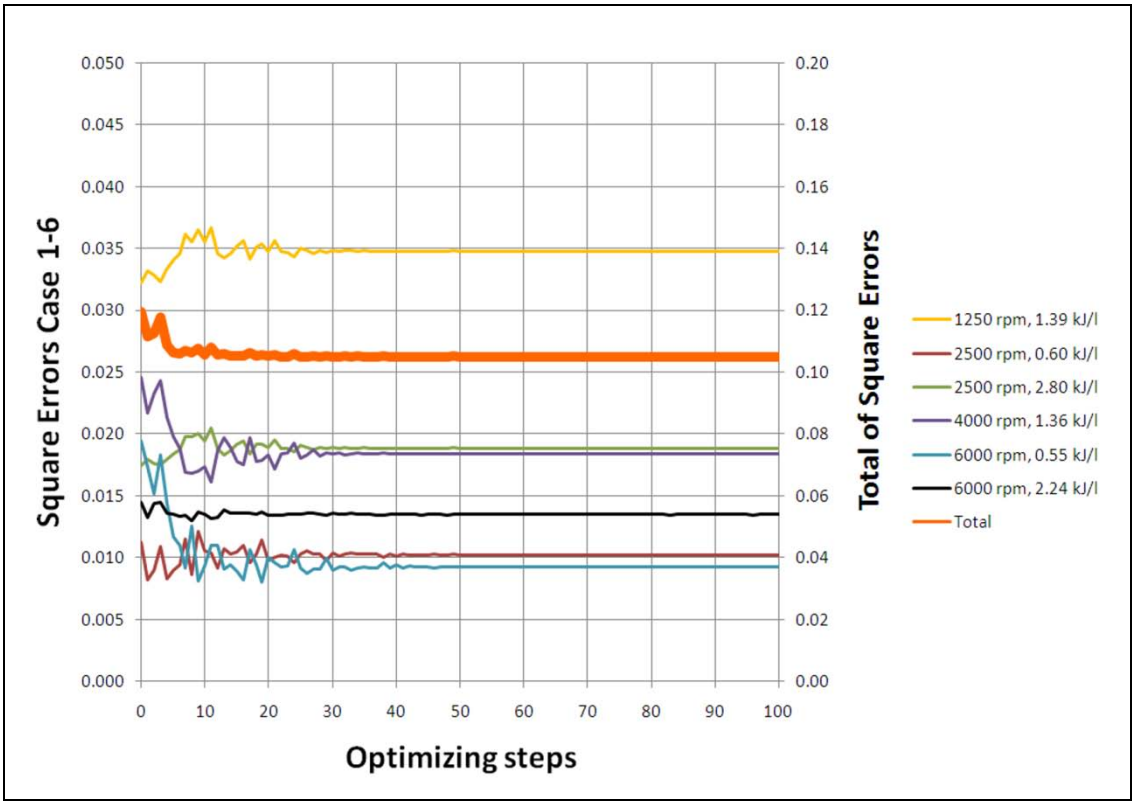

Figure 6-5: Optimization progress of the SI Turbulent Flame Combustion Model (Highly Turbocharged TGDI)

Table 6-1 shows the values of the 3 parameters of the pre-adjustment and the slightly changed parameters as result of the MATLAB optimization.

Parameter	Manual pre-adjustment	MATLAB optimized
TFM	0.72	0.77
DEM	1.00	1.07
CK	2.00	2.07

Table 6-1: Optimized parameters of the SI Turbulent Flame Combustion Model (Highly turbocharged TGDI)

The optimization process for the Nefischer User Model decreased the total of square errors by 24%. Obviously, the optimization algorithm achieved this result after around 40 optimization steps and could not improve the situation further (Figure 6-6).

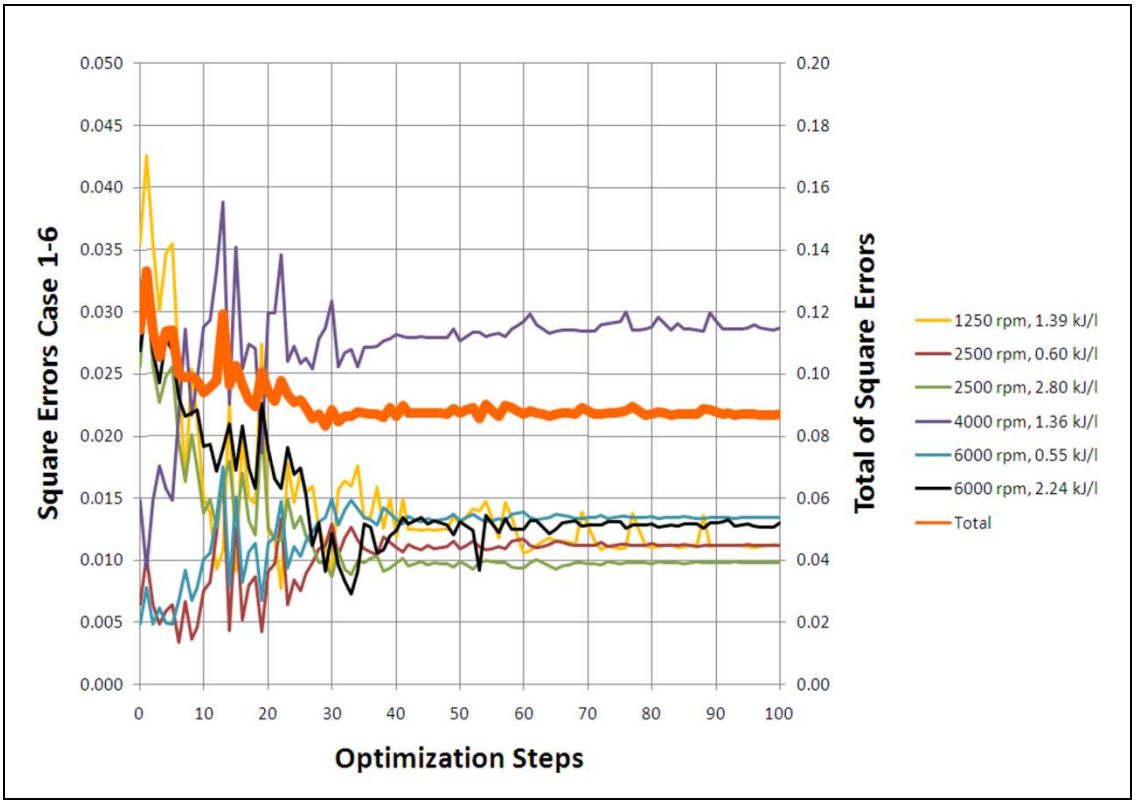

Figure 6-6: Optimization progress of the Nefischer User Model (Highly Turbocharged TGDI)

Table 6-2 shows the values of the 6 parameters after the pre-adjustment and the MATLAB optimization.

Parameter	Manual pre-adjustment	MATLAB optimized
a = b/2	1.00	0.96
c	9.47E-4	9.86E-4
cburn	7.10	8.61
exc	8.40E-3	8.93E-3
dilution_exp	1.00	0.89

Table 6-2: Optimized parameters of the Nefischer User Model (Highly Turbocharged TGDI)

Figure 6-7 compares the total square errors of both models. The Nefischer User Model reached a 17% lower value than the SI Turbulent Flame Combustion Model.

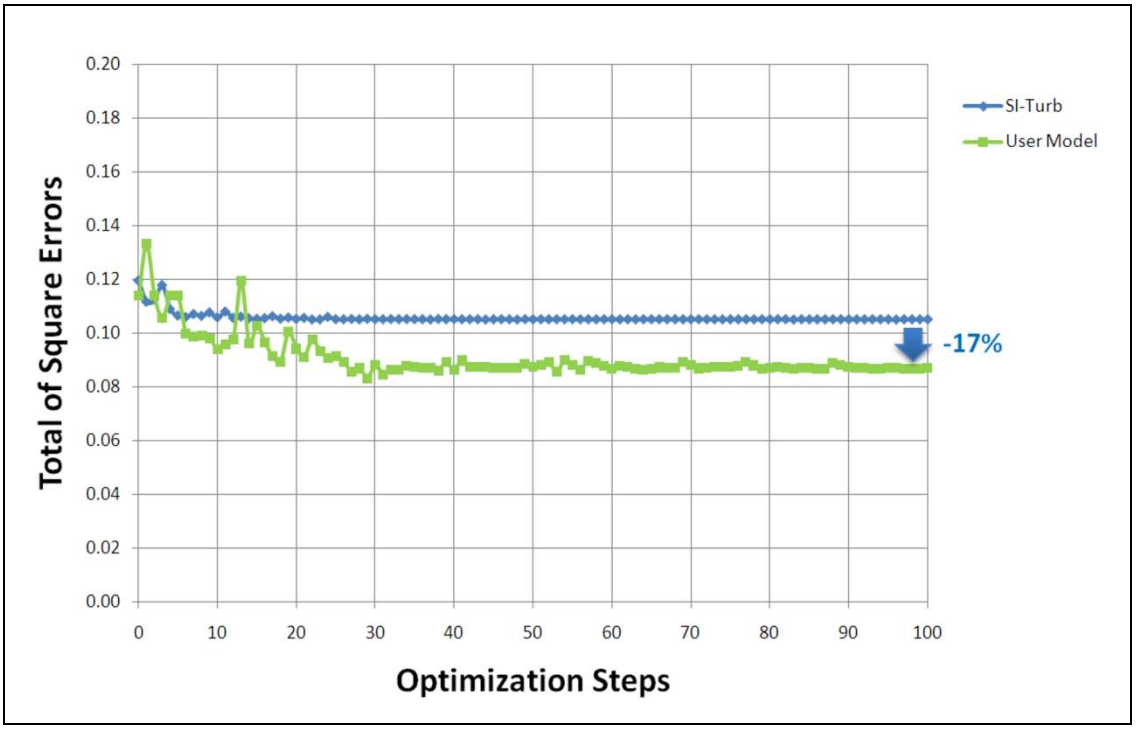

Figure 6-7: Comparison of total square errors of both models (Highly Turbocharged TGDI)

6.2.2 Burn Rates

Figure 6-8 shows the variation of engine speed (at a constant load of 1.70 kJ/l) and a variation of load (at a constant engine speed of 3000 rpm). The Nefischer User Model shows a better match of burn rates, the burn rates of the SI Turbulent Flame Combustion Model have a lower peak but a longer late stage of combustion.

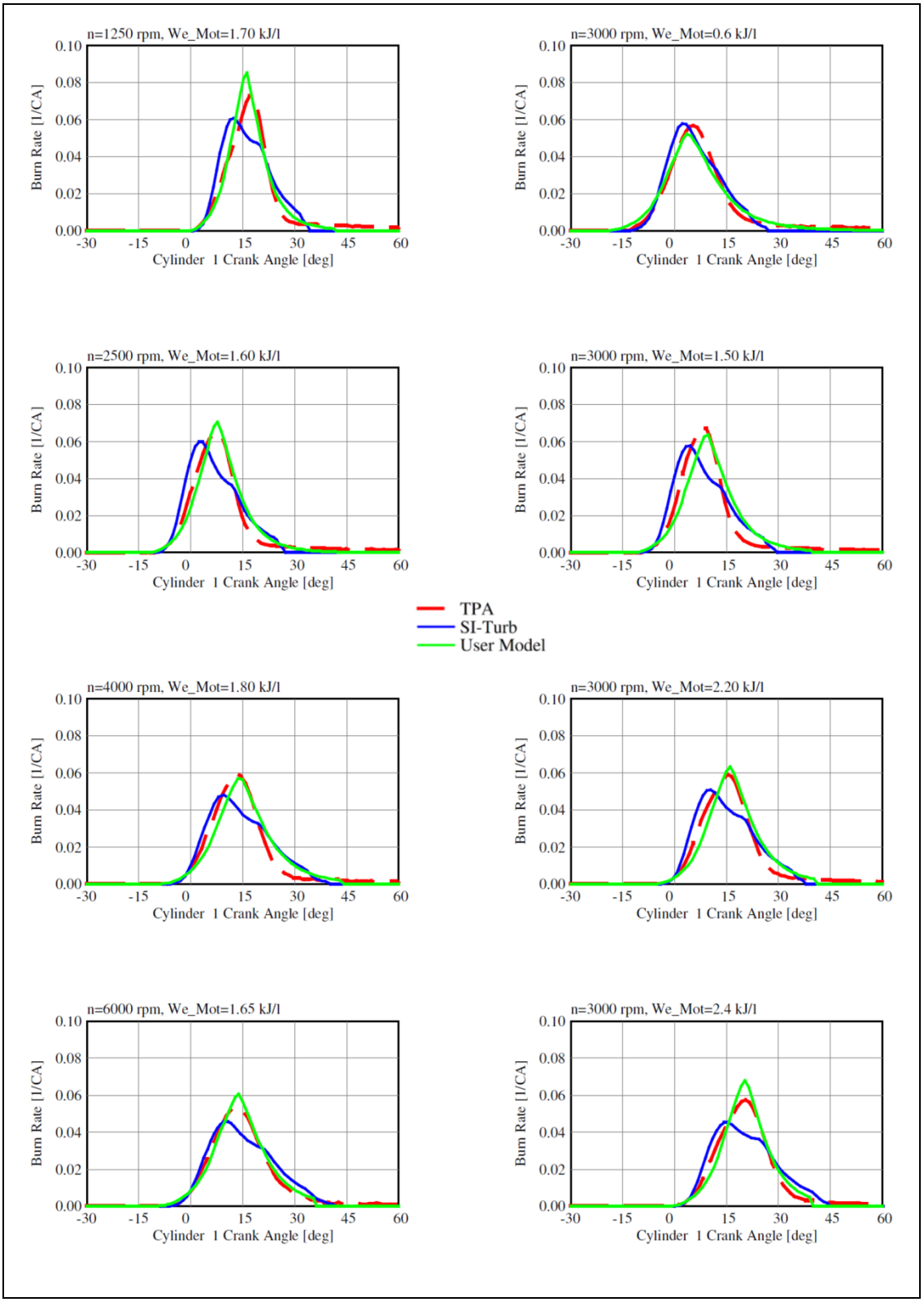

Figure 6-8: Variation of engine speed and load for the burn rate (Highly Turbocharged TGDI)

Figure 6-9 indicates problems of the SI Turbulent Flame Model at high engine speeds and low loads. The ignition delay of the Nefischer User Model works properly except for a few points with low engine speed and low load. The map plots show the deviation of the respective model from the TPA in °CA.

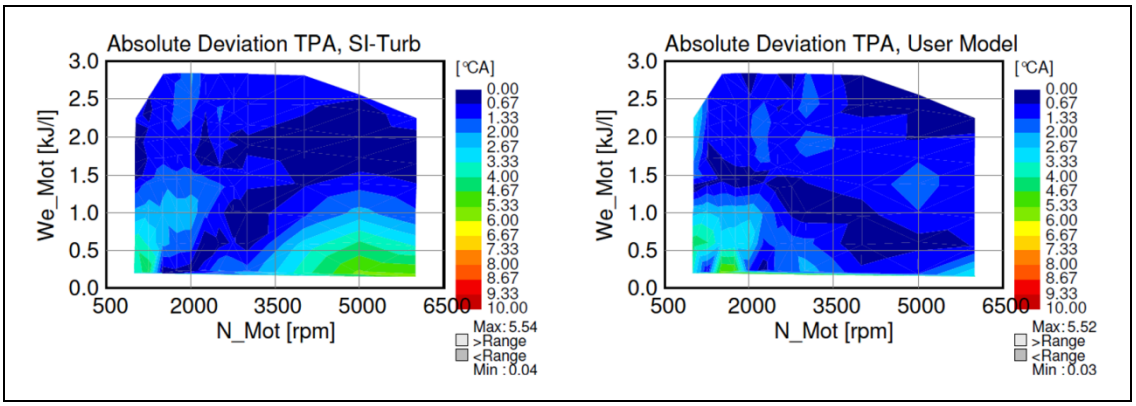

Figure 6-9: 5% BFF, absolute deviations from TPA (Highly Turbocharged TGDI)

The areas with too low ignition delay of course have an effect on the crank angle of 50% burn point. Also, the Nefischer User Model has problems at high engine speeds and low load (Figure 6-10).

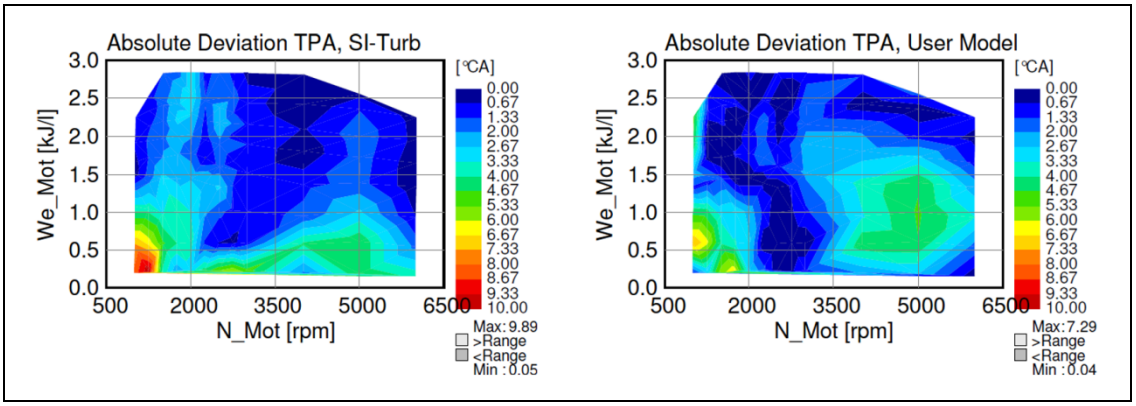

Figure 6-10: 50% BFF, absolute deviations from TPA (Highly Turbocharged TGDI)

Overall, both models deliver acceptable results regarding the burn rates. Figure 6-11 shows the correlation coefficients from 5%, 10%, 50% and 75% BFF of both models with the TPA, which are all higher than 90%. The performance of both models is nearly equal.

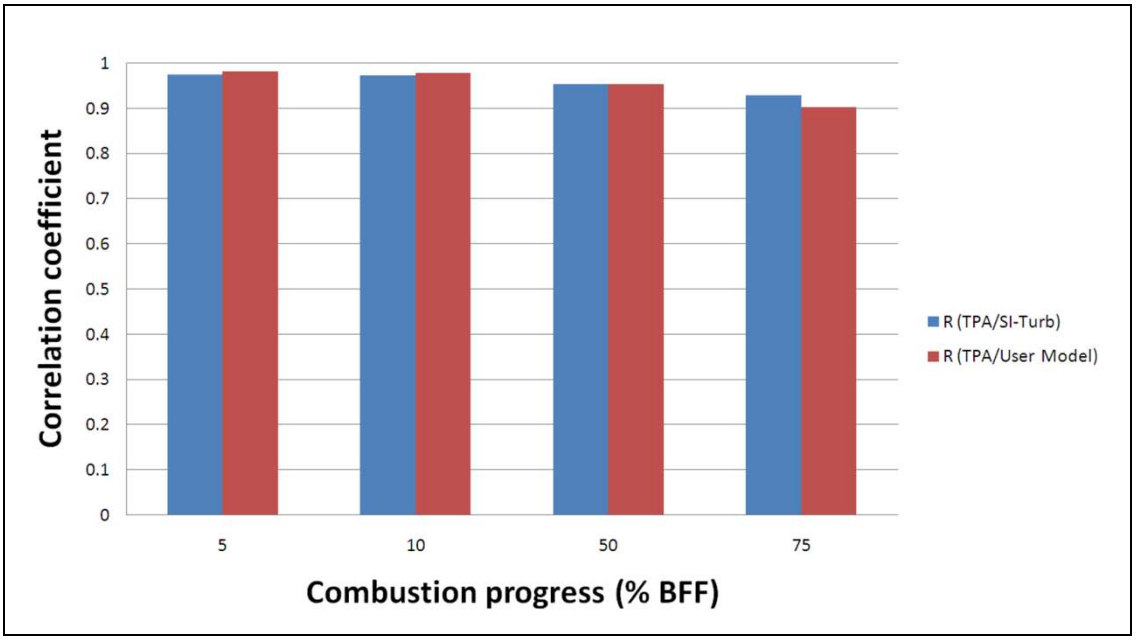

Figure 6-11: Correlation coefficients for both models (Highly Turbocharged TGDI)

6.2.3 Cylinder Pressures, IMEP

Figure 6-12 shows the variation of engine speed and load using the same 8 points as in the plot of burn rates (Figure 6-8). Both models can achieve very good results, whereas the Nefischer User Model is even more accurate.

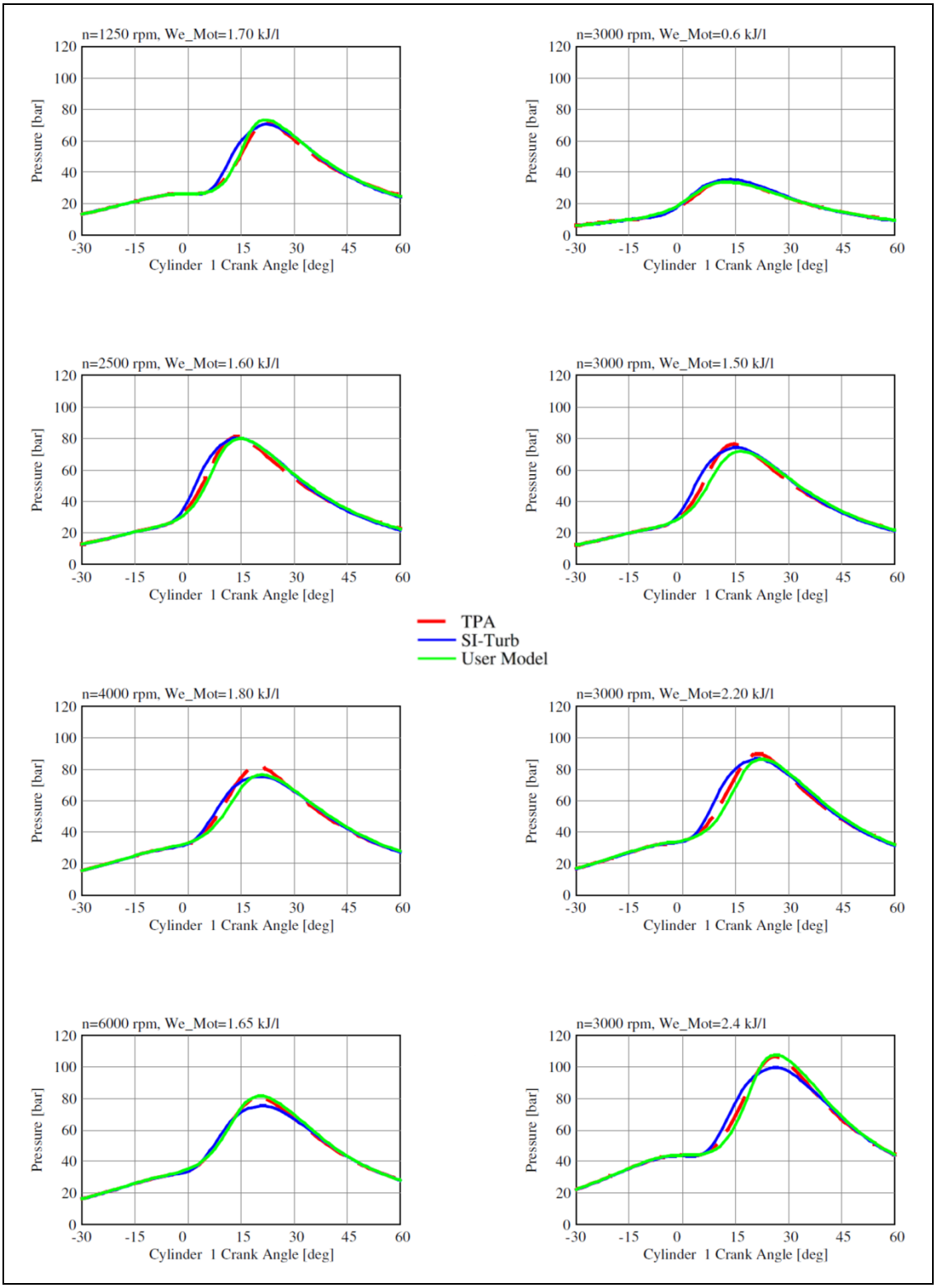

Figure 6-12: Variation of engine speed and load for the cylinder pressure (Highly Turbocharged TGDI)

For the maximum cylinder pressure, the SI Turbulent Flame Combustion model delivers deviations up to 33% and the Nefischer User Model up to 18% (Figure 6-13).

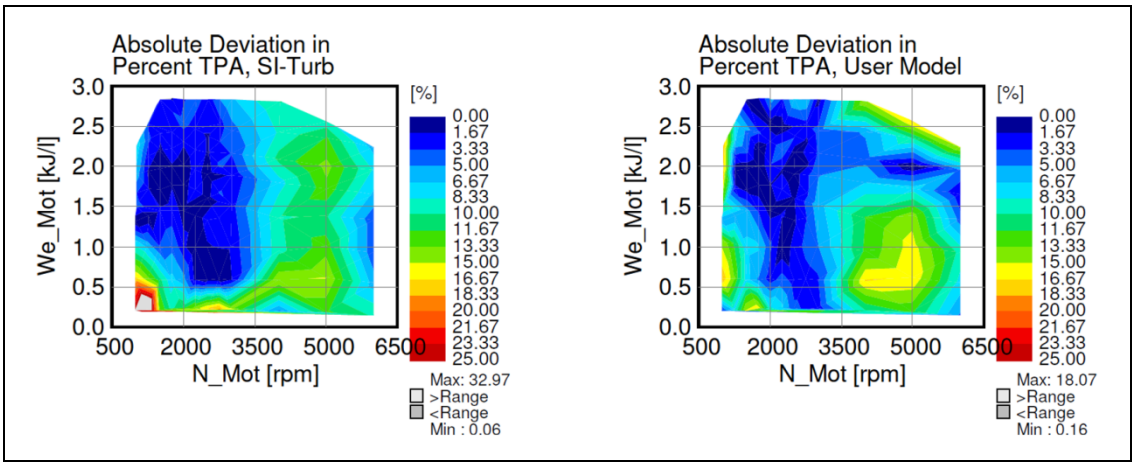

Figure 6-13: Maximum cylinder pressure, absolute deviations from TPA (Highly Turbocharged TGDI)

Finally, both models showed very good results for the Indicated Mean Effective Pressure with decent matches in wide areas of the engine performance map (Figure 6-14).

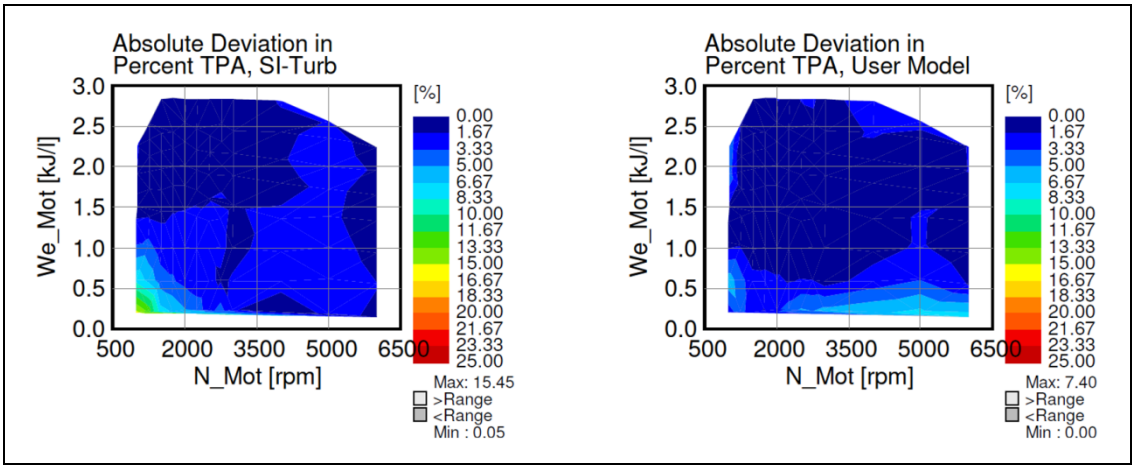

Figure 6-14: IMEP, absolute deviations from TPA (Highly Turbocharged TGDI)

The SI Turbulent Flame Combustion model shows deviations up to 15.5% and the Nefischer User Model up to 7.4%.

6.3 TVDI

Compared to the Highly Turbocharged TGDI, the TVDI caused much more problems for both combustion models. Chapters 6.3.1, 6.3.2 and 6.3.3 show the results and chapter 6.4 discusses the differences in quality of results from the 2 engine concepts.

6.3.1 Optimization Progress

The MATLAB optimization for the SI Turbulent Flame Combustion Model of the TVDI started with almost similar pre-adjusted parameters as for the Highly Turbocharged TGDI (DE = 1.50 instead of 1.0). This time, the total of square errors decreased by 25% and the results did not further improve after about 70 optimizing steps (Figure 6-15).

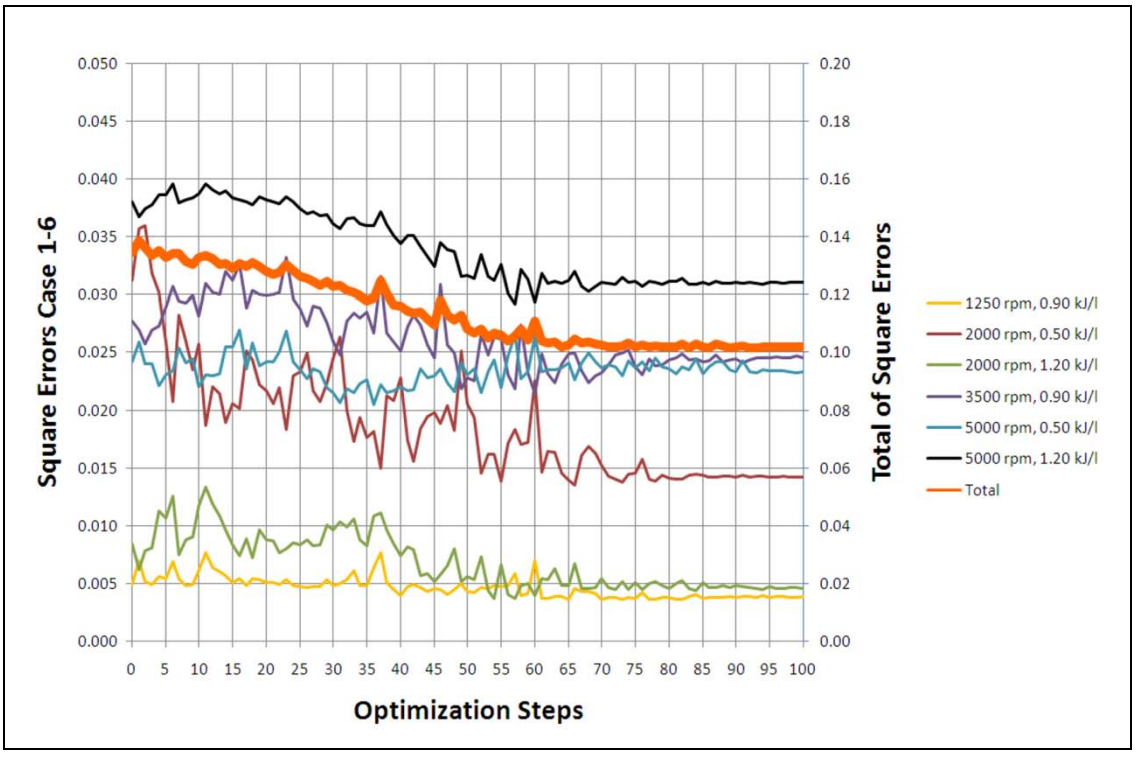

Figure 6-15: Optimization progress of the SI Turbulent Flame Combustion Model (TVDI)

Table 6-3 shows the values of the 3 parameters of the pre-adjustment and the changed parameters as result of the MATLAB optimization. The optimizer delivered an even higher value for CK, but 10.00 is the highest applicable value and therefore used in the model.

Parameter	Manual pre-adjustment	MATLAB optimized
TFM	0.72	0.71
DEM	1.50	1.16
CK	2.00	10.00

Table 6-3: Optimized parameters of the SI Turbulent Flame Combustion Model (TVDI)

The Nefischer User Model also showed a massive decrease of the total square error by about 50%, but started with a relatively high total square error from the pre-adjustment (Figure 6-16).

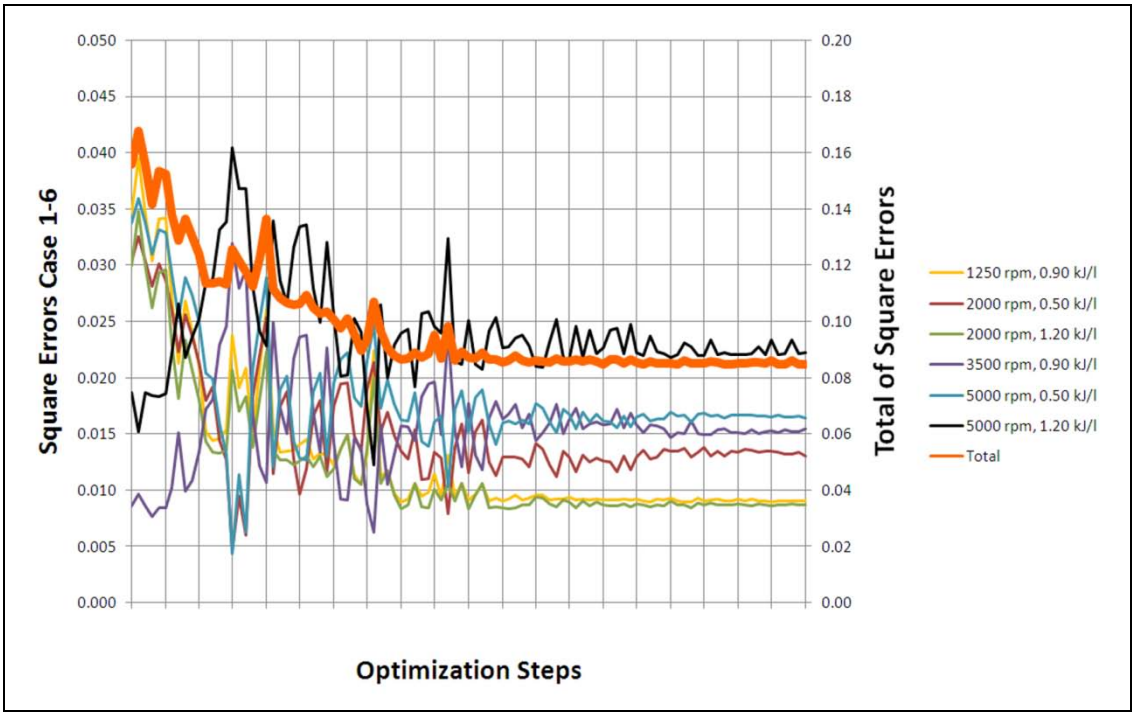

Figure 6-16: Optimization progress of the Nefischer User Model (TVDI)

Table 6-4 shows the values of the 6 parameters after the pre-adjustment and the MATLAB optimization.

Parameter	Manually optimized	MATLAB optimized
a = b/2	0.90	0.91
c	1.00E-3	1.03E-3
cburn	7.00	10.40
exc	8.40E-3	5.69E-3
dilution_exp	1.10	1.38

Table 6-4: Optimized parameters of the Nefischer User Model (TVDI)

A further comparison of the progress of total square errors of both models points out the higher value of the Nefischer User Model at the beginning but also the higher improvements at the end of the optimization process. After 100 optimization steps the Nefischer User Model reached a 16% lower value of total square errors (Figure 6-17).

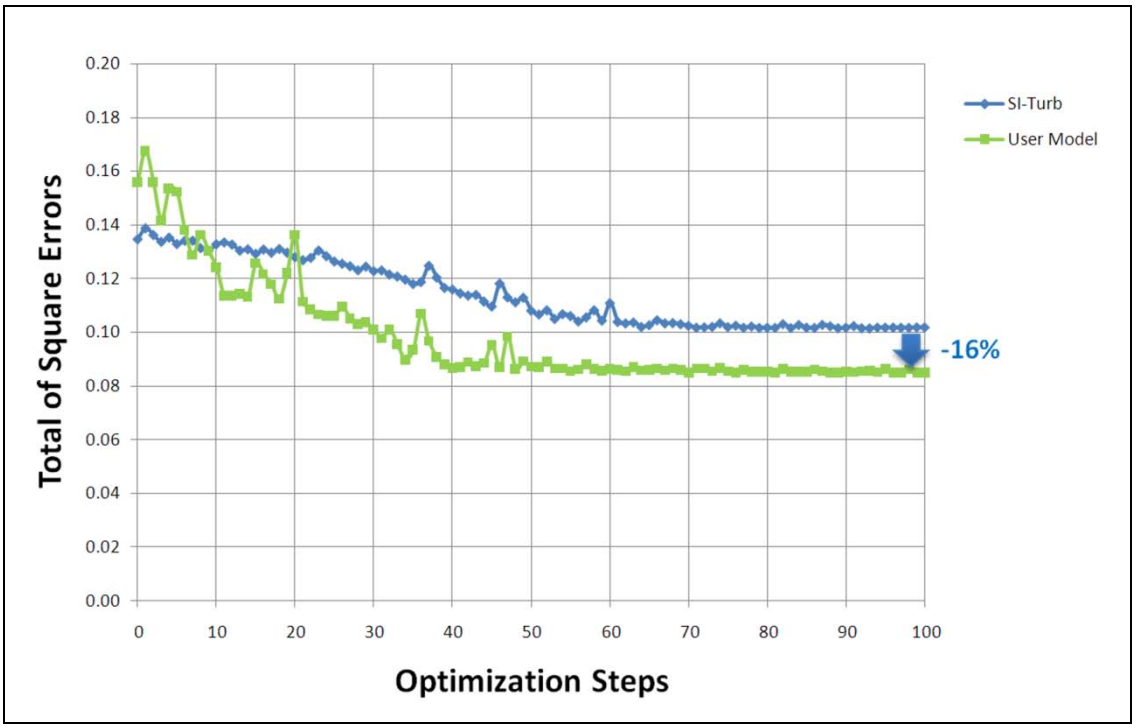

Figure 6-17: Comparison of total square errors of both models (TVDI)

6.3.2 Burn Rates

The variation of engine speed and load (Figure 6-19) this time shows the weaker performance of both models in comparison with the Highly Turbocharged TGDI. Whereas the SI Turbulent Flame Combustion Model seems to have additional problems with a too high ignition delay, both models are not able to model the change of turbulence due to phasing. Figure 6-18 shows the applied phasing levels in the engine performance map (blue = no phasing, red = maximum phasing).

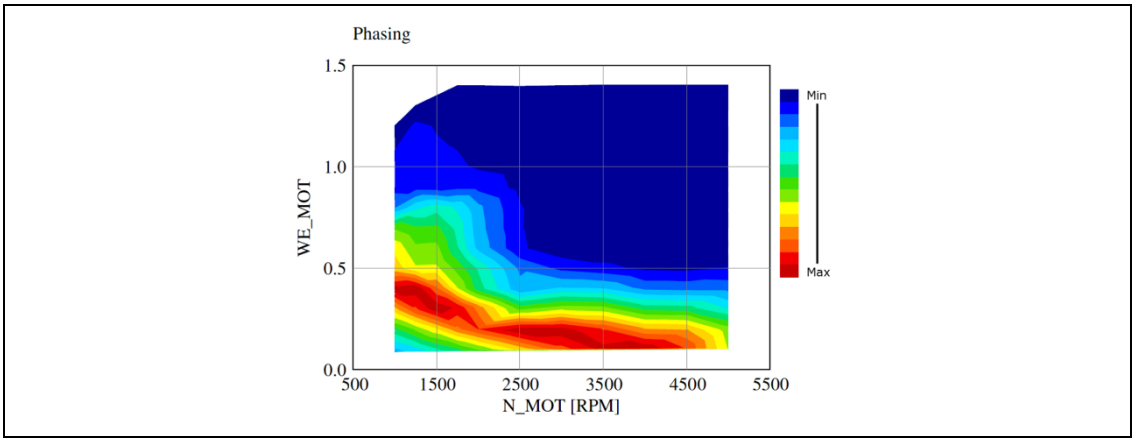

Figure 6-18: Applied phasing levels

The first 3 points in the variation of load plot (right column Figure 6-19) are intentionally taken at lower loads to visualize the deviations caused by phasing.

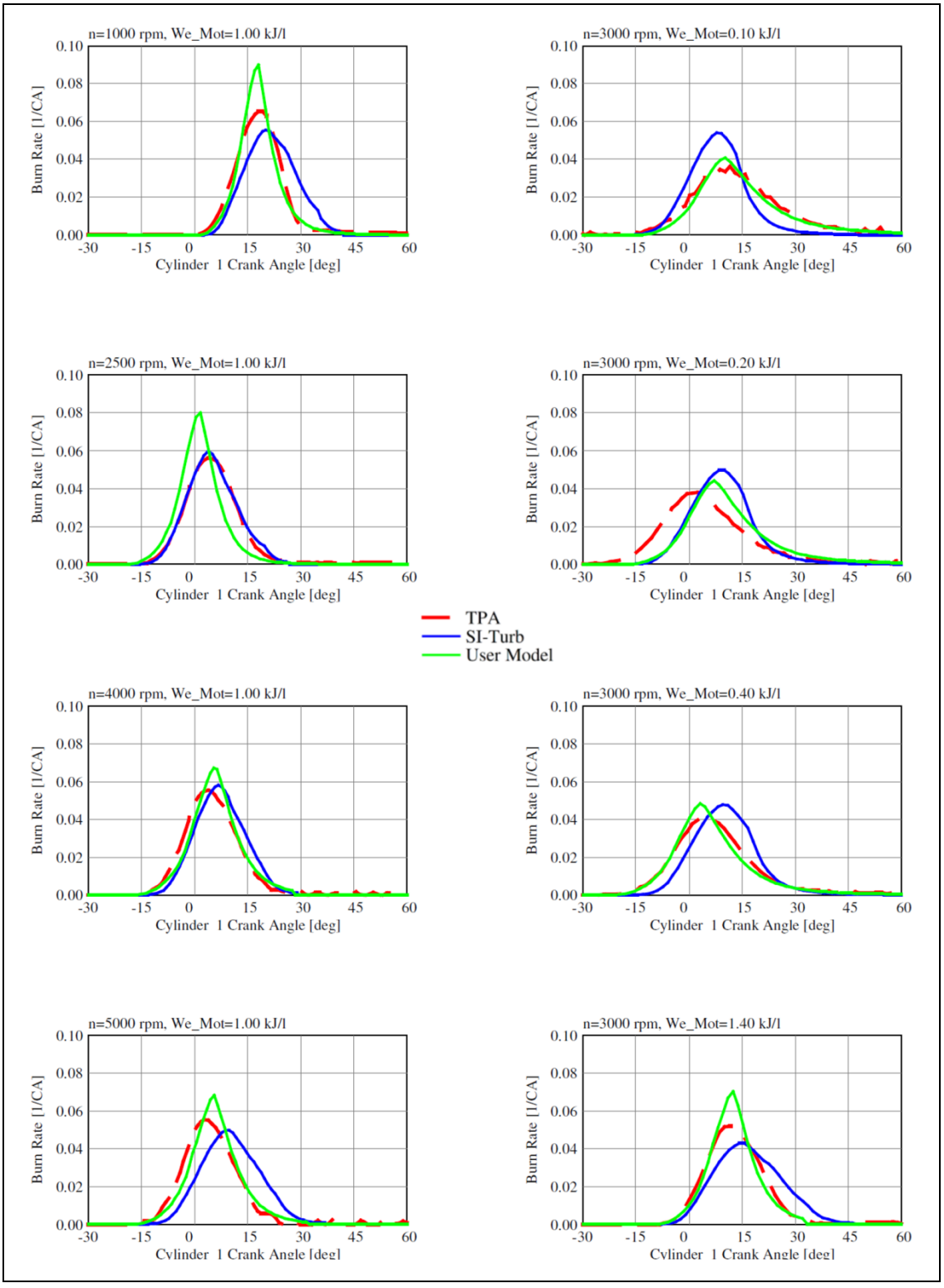

Figure 6-19: Variation of engine speed and load for the burn rate (TVDI)

Whereas the Nefischer User Model matches the burn rate at 0.10 and 0.40 kJ/l quite well, it seems to have too low turbulence at 0.20 kJ/l. This is exactly the area where the highest phasing levels are applied. In chapter 6.4 this will be discussed further and possible solutions will be pointed out.

As the variation of load already indicated, the problems caused by phasing are obvious in the engine performance map at 5% BFF (Figure 6-20). Even though the ignition delay model was adjusted as properly as for the Highly Turbocharged TGDI, the lack of turbulence causes high deviations. Also, the SI Turbulent Flame Combustion Model delivers much too high CA values for 5% BFF in these areas.

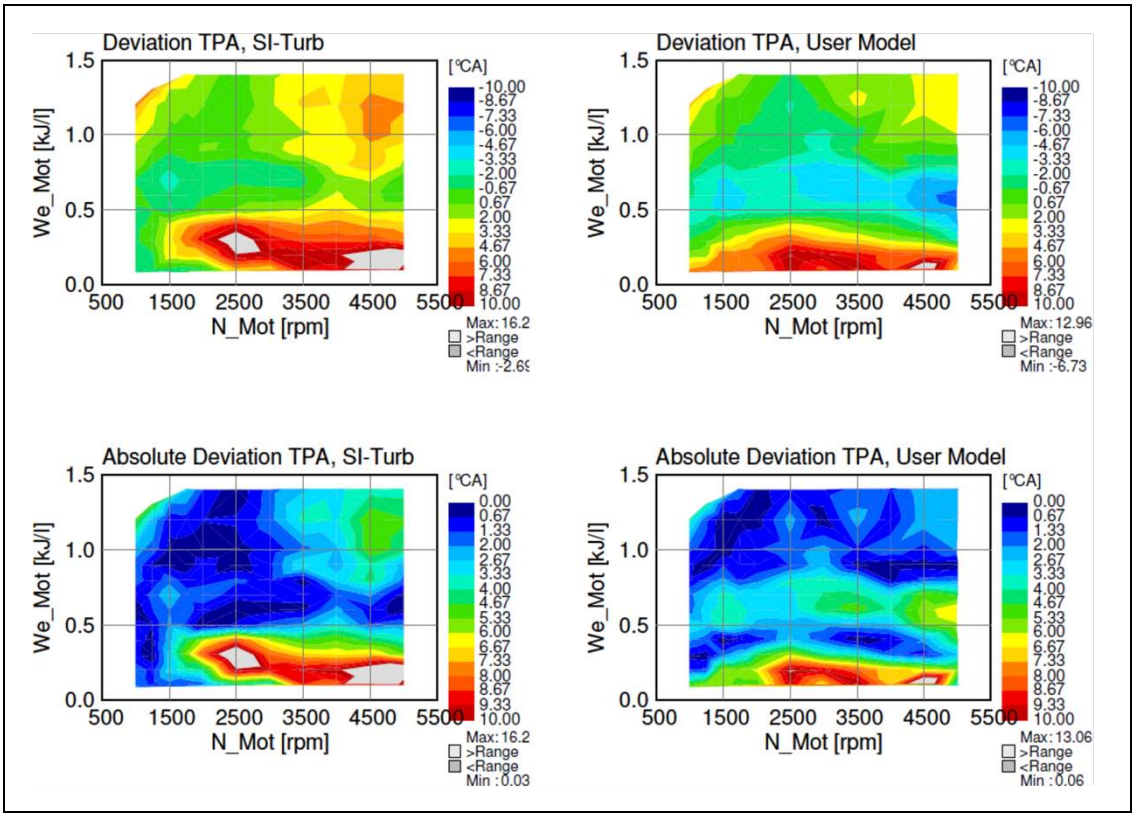

Figure 6-20: 5% BFF, deviations and absolute deviations from TPA (TVDI)

The entire engine performance map is affected in a way because the model has been also adjusted on some points with too low turbulence. This deteriorates the results in other areas where the 5% BFF is too early. So, it is important to have reasonable values for turbulence before the combustion models are adjusted.

Of course the deviations at 5% BFF also affect the 50% burn point, where both models deliver high deviations from the TPA (Figure 6-21).

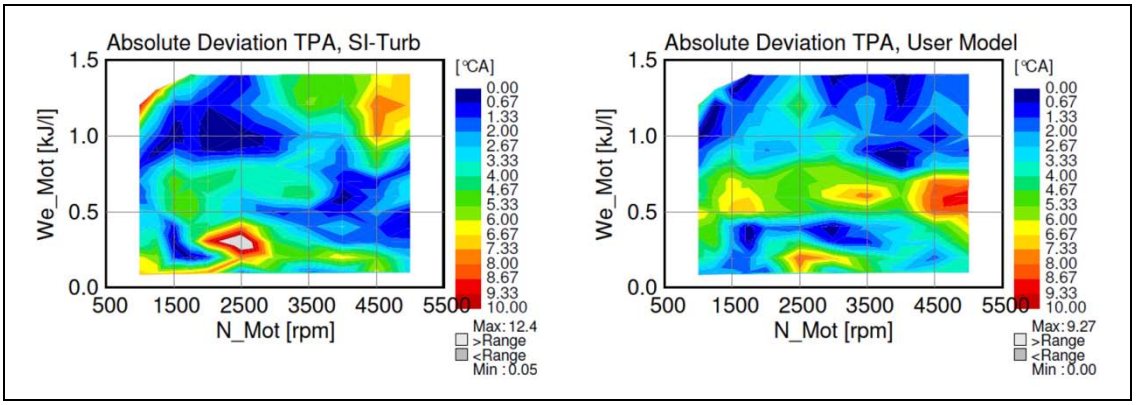

Figure 6-21: 50% BFF, absolute deviations from TPA (TVDI)

Thus, also the correlation coefficients are much lower than for the Highly Turbocharged TGDI, whereas the Nefischer User Model can achieve better results.

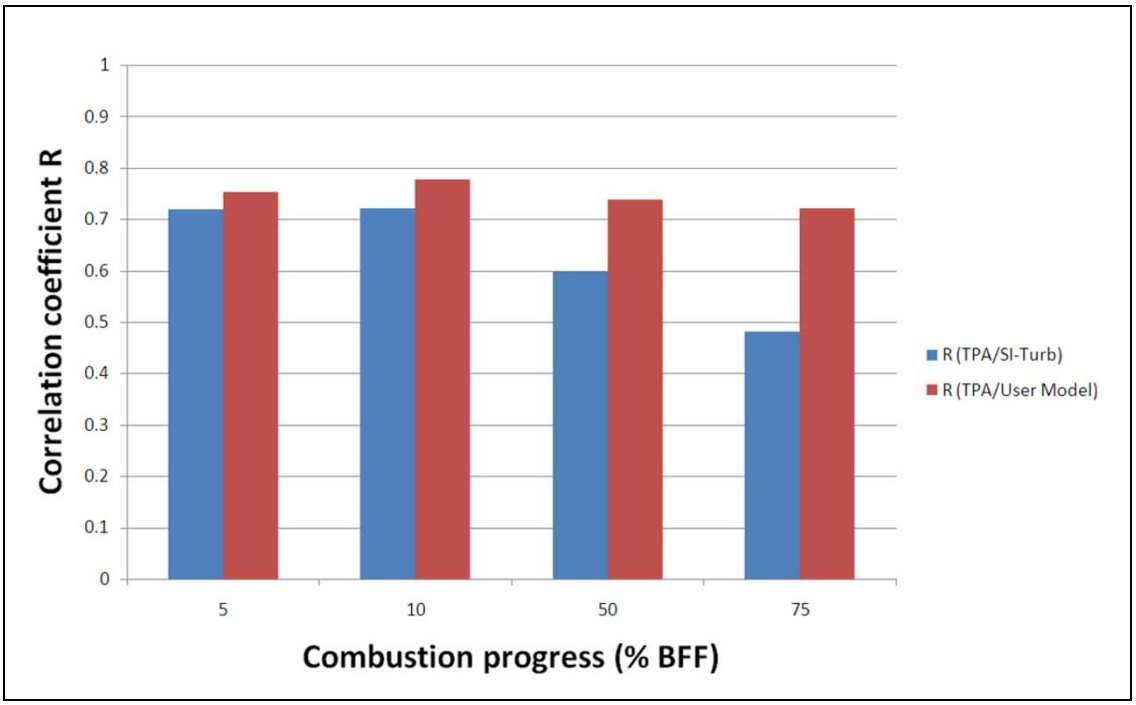

Figure 6-22: Correlation coefficients for both models (TVDI)

6.3.3 Cylinder Pressures, IMEP

Figure 6-23 indicates the variation of engine speed and load, again using the same 8 points as in the plot of burn rates (Figure 6-19). As expected, a similar behavior of the deviations as for the burn rates can be observed.

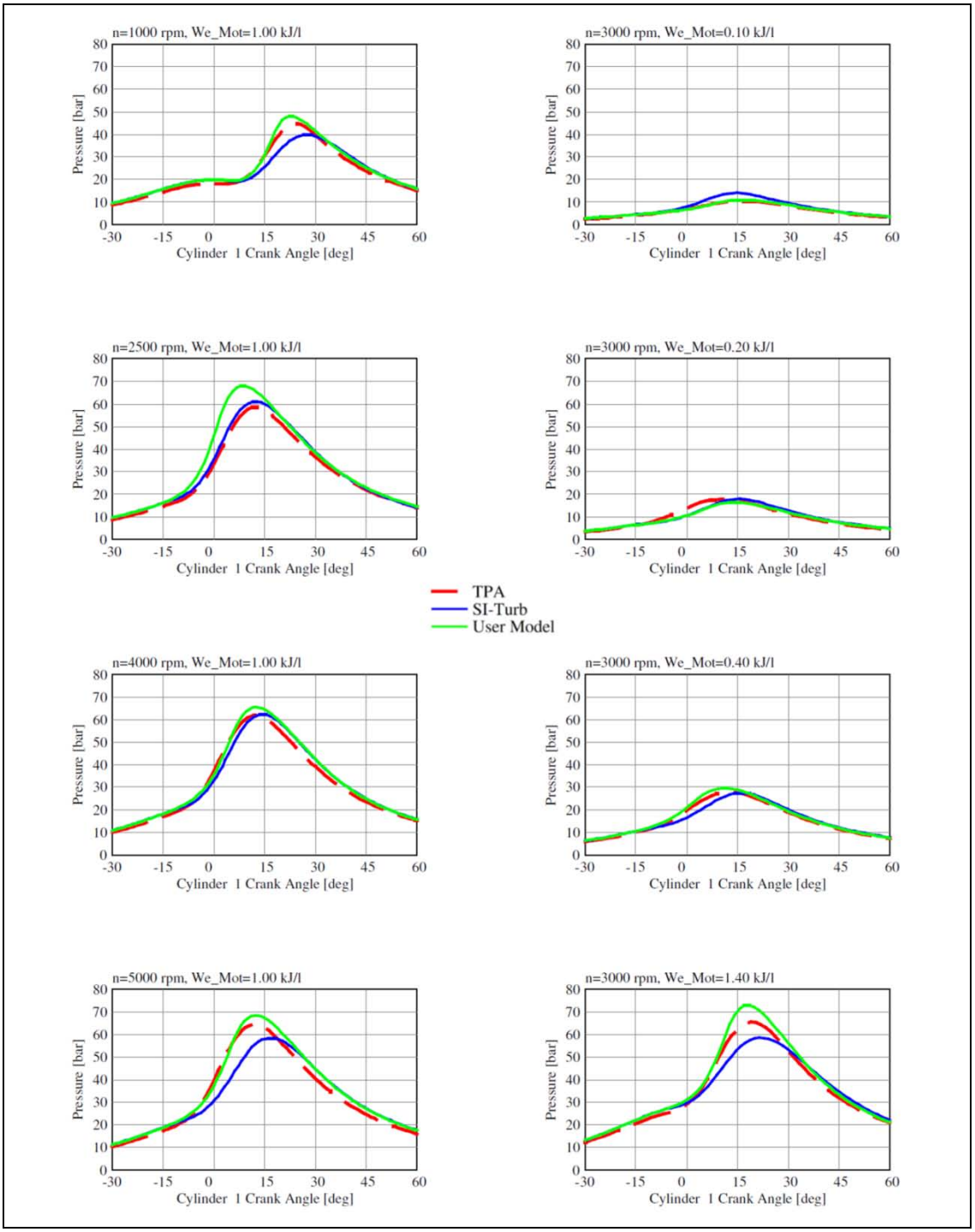

Figure 6-23: Variation of engine speed and load for the cylinder pressure (TVDI)

The map plots for the maximum cylinder pressure point out deviations up to 53% for the SI Turbulent Flame Combustion Model and 34% for the Nefischer User Model (Figure 6-24).

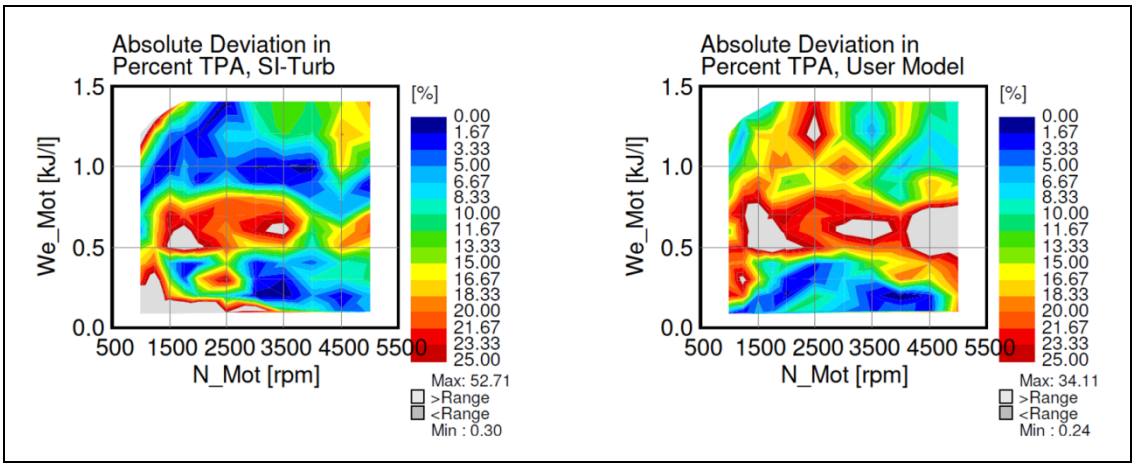

Figure 6-24: Maximum cylinder pressure, absolute deviations from TPA (TVDI)

Despite the bad results for burn rates and maximum cylinder pressure, the map plots for the Indicated Mean Effective Pressure are relatively good with deviations up to 21% for the SI Turbulent Flame Combustion Model and 11% for the Nefischer User Model (Figure 6-25).

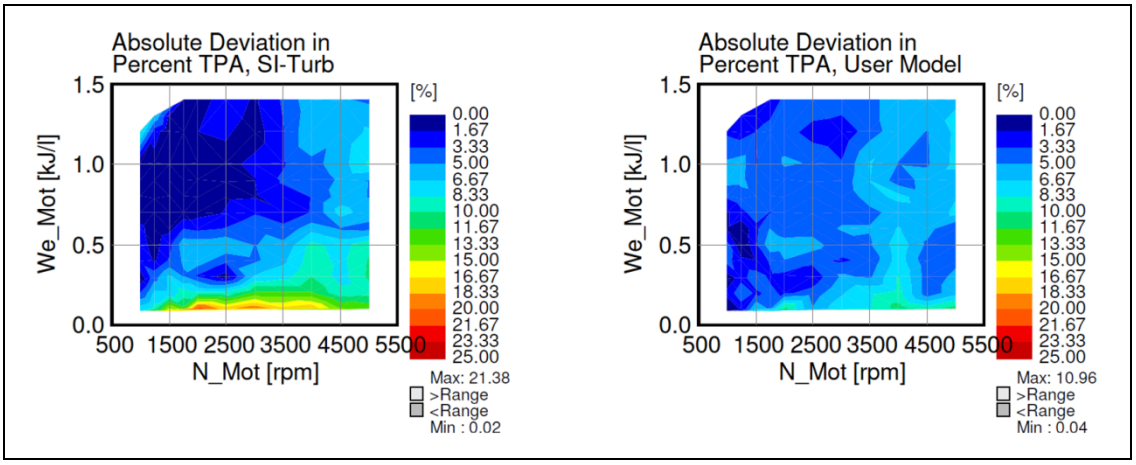

Figure 6-25: IMEP, absolute deviations from TPA (TVDI)

6.4 Discussion

Basically, the results in the preliminary survey at the Base TGDI and the results of the Highly Turbocharged TGDI are much better than of the TVDI.

This is probably caused by the inability of both models to model the effects of phasing of the Variable Valve Timing (VVT).

Due to the fact that phasing effects the turbulence in the cylinder, the adjustments need to be done in the turbulence models of the SI Turbulent Flame Combustion Model and the Nefischer User Model. As the “EngCylFlow” object offers no options to model phasing, the only possibility would be to substitute this object by another User Model created for the turbulence. The turbulence model of the Nefischer User Model can easily be extended.

As internal investigations at BMW showed, the effects of phasing are strongly non-linear and this makes the modeling difficult. It was shown that phasing increases the swirl level but partly also lowers the tumble level. Finally, little phasing had lower TKE in total than no phasing and a medium phasing variant resulted in the highest TKE values. A further increase of the phasing level again decreased the turbulence in the cylinder.

From a scientific point of view, a model, which is able to exactly describe the effects of phasing considering different parameters like valve lifts, geometrical dependencies etc., seems to be difficult. But due to the fact that phasing basically is applied to increase the turbulence level in the cylinder, a practical approach can be proposed.

Basically, the TKE start value, the Anisotropy and Dissipation constant have an influence on the progress of turbulence in the Nefischer User Model (see chapter 5.3.1.3). The most reasonable way to consider phasing seems to be to increase the TKE start value. The idea is to apply a pre-factor to the TKE start value depending on the phasing level (which for instance can be related to the difference of valve lifts). The adjustment of this pre-factor requires 3D-CFD calculations, which are able to compute the effects of different phasing levels. So, the change of this pre-factor needs to be determined for the respective engine, which uses Variable Valve Timing, and can then easily be implemented in the turbulence model.

7 Summary and Future Prospects

This thesis showed a comparison of 2 combustion models, the commercial SI Turbulent Flame Combustion Model from Gamma Technologies and a User Model created by Nefischer (2009) at BMW, which has been enhanced during this thesis.

The comparison of the 2 combustion models showed different aspects, which need to be evaluated. Regarding the general performance, both showed a partly good behavior but also some weaknesses. Overall, the results of the Nefischer User Model are slightly more accurate. For the optimization, it was easier to find appropriate starting values for the SI Turbulent Flame Combustion Model using the default-settings. Two big advantages of the Nefischer User Model are the known source code and thus understanding the processes behind the model as well as the approximately 50% lower calculation time, which is important especially for optimization processes.

Due to the fact that the SI Turbulent Flame Combustion Model is proprietary software from Gamma Technologies, it is perfectly integrated in GT-Power and easy to use. Nevertheless, the user is depending on this black-box-solution.

The worse results of both models on the TVDI seemed to be caused by the inability of modeling the change of turbulence and burn rates in the cylinder due to the phasing of the Variable Valve Timing. Extending the Nefischer User Model with a practical approach to increase TKE depending on the phasing level seems to be feasible (if the required CFD calculations are available) to further improve the results.

Considering 5 different aspects of both models, the radar chart in Figure 7-1 shows a comparison using a value of 100% for the better one, except for the robustness, where a value of 75% has been chosen for both models. This is because the SI Turbulent Flame Combustion Model already achieved roughly acceptable results with default-settings but also showed higher deviations after the optimization process. For the Nefischer User Model no default-settings are available. If once reasonable starting values have been found

and the optimization has been done, it delivers acceptable results throughout the entire engine performance map.

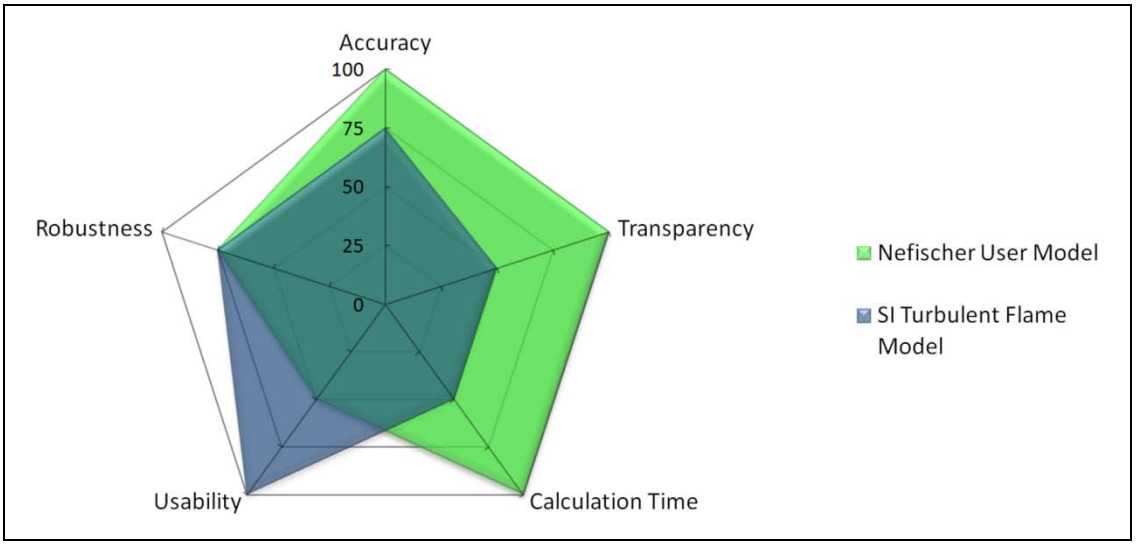

Figure 7-1: Radar chart comparing the 2 combustion models

So, each model has its strengths and weaknesses. Overall, the SI Turbulent Flame Model seems to be a more pragmatic approach, whereas the Nefischer User Model is better for a scientific approach, providing transparency and the instant possibility to modify and improve the model.

8 References

Backhaus, R. (2009, 09). Trends in der Antriebstechnik. *MTZ* .

Blizard, N., & Keck, J. (1976). *Experimental and Theoretical Investigation of a Turbulent Burning Model for Internal Combustion Engines.* SAE Technical Paper Series - 740191.

Borgnakke, C., Arpaci, V., & Tabaczynski, R. (1980). *A Model for the Instantaneous Heat Transfer and Turbulence in a Spark Ignition Engine.* SAE Technical Paper Series - 800287.

Bracco, F. (1974). Introducing a new Generation of more detailed and informative Combustion Models. *SAE Technical Paper Series - 741174* .

Busch, S. (2007). *Analyse und Weiterentwicklung von 1D-Simulationsmethoden zur Verbrennungsmodellierung in GT-Power.* Hochschule Zwickau, Diplomarbeit.

Chmela, F., Dimitrov, D., Pirker, G., & Wimmer, A. (2006). *Konsistente Methodik zur Vorausberechnung der Verbrennung in Kolbenkraftmaschinen.* MTZ - Band 67.

Damköhler, G. (1940). Der Einfluß der Turbulenz auf die Flammengeschwindigkeit in Gasgemischen. *Zeitschrift für Elektrochemie und angewandte physikalische Chemie* .

Eichlseder, H. (2005). *Vorlesungsskriptum - Verbrennungskraftmaschinen - Vertiefte Ausbildung.* Institut für Verbrennungskraftmaschinen und Thermodynamik, Graz.

FH Landshut. (2005). *Skriptum zur Vertiefungsvorlesung Motoren.* Retrieved 09 08, 2009, from http://people.fh-landshut.de/~bmae/Vertiefung_Motoren/Vertiefung_Teil1.pdf

fluent.com. (2009). *What is Computational Fluid Dynamics (CFD).* Retrieved 08 06, 2009, from http://www.fluent.com/solutions/whatcfd.htm

Forschungsvereinigung Verbrennungskraftmaschinen e.V. (2000). Computersimulation der Gemischbildung bei Benzin-Direkteinspritzung. (Heft 700).

Gamma Technologies Inc. (2009). *GT-Power - Analysis of measured cylinder pressure*. Retrieved 07 21, 2009, from http://www.gtisoft.com/applic-test_pressure_analysis.html

Gamma Technologies Inc. (2006). *GT-Power - User Manual.*

Gamma Technologies Inc. (2009). *GT-Power.* Retrieved 08 06, 2009, from http://www.gtisoft.com/applic-engine_performance_simulation.html

Grill, M. (2006). *Objektorientierte Prozessrechnung von Verbrennungsmotoren.* Universität Stuttgart, Dissertation.

Gülder, Ö. (1990). *Turbulent Premixed Flame Propagation Models for Different Combustion Regimes.* 1990: Syposium on Combustion.

Haider, G. (2008). *Begriffe aus dem Fachgebiet der Aufladung von Verbrennungsmotoren*. Retrieved 08 25, 2009, from http://members.aon.at/dihaider/LexiconML.htm

Heywood, J. B. (1988). *Internal Combustion Engine Fundamentals.*

Jobst, J., Chmela, F., & Wimmer, A. (2005). *Simulation von Zündverzug, Brennrate und NO_x-Bildung für direkt gezündete Gasmotoren.* 1. Tagung Motorprozesssimulation und Aufladung.

Kiefer, W., Klauer, N., Krauss, M., Mährle, W., & Schünemann, E. (2004). Der neue Reihensechszylindermotor-Ottomotor von BMW. *MTZ - 12/2004 Jahrgang 65* .

Klaus, B., Drexler, G., Eder, T., Eisenkölbl, M., Luttermann, C., & Schleusener, M. (2005). *Weiterentwicklung der vollvariablen Ventilsteuerung.* MTZ, 06/2005 Jahrgang 66.

Lämmle, C. (2006). *Numerical and experimental study of flame propagation and knock in a compressed natural gas engine.* Retrieved 07 28, 2009, from ETH Zürich, Dissertation: http://e-collection.ethbib.ethz.ch/view/eth:28495?q=lämmle

Linse, D., Hasse, C., & Durst, B. (2009). *An experimental and numerical investigation of turbulent flame propagation and flame structure in a turbo-charged direct injection gasoline engine.* Combustion Theory and Modelling.

Lipatnikov, A., & Chomiak, J. (2002). *Turbulent Flame Speed and Thickness: Phenomenology, Evaluation and Application in Multi-dimensional Simulations.* Progress in Energy and Combustion Science.

Livengood, J., & Wu, P. (1955). *Correlation of Autoignition Phenomenon in Internal Combustion Engines and Rapid Compression Machines.* 5th Symposium on Combustion.

Madel, C. (2008). *Weiterentwicklung der Verbrennungs- und Klopfmodellierung von aufgeladenen Ottomotoren mittels 1D-Simulation basierend auf Motorprüfstandsergebnissen.* RWTH Aachen, Diplomarbeit.

Merker, G., Schwarz, C., Stiesch, G., & Otto, F. (2004). *Verbrennungsmotoren - Simulation der Verbrennung und Schadstoffbildung.* Wiesbaden: Teubner Verlag.

Messner, D. (2007). *Wirkungsgradoptimierung von H2-Verbrennungsmotoren mit innerer Gemischbildung.* Technische Universität Graz, Dissertation.

Morel, T., Rackmill, C., Keribar, R., & Jennings, M. (1988). *Model for Heat Transfer and Combustion in Spark Ignited Engines and It's Comparison with Experiments.* SAE Technical Paper Series - 880198.

Nefischer, A. (2009). *Quasidimensionale Modellierung turbulenzgetriebener Phänomene in Ottomotoren.* Technische Universität Graz, Dissertation.

Pischinger, R., Klell, M., & Sams, T. (2002). *Thermodynamik der Verbrennungskraftmaschine.* Wien: Springer Verlag.

Pivec, R. (2001). *Quasidimensionale Modellierung des gasseitigen Wärmeüberganges in Verbrennungsmotoren.* Technische Universität Graz, Dissertation.

RWTH Aachen. (2000). *Ottomotorische Verbrennung.* Retrieved 07 29, 2009, from http://www.sfb224.rwth-aachen.de/Kapitel/kap3_3.htm

Schubert, C., Wimmer, A., & Chema, F. (2005). *Advanced Heat Transfer Model for CI Engines.* SAE Technical Paper Series.

Stergiou, C., & Siganos, D. (n.d.). *Imperial College London - Neural Networks*. Retrieved 09 08, 2009, from http://www.doc.ic.ac.uk/~nd/surprise_96/journal/vol4/cs11/report.html#What%20is%20a%20Neural%20Network

Tabacznynski, R. (1980). *Further Refinement and Validation of a Turbulent Flame Propagation Model for Spark Ignition Engines.*

University of Illinois. (2009). *Mathematics, Science and Technology Education (MSTE) program - Scatter Plots*. Retrieved 08 06, 2009, from http://www.mste.uiuc.edu/courses/ci330ms/youtsey/scatterinfo.html

Van Basshuysen, R., & Schäfer, F. (2009). *Motorlexikon.de - Downsizing.* Retrieved 08 06, 2009, from http://www.motorlexikon.de/?I=2362

Van Basshuysen, R., & Schäfer, F. (2009). *Motorlexikon.de - Hochaufladung*. Retrieved 08 25, 2009, from http://www.motorlexikon.de/?I=2310&R=H

Vibe, I. I. (1970). *Brennverlauf und Kreißprozeß von Verbrennungsmotoren.* Berlin: VEB Verlag Technik.

Wahiduzzaman, S., Morel, T., & Sheard, S. (1993). *Comparison of Measured and Predicted Combustion Characteristics of a Four-Valve S.I. Engine.* SAE Technical Paper Series - 930613.

Wikipedia, the free encyclopedia. (2009). *Correlation*. Retrieved 08 17, 2009, from http://en.wikipedia.org/wiki/Correlation

Wikipedia, the free encyclopedia. (2010). *Simplex algorithm*. Retrieved 01 12, 2010, from http://en.wikipedia.org/wiki/Simplex_algorithm

Wimmer, A. (2004). *Vorlesungsskriptum - Thermodynamik des Verbrennungsmotors.* Graz.

www.skyroadster.com. (n.d.). *Twin Scroll turbocharger.* Retrieved 08 25, 2009, from http://www.skyroadster.com/forums/attachments/f11/31903d1238843197-openometer-twin-scroll-turbo_01.jpg

9 Lists

9.1 List of Abbreviations

ANN	Artificial Neural Network
CA	Crank Angle
CI	Compression Ignition
BDC	Bottom Dead Center
BFF	Burned Fuel Fraction
Br	Combustion chamber (Brennraum)
CK	Flame Kernel Growth Multiplier
CFD	Computational Fluid Dynamics
CRFD	Computational Reactive Fluid Dynamics
DE	Dilution Exponent
DEM	Dilution Exponent Multiplier
EGR	Exhaust Gas Recirculation
EVO	Exhaust Valve Opening
HCCI	Homogeneous Charge Compression Ignition
IMEP	Indicated Mean Effective Pressure
IP	Ignition Point
IVC	Intake Valve Closing
LHV	Lower Heating Value
SI	Spark Ignition
TDC	Top Dead Center
TGDI	Turbocharged Gasoline Direct Injection
TKE	Turbulent Kinetic Energy
TVDI	Turbocharged Valvetronic Direct Injection
TPA	Three Pressure Analysis
TFM	Turbulent Flame Speed Multiplier
Verd.	Evaporation (Verdampfung)
VVT	Variable Valve Timing

9.2 List of Formula Symbols

a	...	$Anisotropie$
a	...	$Pressure - exponent$
A_e	...	$Surface\ Area\ at\ the\ Edge\ of\ the\ Flame\ Front\ [m^2]$
A_T	...	$Turbulent\ Flame\ Surface\ [m^2]$
B_M	...	$Laminar\ Flame\ Speed\ \left[\frac{m}{s}\right]$
E	...	$Expected\ Value\ Operator$
f	...	$Dilution$
h	...	$Specific\ Enthalpy\ \left[\frac{J}{kg}\right]$
k	...	$Turbulent\ Kinetic\ Energy\ \left[\frac{m^2}{s^2}\right]$
H_u	...	$Lower\ Heating\ Value\ \left[\frac{J}{kg}\right]$
L_t	...	$Turbulent\ Lenght\ Scale\ [m]$
m	...	$Mass\ [kg]$
m	...	$Vibe\ Form\ Factor$
$\dot{m}$	...	$Mass\ Flow$
n	...	$Engine\ Speed\ [rpm]$
M_b	...	$Burned\ mass\ [kg]$
M_e	...	$Entrained\ Mass\ of\ the\ Unburned\ Mixture\ [kg]$
p	...	$Pressure\ \left[\frac{N}{m^2}\right]$
Q_B	...	$Heat\ Release\ [kJ]$
Q_w	...	$Heat\ Flow\ [J]$
R_f	...	$Flame\ Radius\ [m]$
S_L	...	$Laminar\ Flame\ Speed\ \left[\frac{m}{s}\right]$
S_T	...	$Turbulent\ Flame\ Speed\ \left[\frac{m}{s}\right]$

t	...	$Time\,[s]$
T	...	$Temperature\,[K]$
T_a	...	$Activation\ Temperature\,[K]$
u'	...	$Turbulent\ Intensity\ \left[\frac{m}{s}\right]$
U	...	$Internal\ Energy\ [J]$
V	...	$Volume\ [m^3]$
We_Mot	...	$Mean\ Effective\ Pressure\ \left[\frac{kJ}{l}\right] \widehat{=} 10\ [bar]$

Greek

γ	...	$Constant$
δ_L	...	$Flame\ Thickness\ [m]$
ε	...	$Turbulent\ Rate\ of\ Dissipation\ \left[\frac{m^2}{s^3}\right]$
η_u	...	$Degree\ of\ Realization$
λ	...	$Taylor\ Length\ Scale\,[m]$
μ	...	$Expected\ Value$
σ	...	$Standard\ Deviation$
φ	...	$Crank\ Angle\ [°CA]$
φ_{BB}	...	$Start\ of\ Combustion\ [°CA]$
φ_{BD}	...	$Duration\ of\ Combustion\ [°CA]$
Φ	...	$Equivalence\ Ratio$
ρ	...	$Density\ \left[\frac{kg}{m^3}\right]$
ρ_u	...	$Unburned\ Density\ \left[\frac{kg}{m^3}\right]$
$\rho_{X,Y}$	...	$Pearson\ Correlation\ Coefficient$
τ	...	$Time\ Constant\ [s]$

9.3 List of Figures

9.4 List of Formulas

9.5 List of Tables